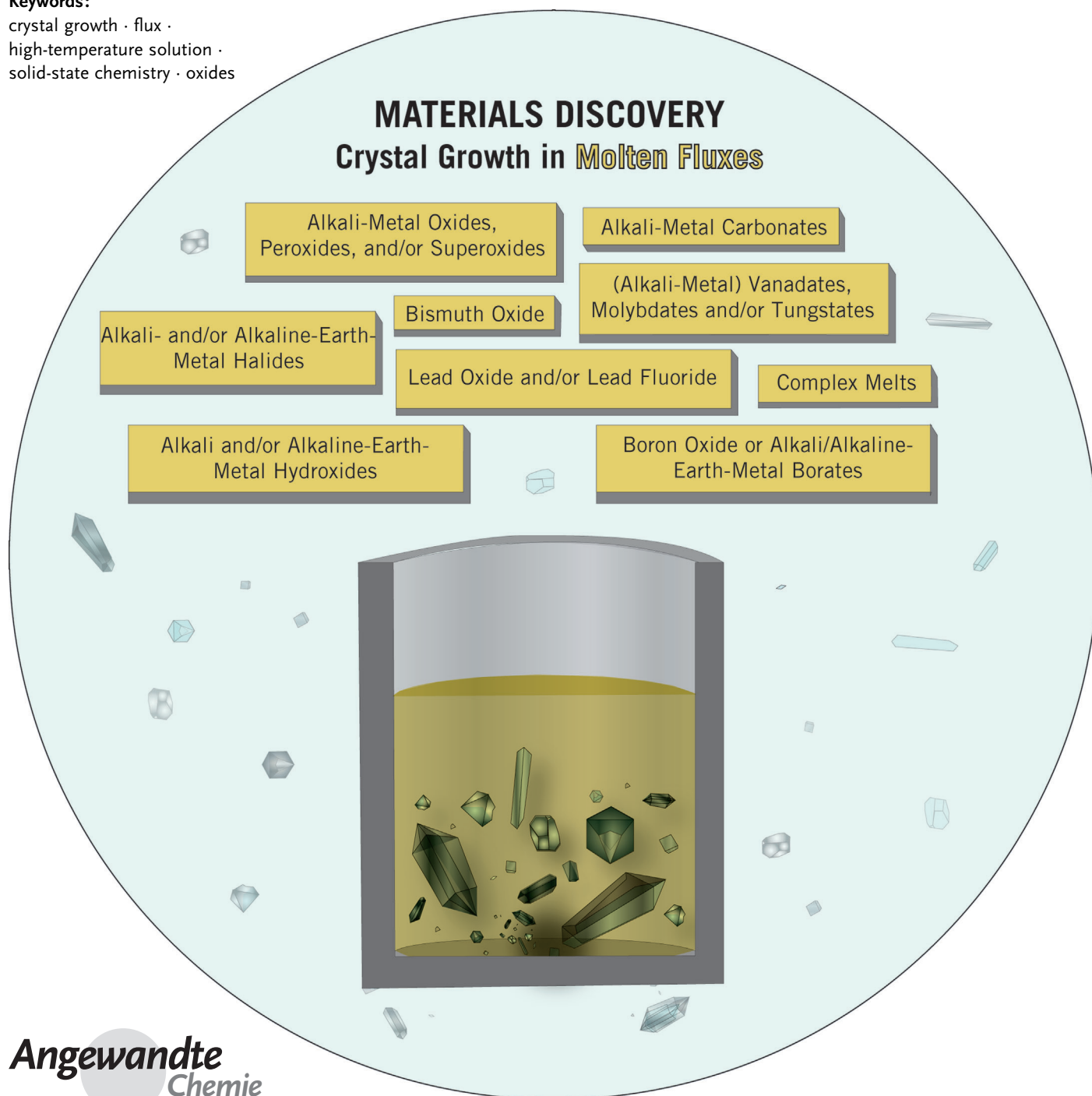


# Materials Discovery by Flux Crystal Growth: Quaternary and Higher Order Oxides

Daniel E. Bugaris\* and Hans-Conrad zur Loye\*

**Keywords:**

crystal growth · flux ·  
high-temperature solution ·  
solid-state chemistry · oxides



**This Review highlights the application of high-temperature solutions for exploratory crystal growth and materials discovery of novel complex oxides. It provides an overview of the method of flux crystal growth of complex oxides and can function as a “how to” guide for those interested in oxide crystal growth. The most commonly used fluxes are discussed in terms of their applicability for dissolving specific elements and the typical reaction conditions are compiled. A large variety of recent quaternary and higher oxides that have been grown as crystals from fluxes are used to illustrate the power of the flux method to grow oxide crystals containing specific elements.**

## 1. Introduction

There exist many diverse synthetic techniques, but none that offer as much reward for success as exploratory crystal growth.<sup>[1–24]</sup> The preparation of a novel chemical composition, coupled with the ready ability to determine the crystal structure, as well as the potential of uncovering the compounds intrinsic properties using single-crystal characterization techniques, can rapidly open up a new field of chemical investigation. Succeeding in this endeavor is difficult, however, and this Review will focus on one approach, crystal growth from high-temperature solutions, to provide a roadmap to the interested scientist. Using quaternary and higher order oxides (three or more elements plus oxygen) as examples, the technique and its underlying subtleties will be illustrated using the diverse classes of high-temperature solutions or fluxes, where the successes over the past 30 years can be readily documented and categorized. Owing to the fact that an enormous number of new and interesting phases have been discovered, it is far beyond the scope of this Review to include and describe but a small fraction. In fact, although the focus will be on the documentation of an extensive list of novel oxide compositions that have been prepared as single crystals by flux growth, together with a detailed compendium of the crystal growth conditions, we further limit those to quaternary and higher phases, not including many borates, silicates, phosphates, arsenates, sulfates, selenates, tellurates, and mixed-anion oxides (oxy-niobates, oxychalcogenides, oxyhalides).

The discovery of new materials and associated desirable properties has been a driving force behind chemical innovation for centuries.<sup>[25–27]</sup> When we look at some of the many recent technological advances and how widespread and significant their impact has been, we appreciate how much they have relied on new materials. Some of these advances include the increase in hard-drive storage capacity because of new magneto-resistive materials, the ever-shrinking cell phone because of new microwave dielectric materials, the enhancement in lithium battery storage capacity because of new intercalation materials, and the improved capacitor because of new ferroelectric materials. This is not to say that all these materials were discovered and used without


## From the Contents

<b>1. Introduction</b>	3781
<b>2. Materials Discovery from High-Temperature Solutions</b>	3782
<b>3. Solvent Systems</b>	3786
<b>4. Summary and Outlook</b>	3806

further chemical optimization, as in fact most of them have been carefully modified prior to being incorporated into devices. However, in all cases, there was a “First Material”, or archetype in which the phenomenon was first observed; the one that led to further investigations and the subsequent preparation of improved 2nd or 3rd generation materials. It is this “First Material” that needs to be discovered. And we do mean “discovered”. It is difficult to predict the composition of a “First Material” that will exhibit the “heretofore never observed property or phenomenon”; after all, where would one start? The concept of an “Energy Landscape” as described by Jansen and Schön<sup>[25,28]</sup> stipulates that *all* compounds capable of existence are present on an energy landscape and that, furthermore, each composition capable of existence is associated with a local minimum on that landscape. A direct result of this “global view” is the concept of *discovery* rather than *design* of a new material, as well as the implication that we are exploring this landscape by carrying out experiments to find the local minima. It turns out that we are very successful at locating these minima for simple compositions, but find it significantly more difficult to extend our success to the more complex compositions. Yet, it is likely that these more complex structures may hold the key to realizing some of the most desirable properties.<sup>[25–28]</sup>

Predicting a simple structure for a simple composition, or vice-versa, is fairly straightforward. Predicting a complex structure for a complex composition, or vice-versa, on the other hand, is extremely challenging, if currently feasible. But at least we have a starting point—either the structure or the composition. What if we had neither? Where would we start and would we run out of choices for new chemical combinations considering how much has been prepared to date? While we can look back at a rich history of materials discovery, it is important to realize that we have barely scratched the surface of what can be made.<sup>[29]</sup> As we consider

[\*] Dr. D. E. Bugaris, Prof. H.-C. zur Loye  
Department of Chemistry and Biochemistry  
University of South Carolina  
631 Sumter Street, Columbia, SC 29208 (USA)  
E-mail: bugaris@mailbox.sc.edu  
zurloye@mailbox.sc.edu

 Supporting information for this article is available on the WWW under <http://dx.doi.org/10.1002/anie.201102676>.

more complex structures containing more components, the combinatorial possibilities are almost limitless, and we can be certain that we will not run out of new materials any time soon, if ever.

Chemists are very good at improving new materials by carrying out carefully planned chemical substitutions that result in new compositions with, in many cases, enhanced properties. These substitutions often rely on radius ratio rules and on our understanding of oxidation states and coordination environment preferences of the elements. For example, for the intensely studied family of perovskite oxides there are detailed structural predictions and approaches for making new compositions based on size, oxidation state preferences, and electronegativities.<sup>[30,31]</sup> Thus, once a new structure/composition has been discovered, the trained chemist can use this as a starting point for a targeted study that may well include additional chemical substitutions to tweak the structure, change oxidation states, and directly influence and modify the observed physical properties. But how can we find this “First Material”? To address this issue, in this Review, we will present one method, crystal growth from high-temperature solutions, that we believe is most likely to result in the discovery of new compositions with complex structures and potentially new properties.

## 2. Materials Discovery from High-Temperature Solutions

Typically there is more than one solvent and often more than one set of conditions that will yield crystals. Nonetheless, it is inevitably true that for each material the specific growth conditions are unique and must be optimized. As crystal growth is a time intensive undertaking,

there needs to be a reason why crystals rather than polycrystalline powders are desired (often simply because crystals provide an opportunity to measure a material’s intrinsic behavior in the absence of grain boundaries).

It is possible to distinguish between two broad approaches to crystal growth—the application driven and the exploration driven (Figure 1). In the first case, the desire is to grow crystals of a specific composition that is known to exhibit a specific property, while in the second case, there is no defined target composition and the goal is to obtain a crystal with a new composition and/or new crystal structure and to investigate its physical properties. Often there is a trade-off between targeting small, high-quality, faceted crystals for crystallographic studies, and preparing large single crystals (boules) of known materials with established and desired properties from which smaller pieces are cut to be used in devices. The focus on small crystals for exploratory work, rather than large crystals for applications will be emphasized in this Review.

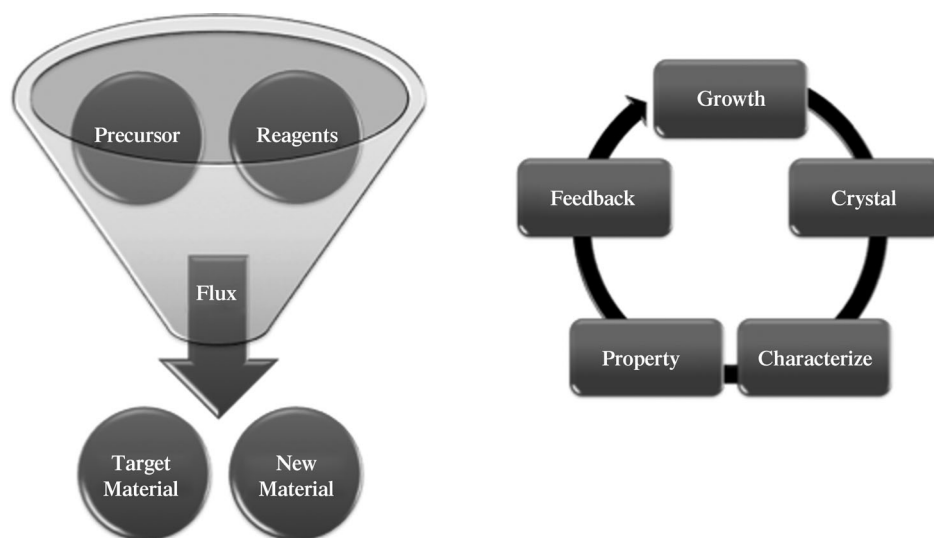


Figure 1. Principle of exploratory crystal growth process.



Daniel E. Bugaris graduated with a B.S. in Chemistry from the University of Notre Dame in 2005, and a Ph.D. from Northwestern University in 2009 under the supervision of Dr. James A. Ibers. He is currently a post-doctoral fellow in the laboratory of Dr. Hans-Conrad zur Loye at the University of South Carolina. His research interests are in the broad area of inorganic materials chemistry and include the crystal growth of novel compositions (oxides and chalcogenides), structure determinations, and physical-property measurements.



Hans-Conrad zur Loye is the David W. Robinson Palmetto Professor in the Department of Chemistry and Biochemistry at the University of South Carolina. He received his B.S. from Brown University in 1983 and his Ph.D. in Chemistry from the University of California, Berkeley in 1988 under the supervision of Dr. A. Stacy. After one year as a postdoctoral fellow at Northwestern University in the group of Dr. D. Shriver, he became an assistant professor in the Chemistry Department of MIT in 1989. In 1996 he moved to the University of South Carolina where his research interests focus on inorganic materials chemistry, in particular the synthesis of inorganic/organic hybrid materials and the crystal growth of new oxide materials.

## 2.1. General Considerations Regarding the Use of Fluxes

Flux growth utilizes a high-temperature melt of an inorganic compound as the solvent for crystallization.<sup>[1]</sup> These high-temperature solutions or fluxes are simple inorganic compounds, such as  $\text{BaCl}_2$ ,  $\text{Bi}_2\text{O}_3$ ,  $\text{B}_2\text{O}_3$ ,  $\text{KOH}$ ,  $\text{PbO}$ , or  $\text{Na}_2\text{CO}_3$ , which melt at conveniently low temperatures. Often combinations of inorganic compounds are used to form an even lower melting eutectic, which can reduce the melting point of a “high-temperature solution” below 200 °C. Furthermore, the presence of water, either as an intentional additive or as waters of hydration, can substantially lower the melting points of some fluxes, such as hydroxides, by forming a “eutectic” melt and ultimately an aqueous solution. The term hydroflux has been suggested for such combinations of hydrothermal and flux techniques, where water is used as a modifier to the solution properties of the melt. As an operational definition for this article, we define fluxes to be melts, thereby excluding crystal growth by strictly hydrothermal/solvothermal methods. In these cases, to differentiate a flux from an aqueous solution, we will rely on the operational temperature. If the crystal growth temperature is above the melting point of the solid, then we are dealing with a flux. If the operational temperature lies below the melting point, and the system is liquid only because of the presence of water or some other solvent, then we consider this to be an aqueous or solvothermal solution.

Of course, for an inorganic compound to make a good flux it has to meet certain criteria, including: 1) the ability to dissolve a substantial quantity of the reagents, 2) a low melting point, 3) a significant change of the solubility with temperature, 4) low volatility, 5) unreactive toward the crucible that contains the melt, 6) easily removed after crystal growth, 7) commercially available at low cost, and 8) low toxicity. In a typical experiment the reagents are dissolved in a suitable solvent (melt) and crystallization occurs as the solution becomes critically supersaturated. There are different routes to achieving supersaturation, including reducing the volume of the melt by evaporation and cooling the melt.

Considering that there are many methods for growing crystals, including crystal pulling, zone refining, chemical vapor transport, hydrothermal/solvothermal, high-pressure, recrystallization from the melt, and flux growth, the advantages and disadvantages of flux growth over other methods must be considered. For example, many oxides are commercially produced by growing them from their own melt, such as sapphire ( $\text{Al}_2\text{O}_3$ ); however, this approach does not work for the vast majority of oxides that melt incongruently, which is not an issue for flux growth. Furthermore, to melt many oxides can require substantially high temperatures (m.p. of  $\text{Al}_2\text{O}_3$  is 2044 °C), or include passing through a structural phase transition upon cooling the crystal (cubic to tetragonal  $\text{ZrO}_2$  at 2287 °C) that often makes growth from the melt impractical. One of the main advantages of flux growth is the ability to achieve crystal growth at much lower temperatures than if the crystal was grown from the melt, and this may also enable the researcher to obtain low-temperature phases that cannot be prepared otherwise. Furthermore, the use of a flux allows crystal growth in the absence of a temperature

gradient, which minimizes the presence of crystal defects, such as vacancies or dislocations, and can lead to crystals of the highest quality for single-crystal X-ray diffraction. And finally, a not insignificant advantage is the simplicity of the technique, which does not require a substantial investment in expensive equipment, such as crystal pullers or high-pressure apparatus. Of course, the method cannot match the high growth rates achievable by crystal pulling, although that is not typically the intention. There are some potential complications with flux growth that are not an issue with growth from the melt. Specifically, the flux can end up incorporated into the crystal, either as an inclusion or as a component of the crystal itself. In the former case the crystal quality is greatly reduced, while in the latter case one refers to a “reactive flux,” where the flux has taken on the role of a reagent, which can lead to the formation of unexpected compositions and structures.

Although there are a large variety of solvents that can be used for crystal growth, there is no single “perfect” solvent. Most crystals can be grown out of more than one solvent system and often there are some advantages and disadvantages to all of them. Depending on the outcome desired (crystal structure, optical properties, magnetic measurements), some fluxes will be superior over others and impurities contained in some fluxes can interfere with properties of interest while others will not. The most critical criterion remains the need for high solubility of the reagents in the flux and a significant change in solubility with temperature. This requirement is best achieved by closely matching the bonding of the molten compound (flux) to that of the final product, that is, ionic to ionic, covalent to covalent. Since most materials are not strictly one or the other, compromises must be made. While it is possible to use a flux in which the bonding is very different from the desired product, the solubility of the reagents in such systems is often quite limited.

So what makes a good flux? There are several factors that positively influence the ability of a flux to dissolve the reagents and to promote crystal growth. Often materials with good solvent properties are those that form a compound with the solute at low temperatures or in different concentration ranges. Furthermore, a common anion or cation often has a positive impact on the solution chemistry and solubility, as does matching the polarizability of the solvent and the solute. The advantages of choosing the flux by matching the physical and chemical properties are reduced flux inclusion and high-quality crystals.

There are several aspects of crystal growth that require adjustment or optimization, including, for example, the use of additives or mineralizers ( $\text{OH}^-$ ,  $\text{F}^-$ ,  $\text{Cl}^-$ ) that are historically used in hydrothermal crystal growth. These mineralizers can have a multitude of effects ranging from promoting the dissolution of the reagents by stabilizing metal complexes in solution, to increasing the width of the metastable region where supersaturation can exist, to altering the viscosity of the melt, and to influencing crystal nucleation and consequently crystal size. Halide salts, such as  $\text{NaCl}$ ,  $\text{KF}$ , or  $\text{BaCl}_2$ , can promote the formation of metal complexes in solution and thereby increase the solubility of reagents. The addition



of monovalent ions, such as  $\text{Li}^+$ ,  $\text{Na}^+$ , or  $\text{Cl}^-$ , can decrease the viscosity of the melt by preventing network formation in melts prone to that, for example in  $\text{B}_2\text{O}_3$  (viscous) as compared to  $\text{Na}_2\text{B}_4\text{O}_7$  (less viscous). Conversely, some additives, such as  $\text{B}_2\text{O}_3$ , which are desirable because they typically broaden the metastable region, can also have adverse effects by increasing the viscosity to undesirable levels when too much is added.

The issue of “inertness” of a flux requires careful consideration. To avoid having a reactive flux, that is, one where flux components become incorporated into the product, it is best to find materials that are chemically similar in bonding, but have different coordination environment preferences, different valence or substantially different sizes. A combination of these differences typically prevents the incorporation of the flux into the product.

There are numerous factors that influence the composition and quality of crystals grown from a melt. For example, the redox equilibria that exist in the melt will dictate the oxidation states of metals, whereas the atmosphere above the melt, which can be controlled by fixing the  $\text{O}_2$  partial pressure ( $P_{\text{O}_2}$ ; for example by choosing an  $\text{O}_2$  vs. a  $\text{N}_2$  vs. a  $\text{CO}/\text{CO}_2$  atmosphere), influences these redox equilibria. This situation is especially important in the case of hydroxide-based melts, where the acid–base properties of the melt are best described by the Lux–Flood concept of oxoacidity.<sup>[32,33]</sup> The practical upshot of this is the ability to grow crystals of both oxidized and reduced phases in fluxes as well as the ability to target kinetic versus thermodynamic phases.

One drawback of flux growth is the lack of knowledge of what exactly goes on in the solution (although the processes taking place during the early stages of crystal growth are beginning to be investigated by in situ methods)<sup>[34]</sup> and, hence, a limited understanding of the growth mechanism. Clearly, while solvent–solute interactions are expected to be important and the crystal–solution interface is expected to influence the growth process, there are no good methods of routinely studying these processes. Likewise, to what extent solution pre-arrangement or clustering impacts the specific crystal structure or composition that is obtained, while undoubtedly important, is not well understood to date. Hence, the researcher must always perform some degree of exploratory work to identify growth issues specific to the system under investigation and optimize the growth conditions.

## 2.2. Solution Growth

The sequence of growing a single crystal begins with the nucleation step that, in flux growth, often takes place in a heterogeneous fashion on the crucible wall or the surface of the melt.<sup>[35–37]</sup> This nucleus must reach a critical size for it to grow rather than be re-absorbed into the melt. The critical size is a function of the degree of supersaturation, where greater supersaturation allows for smaller critical nuclei. This situation is the reason why it is an important requirement of a good flux to be able to dissolve a large amount of the reagents and to have a significant change in solubility with temperature to achieve this supersaturation. The rate of this nucleation process is a function of temperature and below some critical

temperature nucleation will cease altogether. At the same time, there is an optimum temperature range where the nucleation rate is at its maximum and, in fact, the width of this metastable temperature regime, which may span more than  $50^\circ\text{C}$  can be increased by appropriate additives to the flux. The nucleation rate is further influenced by many factors, including the absence or presence of impurities, such as dust particulates in the melt, and the roughness of the crucible surface. Once the crystal has exceeded the critical size it can begin to grow. It is important to realize that the complete process of crystal growth consists of these two separate, sequential, processes—nucleation and growth. The rate of growth is also a function of the degree of supersaturation and typically is simply proportional to supersaturation. Although it might be concluded that the greater the degree of supersaturation the better the process will work, this would not be correct. Too high a degree of supersaturation (system specific) will lead to dendritic growth, rather than nicely faceted crystals, because the growth rate is too fast. On the other hand, too low a degree of supersaturation, typically less than 10% supersaturation, will prevent nucleation altogether. Hence, there is an optimum degree of supersaturation that must be identified for each flux/reagent system to obtain a good yield of high-quality crystals. Still, in the absence of a nucleation step, no crystal growth can occur, and even when nucleation occurs, a critical size must be achieved to lead to growth.

There are many factors that can interfere with the growth of nicely faceted crystals. For example, if the degree of supersaturation is not constant throughout the melt, the concentration gradient can lead to increasingly unstable growth, which typically manifests itself in the shape of the crystals. Thus, it is possible to go rapidly from flat faces to flux inclusions in the crystal, to hopper growth, to dendritic growth. Conversely, too low a degree of supersaturation can lead to hillock growth, which makes crystals less suitable for crystallographic studies.<sup>[1]</sup> Crystal growth from fluxes is generally believed to occur by a BCF (Burton–Cabrera–Frank) type screw-dislocation process,<sup>[38]</sup> although other mechanisms have been proposed. In this process, continuous crystal growth is maintained by the addition of adatoms at dislocations that are coupled to a screw component, generating a spiral growth pattern. In a solution environment, such as a flux, the growth rate is governed by the rate of ions diffusing to kinks in the steps of the spiral. However, since each crystal has its own unique growth history based on the specific flux used, the nature of the dissolved reagents, and the experimental parameters (temperature, concentration, impurities), no strict generalization on the growth mechanism and the rate-determining step can be made.

In some cases a stirred flux can lead to increased growth rates and greater overall uniformity in supersaturation, resulting in higher quality crystals. As diffusion of reagents to the crystal faces typically limits the growth rates, stirring can increase the delivery rate of reagents (beyond what is created by natural convection) and thus increase the crystal growth rate. However, the volume change in going from a crystal with a 0.1 mm edge to one with a 1 mm edge is a factor of 1000. Hence, while most small-scale flux growth experi-

ments yield sub-mm sized crystals, it is possible to increase the crystal size by stirring and, to achieve large crystals (several mm), by utilizing a scaled-up crystal growth system.

The ideal outcome of a crystal growth experiment is a few large crystals, rather than many small crystals. This result clearly is closely tied to the relative rates of nucleation and growth. Achieving growth conditions where there are only a limited number of nucleated crystals that grow, requires excellent temperature control. This control is, on the one hand, not so difficult anymore as programmable controllers can easily achieve cooling rates of 1 °C per hour or less; on the other hand, a high-quality furnace is necessary if this is actually to be achieved in practice. It is important to keep in mind that cooling more slowly than what the furnace can keep stable is counterproductive and a waste of time. For practical crystal growth, to achieve supersaturation in fluxes, a cooling rate between 0.5 to 10 °C per hour is a good starting point. Assuming that at the starting temperature sufficient reagents have dissolved to achieve supersaturation during cooling, the crystal morphology—dendritic versus faceted—can suggest modifications to the reaction conditions that will lead to high-quality crystals. As the width of the metastable regime is system dependent and can be as small as 25 °C, a reasonable approach during the exploratory phase is to change the maximum flux growth temperature in steps of 25–50 °C to identify the optimum temperature range for crystal growth.

### 2.3. Crystal Habit

The crystal habit, or shape, is influenced not only by the underlying crystal structure, for example cubic structures often form in a cubic crystal habit, but also by kinetic factors that are solution controlled. Specifically, the rate at which different faces of a crystal grow will lead to the formation of different crystal habits. Thus, a cubic crystal can grow as a cube or as an octahedron (Figure 2). In the cube case, the [100] face (and equivalent) is the fastest growing, whereas for the octahedron the [111] face (and equivalent) is the fastest growing. Intermediate growth rates will lead to truncated structures, such as a cubeoctahedron. The growth rates of different faces are influenced primarily by the degree of

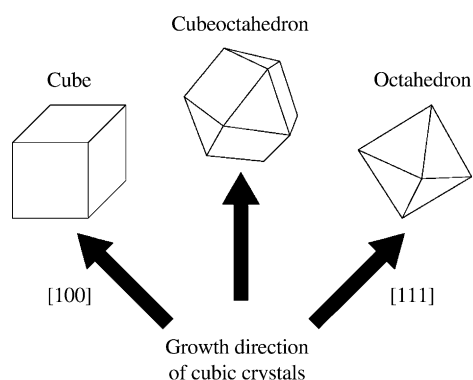


**Figure 2.** The crystal habits of cubic crystals experiencing a maximum growth rate along [100], [111], or an intermediate direction between the two.

supersaturation, but can also be altered by the presence of very small quantities of solution impurities and temperature (cooling rate).

### 2.4. Doping During Crystal Growth

There are numerous applications for which it is desirable to be able to vary the composition of a crystal, either by doping or by creating a solid solution, to control the electronic or optical properties. In cases where isostructural series exist, for example a family of rare-earth-containing oxides, it is feasible to grow crystals with controlled mixed rare-earth-element content. By having both rare-earth elements present in the flux during crystal growth, the final product will have a composition that will depend on the distribution coefficient,  $K'$ , defined as [Eq. (1), Ln = rare-earth element]

$$K' = \frac{\left[ \frac{\text{moles Ln1}}{\text{moles (Ln1+Ln2)}} \right] \text{ in crystal}}{\left[ \frac{\text{moles Ln1}}{\text{moles (Ln1+Ln2)}} \right] \text{ in flux}} \quad (1)$$

Thus, for a distribution coefficient greater than one, the fractional concentration of Ln1 will be greater in the crystal than in the melt. For rare-earths, the closer in size the rare-earth elements are, the closer the distribution coefficient will be to one. For doping or creating solid solutions using other elements, both the size and the chemical similarities will affect the distribution coefficient. This type of crystal growth process allows for the preparation of single crystals of, for example, an  $\text{Eu}^{3+}$ -doped  $\text{La}^{3+}$ -containing oxide material to achieve the desired luminescent properties.<sup>[39]</sup>

### 2.5. Practical Considerations for Crystal Growth Experiments

In addition to deciding what flux to use, the experimenter must decide on how much and which reagents to add to the flux and the initial temperature. A rule of thumb when setting up a flux growth experiment is to start with a 10:1 ratio of flux to reagents and to adjust this ratio up or down as needed as indicated by the crystal morphology. As reagents, the simple binary oxides, nitrates, carbonates, etc., or a pre-synthesized product containing all the elements of interest can be used. Using a pre-synthesized product is most advantageous if the intention is to crystallize a specific phase. In such cases starting with a polycrystalline powder of the correct composition has some advantages over simple binary starting materials. Specifically, the complex oxide, when it dissolves in the flux, will release its constituent elements into the melt in the appropriate ratio and at the same time. Hence, this tends to avoid one known difficulty with simple binaries, namely that they may dissolve at substantially different rates. The kinetics of the dissolution affects the concentrations of reagents in the melt and may drive the melt into a different supersaturated regime from which nucleation takes place. It is of course possible to compensate by increasing the amount of the species that dissolves most slowly. Finally, a temperature and cooling rate has to be chosen. Cooling rates varying

between 1 and 60 °C per hour are typical, where 1 °C per hour is very slow and 60 °C per hour is quite fast. A good trial rate lies between 5–10 °C per hour. To have a reasonable amount of time for crystals to nucleate and grow, the starting temperature should probably lie at least 100 °C above the melting point of the flux, where a “soak” of 12–24 h is typically used to enable reagents to dissolve and to approach saturation. Upon cooling the melt may become supersaturated and favor crystal nucleation and growth. A closed reaction vessel is recommended if at the starting temperature the melt has an appreciable vapor pressure, unless flux evaporation is intentionally chosen as the method for creating supersaturation, crystal nucleation and growth.

Removal of the flux is typically necessary to isolate the crystals and can be achieved by dissolving the flux in a suitable solvent. This process can be straightforward when the flux is, for example, water-soluble and the crystals are not water sensitive. In other cases, however, the dissolution of the flux requires the use of mineral acids, which may also attack the crystals. To minimize the exposure time of the crystals to the mineral acids it is often advisable to decant the flux prior to crystal isolation. To decant the flux, the crucible is cautiously removed from the hot furnace with tongs and the still-liquid flux is carefully decanted. The crucible is then returned to the hot furnace and slow cooled to room temperature to minimize thermal stresses on the crystals. An alternative approach is to puncture the crucible while it is

sitting in the furnace to allow the flux to run out. This approach typically works only if a metal crucible is used. Of course, the crucible must be repaired after the procedure and the furnace cleaned of the flux. Finally, a method commonly used by researchers growing intermetallic crystals, but one that can be adapted to oxides, is to perform the crystal growth in a sealed tube where some quartz wool has been placed above the flux to act as a filter. Upon completion of the crystal growth process, the tube is inverted, placed into a centrifuge and the still-liquid flux is spun through the quartz wool, leaving the crystals behind. Again, returning the tube to the furnace and slow cooling to room temperature is advisable.

### 3. Solvent Systems

There is no limit to the solvent systems that have been used by researchers and we will not discuss all of them herein. Nonetheless, some systems are more prevalent in the literature than others, typically because they are very effective for crystal growth (Figure 3). Of course, since the solvent needs to be matched to the product, many different solvent types with many different intrinsic properties have been used and a representative list of “common” fluxes is included. For each flux we attempt to address solubility behavior, melting and boiling point, and suitable crucibles (Figure 4) that can be used. This is not meant to be a complete

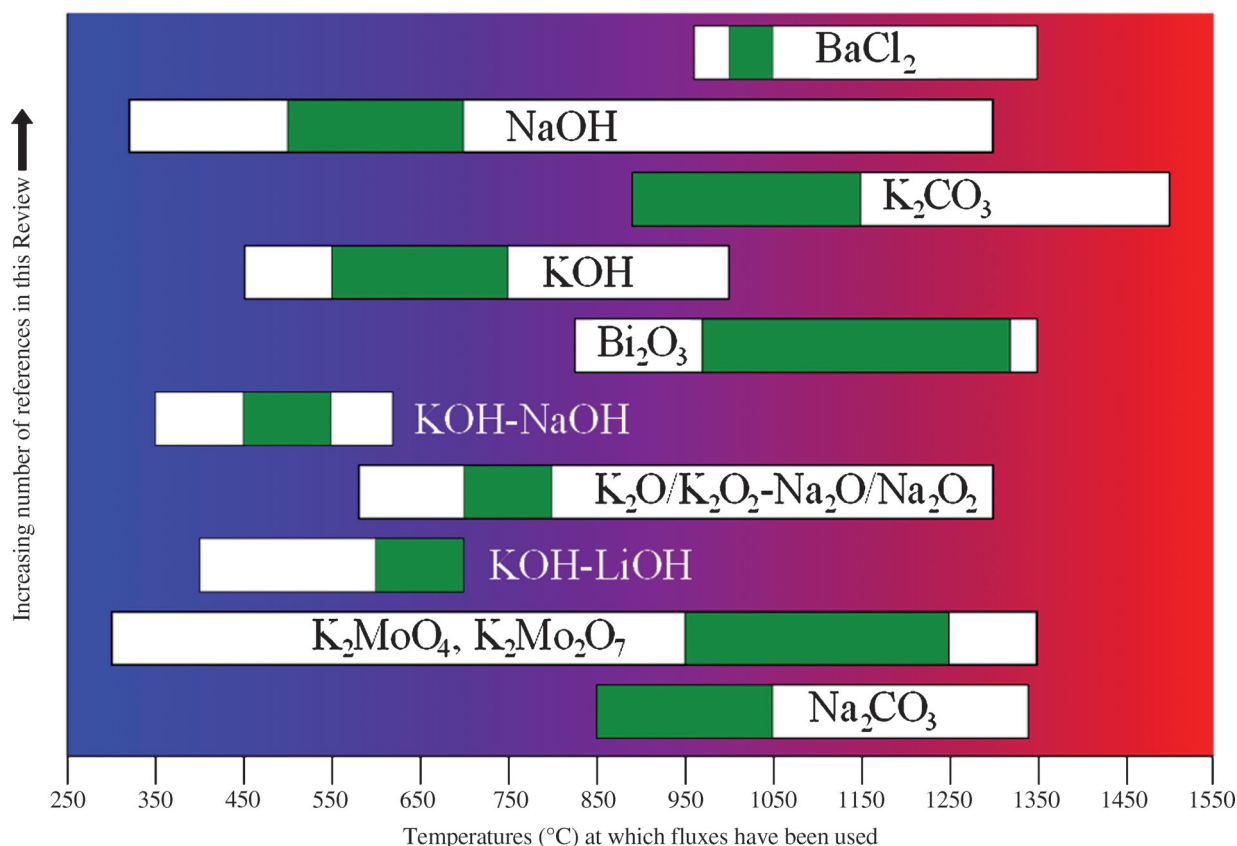


**Figure 3.** The ten flux systems most commonly cited in this Review, as well as the range of reported temperatures for their use. The optimal temperature ranges are denoted in green.

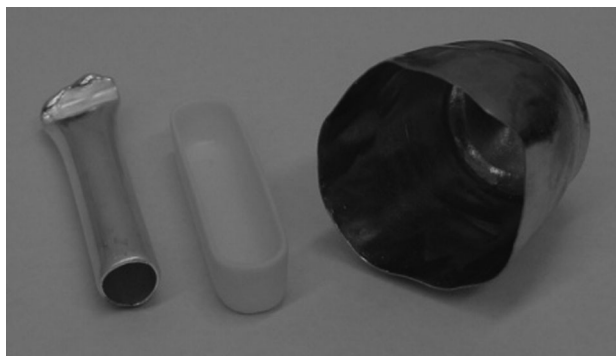


**Figure 4.** Typical reaction vessels used in the flux growth of single crystals of complex oxides (left-to-right): a silver tube, an alumina boat, and a platinum crucible.

list of fluxes and many fluxes not listed have been used with good success for the preparation of specific types of crystal compositions. We have included examples of crystals of complex oxides grown out of each flux or family of fluxes, along with descriptions of the growth conditions that were used. Our intent was to give a flavor of the compositions and structure types that can be grown using each flux rather than be exhaustive in the discussion. For that purpose, an extensive list of over 400 compositions can be found in Table 1 along with crystal growth information, such as the flux used, temperature range, and cooling rate, as well as the citation to the original paper. Additional tables are available in the Supporting Information: Table S1 lists the complex oxides in alphabetical order according to composition, and Table S2 lists the complex oxides according to their elemental groupings (titanates, niobates, rare-earth-containing oxides, etc.).

### 3.1. Lead Oxide and/or Lead Fluoride

Probably one of the oldest and most versatile fluxes is lead oxide because of its superior ability to dissolve oxides and its conveniently low melting point (888 °C). It is quite toxic, however, and exhibits significant volatility because of its low boiling point (1477 °C), which must be taken into consideration. For these reasons, it has fallen somewhat into disuse. It is a frequent additive to other melts to form binary or ternary fluxes with even lower melting points. It is surmised that because of its high polarizability and ionic nature it is capable of dissolving even some of the most refractory oxides. For that reason, PbO is typically used in platinum crucibles that, however, are attacked by the PbO under reducing conditions. Hence, an oxidizing atmosphere (air) is recommended. The divalent lead cation is quite large and is known to substitute (form solid solutions) for other large divalent cations, such as  $\text{Sr}^{2+}$  and  $\text{Ba}^{2+}$ , a consideration when trying to grow compositions that include the heavier alkaline-earth-metal cations.

Lead fluoride is a “variant” of PbO and also a very effective flux for dissolving oxides. Often the two are combined to form a  $\text{PbO-PbF}_2$  (1:1.17) eutectic that melts around 500 °C. By itself,  $\text{PbF}_2$  has a relatively low melting point (824 °C), but significant volatility owing to a low boiling

point (1293 °C). In fact, often the high vapor pressure is taken advantage of for crystal growth by evaporating some of the flux, thereby increasing the supersaturation of the solutes and inducing nucleation and crystal growth. The added benefit of lead fluoride is the presence of the fluoride anions that can have a mineralizing effect, which enhances the dissolution of the reagents and can influence the nature of the metal complex found in solution. It is rarely used by itself and often other metal oxides are added to control the volatility. Just like PbO, it is usually used in platinum crucibles and to prevent reaction with the platinum,  $\text{PbF}_2$  should only be used under oxidizing conditions. Furthermore, because of the presence of the  $\text{F}^-$  ion, it cannot be used with alumina crucibles at high temperatures.

PbO and/or  $\text{PbF}_2$  fluxes have been used to obtain single crystals of a wide variety of oxide compositions that often, but not always, contain lead as one component. Other than alkali-metal cations, all other types of cations appear to be soluble in PbO and/or  $\text{PbF}_2$  fluxes. The typical crystal growth experiment is carried out between 800 °C and 1000 °C and involves either slow cooling or flux evaporation to achieve supersaturation and hence crystal growth. While some crystal growth experiments used ratios of flux to reagent as high as 30:1, others required only a small excess of flux to maintain a melt in which the crystals could grow. More typical, however, is a 5–10-fold excess of flux to reagent. Solidified PbO and/or  $\text{PbF}_2$  melts can be dissolved in hot acids, such as nitric or acetic.

A series of complex aluminum–lead containing oxides,  $\text{Sr}_{1.33}\text{Pb}_{0.67}\text{Al}_6\text{O}_{11}$ ,<sup>[40]</sup>  $\text{BaPb}_{1.5}\text{Mn}_6\text{Al}_2\text{O}_{16}$ ,<sup>[41]</sup> and  $\text{Pb}_3\text{MnAl}_{10}\text{O}_{20}$  (Figure 5),<sup>[42]</sup> were obtained by Müller-Buschbaum’s group using only a slight excess of PbO to lower the melting point of the mixture and to maintain a molten state at the growth temperature of about 800 °C. Using cooling rates of 6–7 °C per hour, small crystals were grown. A different approach to isolating the formed crystals was used by Müller-Buschbaum in the preparation of  $\text{Pb}_2\text{HoAl}_3\text{O}_8$  and  $\text{Pb}_2\text{LuAl}_3\text{O}_8$ ,<sup>[43]</sup> where the PbO– $\text{PbF}_2$  flux was allowed to sublime away at 850 °C over the course of 7 days. Alternatively, Reinen’s group dissolved the  $\text{PbF}_2$  flux used to grow  $\text{CuGaInO}_4$ <sup>[44]</sup> in dilute, warm nitric acid. A stoichiometric reactive oxide precursor was dissolved in  $\text{PbF}_2$  in a platinum boat at 1000 °C and crystals formed during slow cooling to 800 °C. The ditrigonal shaped platelets were readily isolated once some of the flux was removed by the nitric acid treatment. Crystals of the  $\text{BaPb}_{0.85}\text{Bi}_{0.15}\text{O}_3$ <sup>[45]</sup> superconductor were grown by Jansen’s group using PbO as a flux. The melt was heated in a platinum boat to 1000 °C for 3 days, subsequent slow cooling at a rate of 5 °C per hour to 800 °C, and then at 50 °C per hour to room temperature. To isolate the crystals the solidified flux was immersed in dilute NaOH solution and ultrasonicated. This procedure loosened the charge so that crystals could be harvested.

$(\text{Nd}_4\text{Ca}_2)\text{Ti}_6\text{O}_{20}$ <sup>[46]</sup> was obtained by slow cooling from 1280 °C to 850 °C using a PbO flux contained in a platinum crucible. Either the binary oxides or polycrystalline  $(\text{Nd}_4\text{Ca}_2)\text{Ti}_6\text{O}_{20}$  could be used as the starting material, with the wt % of PbO flux increased from 87 % to 92 % for the binary oxides. Crystals up to  $10 \times 1 \times 1 \text{ mm}^3$  were obtained,



**Table 1:** Crystal growth information for quaternary (and higher order) complex oxides. Compositions are sorted first by the family of flux used for crystal growth (with reference to the corresponding Section in the Review), and then alphabetically by elemental composition.<sup>[a]</sup>

Composition	Flux	Temperature range [°C]	Cooling rate [°C/h]	Reference
<b>Lead Oxide and/or Lead Fluoride (3.1)</b>				
Al <sub>2</sub> BaMn <sub>6</sub> Pb <sub>1.5</sub> O <sub>16</sub>	PbO	850–200	100	[41]
Al <sub>3</sub> HoPb <sub>2</sub> O <sub>8</sub>	PbF <sub>2</sub> -PbO	850	–	[43]
Al <sub>10</sub> MnPb <sub>3</sub> O <sub>20</sub>	PbO	900–200	100	[42]
Al <sup>3</sup> LuPb <sub>2</sub> O <sub>8</sub>	PbF <sub>2</sub> -PbO	850	–	[43]
Al <sub>6</sub> Pb <sub>0.67</sub> Sr <sub>1.33</sub> O <sub>11</sub>	PbO	950–800	6.25	[40]
BaBi <sub>0.15</sub> Pb <sub>0.85</sub> O <sub>3</sub>	PbO	1000–800	5	[45]
Ca <sub>2</sub> Nd <sub>4</sub> Ti <sub>6</sub> O <sub>20</sub>	PbO	1280–850	2.3	[46]
CoPb <sub>2</sub> WO <sub>6</sub>	PbO	1130–830	0.3	[47]
CuGaInO <sub>4</sub>	PbF <sub>2</sub>	1000–800	10	[44]
MnNd <sub>0.75</sub> Pb <sub>0.25</sub> O <sub>3</sub>	PbF <sub>2</sub> -PbO	–	–	[49]
PbPt <sub>4</sub> Sr <sub>4</sub> O <sub>11</sub>	PbO	930–850	1	[48]
<b>Bismuth Oxide (3.2)</b>				
Al <sub>12</sub> Cr <sub>2</sub> Sr <sub>8</sub> O <sub>32</sub>	Bi <sub>2</sub> O <sub>3</sub>	–	–	[140]
Al <sub>0.6</sub> Fe <sub>2.4</sub> LaSr <sub>3</sub> O <sub>8.95</sub>	Bi <sub>2</sub> O <sub>3</sub>	1130	–	[59]
Ba <sub>2</sub> BiGa <sub>11</sub> O <sub>20</sub>	Bi <sub>2</sub> O <sub>3</sub>	1350–500	50	[141]
BaBi <sub>0.5</sub> Sb <sub>0.5</sub> O <sub>3</sub>	Bi <sub>2</sub> O <sub>3</sub>	1200–800	5	[55]
BaBi <sub>4</sub> Ti <sub>4</sub> O <sub>15</sub>	Bi <sub>2</sub> O <sub>3</sub>	1150–500	3	[142]
BaCo <sub>0.85</sub> Fe <sub>10.3</sub> Ir <sub>0.85</sub> O <sub>19</sub>	Bi <sub>2</sub> O <sub>3</sub>	1250–1000	2	[57]
BaFe <sub>11</sub> Ir <sub>0.5</sub> Zn <sub>0.5</sub> O <sub>19</sub>	Bi <sub>2</sub> O <sub>3</sub>	1250–1000	2	[57]
Bi <sub>0.6</sub> Ca <sub>0.4</sub> MnO <sub>3</sub>	Bi <sub>2</sub> O <sub>3</sub>	1094–25	4	[51]
Bi <sub>1.64</sub> Ca <sub>2</sub> Co <sub>1.69</sub> O <sub>7.38</sub>	Bi <sub>2</sub> O <sub>3</sub>	1050–700	2	[143]
Bi <sub>4</sub> CaTi <sub>4</sub> O <sub>15</sub>	Bi <sub>2</sub> O <sub>3</sub>	1150–500	3	[142]
Bi <sub>2</sub> Fe <sub>2</sub> Ga <sub>2</sub> O <sub>9</sub>	Bi <sub>2</sub> O <sub>3</sub>	950–700	5	[53]
Bi <sub>2</sub> Fe <sub>2</sub> Mn <sub>2</sub> O <sub>10</sub>	Bi <sub>2</sub> O <sub>3</sub>	1000–700	5	[52]
BiMg <sub>2</sub> VO <sub>6</sub>	Bi <sub>2</sub> O <sub>3</sub>	1000–500	15	[54]
Bi <sub>3.04</sub> Mo <sub>2</sub> Sc <sub>0.96</sub> O <sub>12</sub>	Bi <sub>2</sub> O <sub>3</sub>	1150–900	1.5	[50]
Bi <sub>7</sub> NbTi <sub>4</sub> O <sub>21</sub>	Bi <sub>2</sub> O <sub>3</sub>	1200–700	5	[56]
CuFeSrY <sub>2</sub> O <sub>6.5</sub>	Bi <sub>2</sub> O <sub>3</sub>	1110–1020	–	[144]
CuGe <sub>4</sub> Yb <sub>2</sub> O <sub>12</sub>	Bi <sub>2</sub> O <sub>3</sub>	1250–1055	4	[58]
<b>Boron Oxide or Alkali/Alkaline-Earth-Metal Borates (3.3)</b>				
Al <sub>2</sub> Ga <sub>3</sub> La <sub>3</sub> SnO <sub>14</sub>	LiBO <sub>2</sub>	1475–1350	10	[61]
Ba <sub>4</sub> Ce <sub>0.98</sub> Nb <sub>10</sub> O <sub>30</sub>	B <sub>2</sub> O <sub>3</sub> -BaO	1050–850	6	[63]
BaCo <sub>1.28</sub> Fe <sub>9.44</sub> Sn <sub>1.28</sub> O <sub>19</sub>	B <sub>2</sub> O <sub>3</sub> -BaO	1300–1150	0.8	[145]
BaCo <sub>1.32</sub> Fe <sub>1.44</sub> Sn <sub>3.32</sub> O <sub>11</sub>	B <sub>2</sub> O <sub>3</sub> -BaO	1300–1000	0.8	[145]
Ba <sub>2</sub> CoFe <sub>10</sub> Sn <sub>2</sub> O <sub>22</sub>	B <sub>2</sub> O <sub>3</sub> -BaO	1260–1000	3	[146]
BaFe <sub>6.3</sub> Mn <sub>4.3</sub> Ti <sub>1.4</sub> O <sub>19</sub>	BaB <sub>2</sub> O <sub>4</sub>	1300–1000	1.2	[64]
Ba <sub>12</sub> Fe <sub>28</sub> Ti <sub>15</sub> O <sub>84</sub>	KBO <sub>2</sub>	1300–1050	3	[66]
Ba <sub>0.16</sub> Na <sub>0.84</sub> Nb <sub>0.84</sub> Ti <sub>0.16</sub> O <sub>3</sub>	Na <sub>2</sub> B <sub>4</sub> O <sub>7</sub>	1100–1000	10	[67]
Ba <sub>2</sub> Nb <sub>4</sub> Ti <sub>5</sub> O <sub>18</sub>	B <sub>2</sub> O <sub>3</sub>	1250	–	[147]
Ba <sub>2</sub> V <sub>2</sub> ZnO <sub>8</sub>	B <sub>2</sub> O <sub>3</sub>	880–760	3	[148]
BiK <sub>9</sub> U <sub>6</sub> O <sub>24</sub>	B <sub>2</sub> O <sub>3</sub> -K <sub>2</sub> CO <sub>3</sub>	1200	–	[65]
CoFe <sub>16</sub> SrZnO <sub>27</sub>	B <sub>2</sub> O <sub>3</sub> -SrO	1340–950	2.5	[149]
CrLiSrTi <sub>4</sub> O <sub>11</sub>	LiBO <sub>2</sub>	–	–	[60]
FeLiSrTi <sub>4</sub> O <sub>11</sub>	LiBO <sub>2</sub>	–	–	[60]
Ga <sub>5</sub> La <sub>3</sub> SnO <sub>14</sub>	LiBO <sub>2</sub>	1427–1200	20	[61]
K <sub>2</sub> Nb <sub>5</sub> NdO <sub>15</sub>	B <sub>2</sub> O <sub>3</sub> -K <sub>2</sub> O	1250–800	1.2	[150]
KNb <sub>1.76</sub> Sb <sub>3.24</sub> O <sub>13</sub>	H <sub>3</sub> BO <sub>3</sub>	1000–500	6	[151]
Nb <sub>4</sub> Sr <sub>5</sub> TiO <sub>17</sub>	SrB <sub>4</sub> O <sub>7</sub>	1150–930	2	[152]
Nb <sub>4</sub> Sr <sub>6</sub> TiO <sub>18</sub>	SrB <sub>4</sub> O <sub>7</sub>	1400–1130	3	[62]
<b>Alkali and/or Alkaline-Earth-Metal Halides (3.4)</b>				
Al <sub>2</sub> Ba <sub>5.5</sub> Ca <sub>0.5</sub> Rh <sub>2</sub> Y <sub>2</sub> O <sub>15</sub>	BaCl <sub>2</sub>	1050	–	[153]
Al <sub>1.5</sub> Ba <sub>6</sub> Co <sub>2.5</sub> Sm <sub>2</sub> O <sub>15</sub>	BaCl <sub>2</sub>	1000	–	[154]
Al <sub>4</sub> Ba <sub>6</sub> Dy <sub>2</sub> O <sub>15</sub>	BaCl <sub>2</sub>	1030	–	[155]
Al <sub>2</sub> Ba <sub>6</sub> Ho <sub>2</sub> Rh <sub>2</sub> O <sub>15</sub>	BaCl <sub>2</sub>	1040–25	10	[68]
AlBa <sub>4</sub> Ir <sub>2</sub> O <sub>10</sub>	BaCl <sub>2</sub>	1000	–	[156]
AlBa <sub>2</sub> InO <sub>5</sub>	BaCl <sub>2</sub>	1050	–	[157]
AlBa <sub>5</sub> Ir <sub>2</sub> O <sub>11</sub>	BaCl <sub>2</sub>	1000	–	[158]
Al <sub>2</sub> Ba <sub>6</sub> Rh <sub>4</sub> O <sub>15</sub>	BaCl <sub>2</sub>	1050	–	[153]
Al <sub>1.67</sub> Ba <sub>6</sub> Rh <sub>2.33</sub> Yb <sub>2</sub> O <sub>15</sub>	BaCl <sub>2</sub>	1050	–	[153]
Al <sub>2</sub> Na <sub>3</sub> Nb <sub>34</sub> O <sub>64</sub>	NaF	850	–	[77]

Table 1: (Continued)

Composition	Flux	Temperature range [°C]	Cooling rate [°C/h]	Reference
Al <sub>2</sub> Nb <sub>35</sub> Rb <sub>4</sub> O <sub>70</sub>	RbCl	1050–700	9.72	[76]
Ba <sub>2</sub> CaPd <sub>3</sub> O <sub>6</sub>	BaCl <sub>2</sub>	1050	–	[159]
Ba <sub>3</sub> CaRu <sub>2</sub> O <sub>9</sub>	BaCl <sub>2</sub>	1025	–	[69]
Ba <sub>3</sub> Ca <sub>0.8</sub> Ru <sub>2</sub> Sr <sub>0.2</sub> O <sub>9</sub>	BaCl <sub>2</sub>	1040	–	[160]
BaCo <sub>1.85</sub> Ru <sub>4.15</sub> O <sub>11</sub>	BaCl <sub>2</sub>	1350–25	–	[161]
Ba <sub>2</sub> EuIrO <sub>6</sub>	BaCl <sub>2</sub>	1000	–	[162]
BaFe <sub>3.39</sub> Ru <sub>2.61</sub> O <sub>11</sub>	BaCl <sub>2</sub>	1350–25	–	[161]
BaGd <sub>2</sub> PtO <sub>5</sub>	BaCl <sub>2</sub>	1000	–	[7]
Ba <sub>9</sub> Ir <sub>3.2</sub> Mn <sub>5.8</sub> O <sub>27</sub>	BaCl <sub>2</sub>	1000	–	[163]
Ba <sub>12</sub> Ir <sub>9.6</sub> Nb <sub>2.4</sub> O <sub>36</sub>	BaCl <sub>2</sub>	1100	–	[164]
Ba <sub>2</sub> La <sub>4</sub> Ti <sub>5</sub> O <sub>18</sub>	BaCl <sub>2</sub>	1200–25	–	[165]
BaMg <sub>6</sub> Ti <sub>6</sub> O <sub>19</sub>	BaF <sub>2</sub>	1450–1200	8	[166]
BaPdPr <sub>2</sub> O <sub>5</sub>	BaCl <sub>2</sub>	800	–	[7]
BaPdTb <sub>2</sub> O <sub>5</sub>	BaCl <sub>2</sub>	800	–	[7]
BaPtSm <sub>2</sub> O <sub>5</sub>	BaCl <sub>2</sub>	1000	–	[7]
Ba <sub>3</sub> Ru <sub>0.6</sub> SrTa <sub>1.4</sub> O <sub>9</sub>	BaCl <sub>2</sub>	1025	–	[167]
Ba <sub>3</sub> Ru <sub>1.2</sub> SrTa <sub>0.8</sub> O <sub>9</sub>	BaCl <sub>2</sub>	1025	–	[167]
BiNdSr <sub>2</sub> O <sub>6</sub>	KCl–SrCl <sub>2</sub>	900	–	[168]
Ca <sub>3</sub> CuIrO <sub>6</sub>	CaF <sub>2</sub> –KF	1020–25	20	[70]
Ca <sub>3.34</sub> IrMg <sub>0.66</sub> O <sub>6</sub>	CaCl <sub>2</sub> –KCl–NaCl	925–600	15	[169]
Ca <sub>3.75</sub> IrNi <sub>0.25</sub> O <sub>6</sub>	CaCl <sub>2</sub> –KCl–NaCl	900	12	[170]
Ca <sub>3.50</sub> IrZn <sub>0.50</sub> O <sub>6</sub>	CaCl <sub>2</sub> –KCl–NaCl	925–600	15	[169]
Co <sub>1.29</sub> Li <sub>0.65</sub> Mn <sub>1.06</sub> O <sub>4</sub>	LiCl	750–25	50	[75]
Co <sub>1.89</sub> Ru <sub>4.11</sub> SrO <sub>11</sub>	SrCl <sub>2</sub>	1350–25	–	[171]
Cr <sub>0.5</sub> LiMn <sub>1.5</sub> O <sub>4</sub>	LiCl	750–25	50	[75]
CsLuW <sub>2</sub> O <sub>8</sub>	CsCl	1100–25	6	[172]
Cu <sub>3</sub> Ge <sub>5</sub> K <sub>2</sub> O <sub>14</sub>	KCl	900–850	1	[173]
Cu <sub>3</sub> NaRu <sub>4</sub> O <sub>12</sub>	NaCl	820	–	[174]
Fe <sub>2.54</sub> Ru <sub>3.46</sub> SrO <sub>11</sub>	SrCl <sub>2</sub>	1350–25	–	[171]
Fe <sub>3.04</sub> Ru <sub>2.96</sub> SrO <sub>11</sub>	SrCl <sub>2</sub>	1350–25	–	[171]
Fe <sub>3.47</sub> Ru <sub>2.53</sub> SrO <sub>11</sub>	SrCl <sub>2</sub>	1350–25	–	[171]
K <sub>8</sub> Na <sub>4</sub> Sb <sub>12</sub> O <sub>36</sub>	KF–NaF	1100–25	3	[175]
K <sub>6</sub> U <sub>5</sub> V <sub>2</sub> O <sub>23</sub>	KCl	775	–	[72]
LaRu <sub>1.2</sub> Sr <sub>2.4</sub> O <sub>7</sub>	BaCl <sub>2</sub>	1250–900	10	[176]
Li <sub>0.92</sub> Mn <sub>1.62</sub> Ni <sub>0.46</sub> O <sub>4</sub>	LiCl	700–25	50	[75]
Li <sub>3</sub> Mo <sub>3</sub> ScO <sub>12</sub>	LiF	1150–900	1.5	[73]
NaNb <sub>7.5</sub> V <sub>1.5</sub> O <sub>14</sub>	NaF	900	–	[177]
Na <sub>7</sub> Nb <sub>15</sub> W <sub>13</sub> O <sub>80</sub>	NaCl	1170	1	[74]
Na <sub>0.75</sub> Nd <sub>0.75</sub> Re <sub>3</sub> O <sub>12</sub>	NaCl	830–30	5	[178]
NiPbSr <sub>3</sub> O <sub>6</sub>	NaCl	1000–750	50	[71]
Rb <sub>6</sub> U <sub>5</sub> V <sub>2</sub> O <sub>23</sub>	RbI	650–25	5	[179]
<b>Alkali-Metal Carbonates (3.5)</b>				
Ba <sub>8</sub> CoRh <sub>6</sub> O <sub>21</sub>	K <sub>2</sub> CO <sub>3</sub>	1050–875	12	[82]
Ba <sub>1.2708</sub> Cu <sub>0.2708</sub> Ir <sub>0.7292</sub> O <sub>3</sub>	K <sub>2</sub> CO <sub>3</sub>	1150–880	6	[180]
Ba <sub>1.18</sub> Cu <sub>0.29</sub> Rh <sub>0.71</sub> O <sub>3</sub>	K <sub>2</sub> CO <sub>3</sub>	1150–880	6	[181]
BaFe <sub>16</sub> Zn <sub>27</sub> O <sub>27</sub>	Na <sub>2</sub> CO <sub>3</sub>	1340–1050	4	[90]
Ba <sub>1.06</sub> Ir <sub>0.56</sub> Ni <sub>0.44</sub> O <sub>3</sub>	K <sub>2</sub> CO <sub>3</sub>	1050–880	6	[181]
Ba <sub>12</sub> Ir <sub>1.75</sub> Rh <sub>9.25</sub> O <sub>33</sub>	K <sub>2</sub> CO <sub>3</sub>	1150–800	15	[182]
Ba <sub>2</sub> Li <sub>0.67</sub> Ti <sub>5.33</sub> O <sub>13</sub>	Li <sub>2</sub> CO <sub>3</sub>	1250–25	5	[183]
Ba <sub>1.16</sub> Ni <sub>0.23</sub> Rh <sub>0.77</sub> O <sub>3</sub>	K <sub>2</sub> CO <sub>3</sub>	1150–880	6	[181]
BiCa <sub>2</sub> Na <sub>3</sub> O <sub>6</sub>	Na <sub>2</sub> CO <sub>3</sub>	1050–800	15	[184]
Ca <sub>3</sub> Co <sub>1.34</sub> Rh <sub>0.66</sub> O <sub>6</sub>	K <sub>2</sub> CO <sub>3</sub>	1050–850	15	[80]
Ca <sub>3</sub> CuRhO <sub>6</sub>	K <sub>2</sub> CO <sub>3</sub>	1050–850	15	[80]
Ca <sub>3</sub> FeRhO <sub>6</sub>	K <sub>2</sub> CO <sub>3</sub>	1050–850	15	[80]
Ca <sub>3</sub> IrNaO <sub>6</sub>	Na <sub>2</sub> CO <sub>3</sub>	925	–	[185]
Ca <sub>3</sub> LiRuO <sub>6</sub>	K <sub>2</sub> CO <sub>3</sub> –Li <sub>2</sub> CO <sub>3</sub>	1025–750	6	[83]
Ca <sub>3</sub> NaRuO <sub>6</sub>	Na <sub>2</sub> CO <sub>3</sub>	925	–	[185]
Ca <sub>2</sub> Na <sub>3</sub> TaO <sub>6</sub>	Na <sub>2</sub> CO <sub>3</sub>	1000–800	3	[85]
Ca <sub>3</sub> Na <sub>2</sub> Ta <sub>2</sub> O <sub>9</sub>	Na <sub>2</sub> CO <sub>3</sub>	1000–800	3	[86]
CsNbUO <sub>6</sub>	Cs <sub>2</sub> CO <sub>3</sub>	1200	–	[186]
Cu <sub>0.91</sub> Mn <sub>2.09</sub> Sr <sub>4</sub> O <sub>9</sub>	K <sub>2</sub> CO <sub>3</sub>	927–607	6	[92]
CuPtSr <sub>3</sub> O <sub>6</sub>	K <sub>2</sub> CO <sub>3</sub>	1050–880	15	[78]

Table 1: (Continued)

Composition	Flux	Temperature range [°C]	Cooling rate [°C/h]	Reference
Cu <sub>0.38</sub> Rh <sub>0.62</sub> Sr <sub>1.10</sub> O <sub>3</sub>	K <sub>2</sub> CO <sub>3</sub>	1150–880	6	[181]
FeLi <sub>1.746</sub> Nd <sub>4.494</sub> O <sub>9.493</sub>	Li <sub>2</sub> CO <sub>3</sub>	760	–	[93]
Fe <sub>0.71</sub> Rh <sub>0.29</sub> SrO <sub>3</sub>	K <sub>2</sub> CO <sub>3</sub>	1050–800	15	[81]
Fe <sub>0.73</sub> Rh <sub>2.27</sub> Sr <sub>4</sub> O <sub>9</sub>	K <sub>2</sub> CO <sub>3</sub>	1050–800	15	[81]
K <sub>1.76</sub> Mg <sub>3.25</sub> Sb <sub>4.75</sub> O <sub>16</sub>	K <sub>2</sub> CO <sub>3</sub>	1500–1300	10	[89]
K <sub>2</sub> Mo <sub>2</sub> U <sub>2</sub> O <sub>10</sub>	K <sub>2</sub> CO <sub>3</sub>	950–25	5	[87]
K <sub>8</sub> Mo <sub>3</sub> U <sub>8</sub> O <sub>37</sub>	K <sub>2</sub> CO <sub>3</sub>	950–25	5	[87]
KNbUO <sub>6</sub>	K <sub>2</sub> CO <sub>3</sub>	1300	–	[187]
K <sub>2</sub> U <sub>2</sub> WO <sub>10</sub>	K <sub>2</sub> CO <sub>3</sub>	950–25	5	[88]
La <sub>3</sub> Li <sub>7</sub> Zr <sub>2</sub> O <sub>12</sub>	Li <sub>2</sub> CO <sub>3</sub>	1040	–	[84]
La <sub>3</sub> NaPtO <sub>7</sub>	Na <sub>2</sub> CO <sub>3</sub>	1050–800	15	[188]
Mn <sub>2</sub> NiSr <sub>4</sub> O <sub>9</sub>	K <sub>2</sub> CO <sub>3</sub>	1100–880	6	[91]
NaNd <sub>3</sub> PtO <sub>7</sub>	Na <sub>2</sub> CO <sub>3</sub>	1050–800	15	[188]
Na <sub>1.55</sub> Nd <sub>2.45</sub> RhO <sub>6</sub>	Na <sub>2</sub> CO <sub>3</sub>	1050–800	15	[79]
Na <sub>1.55</sub> Pr <sub>2.45</sub> RhO <sub>6</sub>	Na <sub>2</sub> CO <sub>3</sub>	1050–800	15	[79]
NbRbUO <sub>6</sub>	Rb <sub>2</sub> CO <sub>3</sub>	1300	–	[187]
Nb <sub>2</sub> TiU <sub>2</sub> O <sub>11.5</sub>	Ti <sub>2</sub> CO <sub>3</sub>	1150	–	[187]
NiPtSr <sub>3</sub> O <sub>6</sub>	K <sub>2</sub> CO <sub>3</sub>	1050–880	12	[78]
Rb <sub>2</sub> U <sub>2</sub> WO <sub>10</sub>	Rb <sub>2</sub> CO <sub>3</sub>	950–25	5	[88]
<b>(Alkali-Metal) Vanadates, Molybdates, and/or Tungstates (3.6)</b>				
Al <sub>0.2</sub> Cr <sub>0.8</sub> KMo <sub>2</sub> O <sub>8</sub>	MoO <sub>3</sub>	1000	50	[189]
AlCsMo <sub>2</sub> O <sub>8</sub>	Cs <sub>2</sub> Mo <sub>2</sub> O <sub>7</sub>	–	2	[190]
AlGeNaO <sub>4</sub>	MoO <sub>3</sub> -Na <sub>2</sub> O-V <sub>2</sub> O <sub>5</sub>	1000–600	1	[59]
Al <sub>1.6</sub> K <sub>1.6</sub> Ti <sub>6.4</sub> O <sub>16</sub>	K <sub>2</sub> MoO <sub>4</sub> -MoO <sub>3</sub>	–	–	[191]
AlMo <sub>7</sub> NaO <sub>8</sub>	Na <sub>2</sub> Mo <sub>2</sub> O <sub>7</sub>	720–25	2	[192]
Ca <sub>2</sub> Co <sub>2</sub> NaV <sub>3</sub> O <sub>12</sub>	NaVO <sub>3</sub>	705–640	130	[97]
Ca <sub>3</sub> Fe <sub>2</sub> Ge <sub>3</sub> O <sub>12</sub>	K <sub>2</sub> Mo <sub>2</sub> O <sub>7</sub>	1250–950	3	[193]
Ca <sub>3</sub> Ge <sub>3</sub> Y <sub>2</sub> O <sub>12</sub>	K <sub>2</sub> MoO <sub>4</sub>	1250–850	3	[193]
Ca <sub>2</sub> Mg <sub>2</sub> NaV <sub>3</sub> O <sub>12</sub>	NaVO <sub>3</sub>	735–670	130	[97]
Ca <sub>2</sub> NaNi <sub>2</sub> V <sub>3</sub> O <sub>12</sub>	NaVO <sub>3</sub>	756–690	132	[97]
Co <sub>2</sub> Cs <sub>3</sub> LiMo <sub>4</sub> O <sub>16</sub>	Cs <sub>2</sub> Mo <sub>2</sub> O <sub>7</sub>	600–400	3	[102]
CrLiMo <sub>2</sub> O <sub>8</sub>	Li <sub>2</sub> MoO <sub>4</sub>	750	–	[194]
CrLi <sub>3</sub> Mo <sub>3</sub> O <sub>12</sub>	Li <sub>2</sub> MoO <sub>4</sub>	750	–	[194]
Cr <sub>1.2</sub> Li <sub>1.8</sub> Mo <sub>3</sub> O <sub>12</sub>	Li <sub>2</sub> MoO <sub>4</sub>	750	–	[194]
Cr <sub>1.7</sub> Na <sub>1.7</sub> Ti <sub>6.3</sub> O <sub>16</sub>	MoO <sub>3</sub> -Na <sub>2</sub> CO <sub>3</sub>	1300–1200	4	[100]
CsGa <sub>17</sub> Ti <sub>15</sub> O <sub>56</sub>	Cs <sub>2</sub> CO <sub>3</sub> -MoO <sub>3</sub>	1300	4	[195]
Dy <sub>2</sub> Mo <sub>4</sub> Sb <sub>2</sub> O <sub>18</sub>	MoO <sub>3</sub>	900–25	36.46	[99]
DyNaW <sub>2</sub> O <sub>8</sub>	Na <sub>2</sub> CO <sub>3</sub> -WO <sub>3</sub>	1000–400	4	[196]
FeGeKO <sub>4</sub>	K <sub>2</sub> MoO <sub>4</sub> -KVO <sub>3</sub>	875–725	0.6	[104]
FeGe <sub>3</sub> KO <sub>8</sub>	K <sub>2</sub> Mo <sub>2</sub> O <sub>7</sub>	1050–600	2.4	[197]
FeLiMo <sub>2</sub> O <sub>8</sub>	Li <sub>2</sub> Mo <sub>3</sub> O <sub>10</sub>	700–450	2	[198]
GaGeKO <sub>4</sub>	K <sub>2</sub> O-MoO <sub>3</sub> -V <sub>2</sub> O <sub>5</sub>	1000–600	1	[199]
GaGeNaO <sub>4</sub>	MoO <sub>3</sub> -Na <sub>2</sub> O-V <sub>2</sub> O <sub>5</sub>	1000–600	1	[199]
GaInZn <sub>2</sub> O <sub>5</sub>	K <sub>2</sub> MoO <sub>4</sub>	1350–600	6	[101]
Ga <sub>4.78</sub> K <sub>0.78</sub> Ti <sub>2.22</sub> O <sub>12</sub>	K <sub>2</sub> CO <sub>3</sub> -MoO <sub>3</sub>	1300–1000	4	[200]
Ga <sub>17</sub> KTi <sub>15</sub> O <sub>56</sub>	K <sub>2</sub> CO <sub>3</sub> -MoO <sub>3</sub>	1300	4	[195]
GaLiMo <sub>2</sub> O <sub>8</sub>	Li <sub>2</sub> Mo <sub>3</sub> O <sub>10</sub>	950–600	1	[198]
GaLi <sub>3</sub> Mo <sub>3</sub> O <sub>12</sub>	Li <sub>2</sub> Mo <sub>3</sub> O <sub>10</sub>	950–600	1	[198]
Ga <sub>0.81</sub> Na <sub>0.81</sub> Ti <sub>3.19</sub> O <sub>8</sub>	MoO <sub>3</sub> -Na <sub>2</sub> CO <sub>3</sub>	1300–1000	5	[201]
GaNaTi <sub>5</sub> O <sub>12</sub>	MoO <sub>3</sub> -Na <sub>2</sub> CO <sub>3</sub>	1350–1000	4	[202]
Ga <sub>4.8</sub> Na <sub>0.8</sub> Ti <sub>1.2</sub> O <sub>10</sub>	MoO <sub>3</sub> -Na <sub>2</sub> CO <sub>3</sub>	1300–1200	4	[203]
Ga <sub>17</sub> RbTi <sub>15</sub> O <sub>56</sub>	MoO <sub>3</sub> -Rb <sub>2</sub> CO <sub>3</sub>	1300	4	[195]
Gd <sub>2</sub> Mo <sub>4</sub> Sb <sub>2</sub> O <sub>18</sub>	MoO <sub>3</sub>	900–25	36.46	[99]
GdRbW <sub>2</sub> O <sub>8</sub>	Rb <sub>2</sub> W <sub>2</sub> O <sub>7</sub>	–	2	[204]
Ge <sub>3</sub> Mg <sub>3</sub> Y <sub>2</sub> O <sub>12</sub>	K <sub>2</sub> Mo <sub>2</sub> O <sub>7</sub>	1350–1152	3	[193]
Ge <sub>6</sub> Mn <sub>5.26</sub> Na <sub>2.74</sub> O <sub>20</sub>	Li <sub>2</sub> MoO <sub>4</sub> -LiVO <sub>3</sub>	1200–700	1.8	[205]
In <sub>0.6</sub> Li <sub>1.2</sub> VO <sub>4</sub>	Li <sub>3</sub> VO <sub>4</sub>	800	–	[206]
K <sub>1.6</sub> Mg <sub>0.8</sub> Ti <sub>7.2</sub> O <sub>16</sub>	K <sub>2</sub> MoO <sub>4</sub> -MoO <sub>3</sub>	–	–	[191]
K <sub>2</sub> Mo <sub>3</sub> ThO <sub>12</sub>	K <sub>2</sub> MoO <sub>4</sub>	755	6	[95]
K <sub>4</sub> Mo <sub>4</sub> ThO <sub>16</sub>	K <sub>2</sub> Mo <sub>2</sub> O <sub>7</sub>	600–300	3	[207]
K <sub>8</sub> Mo <sub>6</sub> ThO <sub>24</sub>	K <sub>2</sub> MoO <sub>4</sub>	707	30	[96]
KNbWO <sub>6</sub>	K <sub>2</sub> O-WO <sub>3</sub>	1170–1000	2	[103]

Table 1: (Continued)

Composition	Flux	Temperature range [°C]	Cooling rate [°C/h]	Reference
KNb <sub>2</sub> WO <sub>9</sub>	K <sub>2</sub> O-WO <sub>3</sub>	1050–700	1	[103]
KTaTi <sub>3</sub> O <sub>9</sub>	MoO <sub>3</sub>	1000	–	[208]
KTa <sub>5</sub> Ti <sub>2</sub> O <sub>17</sub>	MoO <sub>3</sub>	1000	–	[209]
K <sub>3</sub> Ta <sub>7</sub> TiO <sub>21</sub>	V <sub>2</sub> O <sub>5</sub>	1000	–	[208]
La <sub>2</sub> Mo <sub>4</sub> Sb <sub>2</sub> O <sub>18</sub>	MoO <sub>3</sub>	900–25	36.46	[99]
LiMnVO <sub>4</sub>	LiVO <sub>3</sub>	1297–797	1	[210]
LiMo <sub>4</sub> Rb <sub>3</sub> Zn <sub>2</sub> O <sub>16</sub>	Rb <sub>2</sub> Mo <sub>2</sub> O <sub>7</sub>	520–400	3	[102]
LiMo <sub>2</sub> YbO <sub>12</sub>	Li <sub>2</sub> MoO <sub>4</sub>	970–860	0.5	[211]
MnRbVO <sub>4</sub>	RbVO <sub>3</sub>	950–25	5	[98]
Mo <sub>4</sub> Nd <sub>2</sub> Sb <sub>2</sub> O <sub>18</sub>	MoO <sub>3</sub>	900–25	36.46	[99]
Mo <sub>4</sub> Sb <sub>2</sub> Sm <sub>2</sub> O <sub>18</sub>	MoO <sub>3</sub>	900–25	36.46	[99]
Mo <sub>4</sub> Sb <sub>2</sub> Y <sub>2</sub> O <sub>18</sub>	MoO <sub>3</sub>	900–25	36.46	[99]
Na <sub>6</sub> U <sub>5</sub> V <sub>2</sub> O <sub>23</sub>	V <sub>2</sub> O <sub>5</sub>	800–25	5	[72]
NbRbWO <sub>6</sub>	Rb <sub>2</sub> O-WO <sub>3</sub>	1170–1000	2	[103]
NbRbW <sub>2</sub> O <sub>9</sub>	Rb <sub>2</sub> O-WO <sub>3</sub>	1050–700	1	[103]
NbTiWO <sub>6</sub>	Ti <sub>2</sub> O-WO <sub>3</sub>	1170–1000	2	[103]
PbUV <sub>2</sub> O <sub>9</sub>	V <sub>2</sub> O <sub>5</sub>	680–25	5	[94]
<b>Alkali-Metal Oxides, Peroxides, and/or Superoxides (3.7)</b>				
AlKLi <sub>4</sub> O <sub>4</sub>	K <sub>2</sub> O	950	–	[212]
Ba <sub>2</sub> Cu <sub>3</sub> NaO <sub>6</sub>	Na <sub>2</sub> O <sub>2</sub>	750	–	[213]
Ba <sub>25</sub> Cu <sub>18</sub> Zn <sub>4</sub> O <sub>49</sub>	KO <sub>2</sub>	750–25	2.5	[214]
Ba <sub>6</sub> Ga <sub>7</sub> KZn <sub>4</sub> O <sub>21</sub>	KO <sub>2</sub>	750–25	2.5	[215]
Ba <sub>3</sub> In <sub>2</sub> Zn <sub>5</sub> O <sub>11</sub>	KO <sub>2</sub>	750–25	2.5	[109]
BaMnRbO <sub>4</sub>	Rb <sub>2</sub> O	600	–	[216]
Ba <sub>3</sub> NaNbO <sub>6</sub>	Na <sub>2</sub> O	1100	–	[217]
Ba <sub>3</sub> NaTaO <sub>6</sub>	Na <sub>2</sub> O	1100	–	[217]
Be <sub>2</sub> K <sub>2</sub> Na <sub>4</sub> O <sub>5</sub>	K <sub>2</sub> O-Na <sub>2</sub> O	750	–	[218]
Be <sub>3</sub> Na <sub>5</sub> RbO <sub>11</sub>	Na <sub>2</sub> O-Rb <sub>2</sub> O	660	–	[219]
Cd <sub>3</sub> NaRbO <sub>4</sub>	Rb <sub>2</sub> O	700–400	1.5	[220]
Co <sub>2</sub> K <sub>2</sub> Na <sub>4</sub> O <sub>5</sub>	K <sub>2</sub> O-Na <sub>2</sub> O	600	–	[221]
Co <sub>2</sub> K <sub>4</sub> Rb <sub>2</sub> O <sub>5</sub>	K <sub>2</sub> O-Rb <sub>2</sub> O	570	–	[222]
CoLi <sub>3</sub> Na <sub>2</sub> O <sub>4</sub>	Li <sub>2</sub> O-Na <sub>2</sub> O <sub>2</sub>	760	–	[223]
Co <sub>2</sub> Na <sub>4</sub> Rb <sub>2</sub> O <sub>5</sub>	Na <sub>2</sub> O-Rb <sub>2</sub> O	600	–	[221]
Co <sub>2</sub> Na <sub>7</sub> RbO <sub>6</sub>	Li <sub>2</sub> O	600	–	[224]
Cs <sub>2</sub> Fe <sub>2</sub> K <sub>4</sub> O <sub>5</sub>	Cs <sub>2</sub> O-K <sub>2</sub> O	470	–	[225]
Cs <sub>2</sub> GaLi <sub>3</sub> O <sub>4</sub>	Cs <sub>2</sub> O	750	–	[106]
CsGaK <sub>4</sub> O <sub>4</sub>	Cs <sub>2</sub> O-K <sub>2</sub> O	580	–	[226]
Cs <sub>2</sub> GeLi <sub>2</sub> O <sub>4</sub>	Cs <sub>2</sub> O-Li <sub>2</sub> O	600	23.96	[227]
CsGe <sub>4</sub> Li <sub>12</sub> Na <sub>3</sub> O <sub>16</sub>	Cs <sub>2</sub> O-Li <sub>2</sub> O-Na <sub>2</sub> O	600	–	[228]
Cs <sub>2</sub> InNa <sub>3</sub> O <sub>4</sub>	Cs <sub>2</sub> O	600	–	[229]
CsK <sub>5</sub> Ru <sub>2</sub> O <sub>9</sub>	Cs <sub>2</sub> O <sub>2</sub> -K <sub>2</sub> O <sub>2</sub>	750	–	[105]
CsLaNb <sub>2</sub> O <sub>7</sub>	Cs <sub>2</sub> CO <sub>3</sub>	1000	–	[230]
Cs <sub>2</sub> LiMnO <sub>4</sub>	Cs <sub>2</sub> O <sub>2</sub>	580	–	[231]
Cs <sub>2</sub> Li <sub>2</sub> TiO <sub>4</sub>	Cs <sub>2</sub> O-Li <sub>2</sub> O	650	–	[232]
Cs <sub>2</sub> LiVO <sub>4</sub>	Cs <sub>2</sub> O-Li <sub>2</sub> O	750	–	[233]
Cs <sub>2</sub> Na <sub>2</sub> IrO <sub>4</sub>	Cs <sub>2</sub> O-Na <sub>2</sub> O <sub>2</sub>	760	–	[5]
CsNaTiO <sub>3</sub>	Cs <sub>2</sub> O-Na <sub>2</sub> O	600	0.83	[234]
CsNa <sub>3</sub> TiO <sub>4</sub>	Cs <sub>2</sub> O-Na <sub>2</sub> O	600	–	[235]
Cs <sub>2</sub> Na <sub>3</sub> TiO <sub>4</sub>	Cs <sub>2</sub> O	580	–	[229]
Cs <sub>2</sub> NaVO <sub>4</sub>	Cs <sub>2</sub> O-Na <sub>2</sub> O	750	–	[236]
CuKNa <sub>2</sub> O <sub>2</sub>	K <sub>2</sub> O-Na <sub>2</sub> O	680	–	[237]
Fe <sub>2</sub> K <sub>2</sub> Na <sub>4</sub> O <sub>6</sub>	Na <sub>2</sub> O	500	–	[238]
FeLi <sub>3</sub> K <sub>2</sub> O <sub>4</sub>	K <sub>2</sub> O-Li <sub>2</sub> O	700	–	[239]
FeLi <sub>3</sub> Na <sub>2</sub> O <sub>4</sub>	Li <sub>2</sub> O-Na <sub>2</sub> O	720	–	[239]
GaKNa <sub>4</sub> O <sub>4</sub>	K <sub>2</sub> O-Na <sub>2</sub> O	650	–	[226]
GaLi <sub>3</sub> Na <sub>2</sub> O <sub>4</sub>	Li <sub>2</sub> O	700	–	[240]
GeKLi <sub>3</sub> O <sub>4</sub>	K <sub>2</sub> O-Li <sub>2</sub> O	800	50	[241]
Ge <sub>2</sub> K <sub>5</sub> LiO <sub>7</sub>	K <sub>2</sub> O-Li <sub>2</sub> O	600	–	[242]
InNa <sub>3</sub> Rb <sub>2</sub> O <sub>4</sub>	Rb <sub>2</sub> O	620	–	[229]
IrKLi <sub>6</sub> O <sub>6</sub>	Li <sub>2</sub> O	750	–	[243]
IrK <sub>3</sub> LiO <sub>4</sub>	K <sub>2</sub> O	800–25	50	[244]
IrK <sub>2</sub> Na <sub>2</sub> O <sub>4</sub>	K <sub>2</sub> O-Na <sub>2</sub> O <sub>2</sub>	740	–	[245]



Table 1: (Continued)

Composition	Flux	Temperature range [°C]	Cooling rate [°C/h]	Reference
KLiMnO <sub>2</sub>	K <sub>2</sub> O-Li <sub>2</sub> O	640	—	[246]
K <sub>11</sub> LiMn <sub>4</sub> O <sub>16</sub>	K <sub>2</sub> O <sub>2</sub>	580	—	[247]
KLi <sub>4</sub> NbO <sub>5</sub>	K <sub>2</sub> O-Li <sub>2</sub> O	1100	—	[248]
KLi <sub>6</sub> TaO <sub>6</sub>	K <sub>2</sub> O-Li <sub>2</sub> O	800	—	[249]
K <sub>2</sub> Li <sub>4</sub> UO <sub>6</sub>	K <sub>2</sub> O	750	—	[250]
K <sub>2</sub> LiVO <sub>4</sub>	K <sub>2</sub> O-Li <sub>2</sub> O	900	—	[251]
KLiZnO <sub>2</sub>	K <sub>2</sub> O-Li <sub>2</sub> O	800	—	[252]
KMnNaO <sub>2</sub>	K <sub>2</sub> O-Na <sub>2</sub> O	650	—	[253]
K <sub>2</sub> MnNaO <sub>4</sub>	K <sub>2</sub> O <sub>2</sub> -Na <sub>2</sub> O <sub>2</sub>	580	—	[254]
K <sub>3</sub> NaTh <sub>2</sub> O <sub>6</sub>	K <sub>2</sub> O-Na <sub>2</sub> O	1300	2	[255]
KNaTiO <sub>3</sub>	K <sub>2</sub> O-Na <sub>2</sub> O	900	—	[256]
K <sub>2</sub> Na <sub>3</sub> TiO <sub>4</sub>	K <sub>2</sub> O-Na <sub>2</sub> O	550	—	[257]
KNa <sub>3</sub> WO <sub>5</sub>	K <sub>2</sub> O	750	—	[258]
KNaZnO <sub>2</sub>	K <sub>2</sub> O-Na <sub>2</sub> O	700	—	[259]
Li <sub>2</sub> Mn <sub>4</sub> Na <sub>10</sub> O <sub>16</sub>	Na <sub>2</sub> O <sub>2</sub>	580	—	[260]
Li <sub>5</sub> Mn <sub>5</sub> Na <sub>3</sub> O <sub>9</sub>	Li <sub>2</sub> O-Na <sub>2</sub> O	700	—	[261]
Li <sub>12</sub> Na <sub>3</sub> RbTi <sub>4</sub> O <sub>16</sub>	Li <sub>2</sub> O-Na <sub>2</sub> O-Rb <sub>2</sub> O	780	—	[262]
Li <sub>2</sub> Na <sub>6</sub> W <sub>2</sub> O <sub>10</sub>	Li <sub>2</sub> O-Na <sub>2</sub> O	840	5	[263]
Li <sub>14</sub> Rb <sub>2</sub> Tb <sub>3</sub> O <sub>14</sub>	Rb <sub>2</sub> O	500	—	[264]
LiRb <sub>2</sub> VO <sub>4</sub>	Li <sub>2</sub> O-Rb <sub>2</sub> O	750	—	[233]
LiRbZnO <sub>2</sub>	Li <sub>2</sub> O-Rb <sub>2</sub> O	770	—	[265]
LiRbZn <sub>2</sub> O <sub>3</sub>	Li <sub>2</sub> O-Rb <sub>2</sub> O	850	—	[265]
NaNi <sub>7</sub> Sr <sub>12</sub> O <sub>23</sub>	Na <sub>2</sub> O <sub>2</sub>	750	—	[108]
NaPbRb <sub>3</sub> O <sub>4</sub>	Rb <sub>2</sub> O	480	3	[107]
NaRbTiO <sub>3</sub>	Na <sub>2</sub> O-Rb <sub>2</sub> O	750	2.08	[234]
NaRb <sub>3</sub> TiO <sub>4</sub>	Na <sub>2</sub> O <sub>2</sub> -Rb <sub>2</sub> O	1000	—	[266]
NaRb <sub>7</sub> Zn <sub>2</sub> O <sub>6</sub>	Na <sub>2</sub> O-Rb <sub>2</sub> O	950	—	[267]
<b>Alkali- and/or Alkaline-Earth-Metal Hydroxides (3.8)</b>				
Al <sub>2</sub> Ba <sub>4</sub> Ti <sub>10</sub> O <sub>27</sub>	NaOH	1300	—	[122]
Au <sub>0.5</sub> La <sub>2</sub> Li <sub>0.5</sub> O <sub>4</sub>	LiOH	750–400	5	[124]
Ba <sub>5</sub> Bi <sub>2</sub> Li <sub>2</sub> O <sub>11</sub>	Ba(OH) <sub>2</sub> -LiOH-RbOH	550	remove	[268]
Ba <sub>3</sub> BiNaO <sub>6</sub>	Ba(OH) <sub>2</sub> -KOH-NaOH	550	remove	[268]
Ba <sub>0.41</sub> BiNaSr <sub>2.59</sub> O <sub>6</sub>	Ba(OH) <sub>2</sub> -NaOH-Sr(OH) <sub>2</sub>	600–500	100	[269]
Ba <sub>2</sub> Co <sub>0.77</sub> Os <sub>1.23</sub> O <sub>6</sub>	Ba(OH) <sub>2</sub> -KOH	600–400	60	[270]
BaFeKO <sub>3</sub>	Ba(OH) <sub>2</sub> -KOH	750–600	4.69	[121]
Ba <sub>2</sub> Fe <sub>0.92</sub> Os <sub>1.08</sub> O <sub>6</sub>	Ba(OH) <sub>2</sub> -KOH	600–400	60	[270]
Ba <sub>3</sub> Ir <sub>2</sub> LiO <sub>9</sub>	Ba(OH) <sub>2</sub> -KOH-LiOH	650	turn off	[271]
Ba <sub>3</sub> Ir <sub>2</sub> NaO <sub>9</sub>	Ba(OH) <sub>2</sub> -NaOH	650	turn off	[271]
BaKVO <sub>4</sub>	Ba(OH) <sub>2</sub> -KOH	700–600	100	[272]
Ba <sub>2</sub> LiOsO <sub>6</sub>	Ba(OH) <sub>2</sub> -KOH-LiOH	600	turn off	[115]
Ba <sub>3</sub> LiOs <sub>2</sub> O <sub>9</sub>	Ba(OH) <sub>2</sub> -KOH-LiOH	600	turn off	[273]
Ba <sub>2</sub> LiReO <sub>6</sub>	Ba(OH) <sub>2</sub> -LiOH	750–600	5	[114]
Ba <sub>3</sub> LiRu <sub>2</sub> O <sub>9</sub>	Ba(OH) <sub>2</sub> -KOH-LiOH	700–600	15	[274]
Ba <sub>7</sub> Li <sub>3</sub> Ru <sub>4</sub> O <sub>20</sub>	Ba(OH) <sub>2</sub> -KOH-LiOH	700–600	15	[275]
Ba <sub>2</sub> NaNi <sub>3</sub> O <sub>6</sub>	Ba(OH) <sub>2</sub> -NaOH	750–25	30	[276]
Ba <sub>2</sub> NaOsO <sub>6</sub>	Ba(OH) <sub>2</sub> -NaOH	600	turn off	[115]
Ba <sub>3</sub> NaOs <sub>2</sub> O <sub>9</sub>	Ba(OH) <sub>2</sub> -NaOH	600	turn off	[273]
Ba <sub>2</sub> NaReO <sub>6</sub>	Ba(OH) <sub>2</sub> -NaOH	750–600	5	[114]
Ba <sub>3</sub> NaRu <sub>2</sub> O <sub>9</sub>	Ba(OH) <sub>2</sub> -NaOH	700–600	15	[274]
Ba <sub>4</sub> NaRu <sub>3</sub> O <sub>12</sub>	Ba(OH) <sub>2</sub> -NaOH	700–600	15	[275]
BiKLi <sub>6</sub> O <sub>6</sub>	KOH-LiOH	550	remove	[268]
BiLi <sub>6</sub> RbO <sub>6</sub>	LiOH-RbOH	550	remove	[268]
BiLiSr <sub>3</sub> O <sub>6</sub>	LiOH-Sr(OH) <sub>2</sub>	550	remove	[268]
BiNaSr <sub>3</sub> O <sub>6</sub>	KOH-NaOH-Sr(OH) <sub>2</sub>	550	remove	[268]
Bi <sub>4.1</sub> Ru <sub>1.9</sub> Sr <sub>18</sub> O <sub>33</sub>	KOH-Sr(OH) <sub>2</sub>	750–600	3.125	[120]
CdPtSr <sub>3</sub> O <sub>6</sub>	KOH	1000–750	1	[277]
Co <sub>0.5</sub> La <sub>2</sub> Li <sub>0.5</sub> O <sub>4</sub>	LiOH	800	—	[123]
CuK <sub>0.22</sub> La <sub>1.78</sub> O <sub>4</sub>	KOH	450	remove	[278]
Cu <sub>0.14</sub> KPd <sub>0.86</sub> PrO <sub>3</sub>	KOH	750–600	4.17	[113]
Cu <sub>0.5</sub> La <sub>2</sub> Li <sub>0.5</sub> O <sub>4</sub>	LiOH	800	—	[123]
CuLa <sub>1.88</sub> Na <sub>0.12</sub> O <sub>4</sub>	NaOH	320	remove	[278]
Dy <sub>0.94</sub> IrNa <sub>1.06</sub> O <sub>4</sub>	CsOH-NaOH	700	turn off	[279]

Table 1: (Continued)

Composition	Flux	Temperature range [°C]	Cooling rate [°C/h]	Reference
DyNaPd <sub>6</sub> O <sub>8</sub>	NaOH	700	turn off	[280]
Er <sub>0.75</sub> IrNa <sub>1.25</sub> O <sub>4</sub>	CsOH-NaOH	700	turn off	[279]
ErNaPd <sub>6</sub> O <sub>8</sub>	NaOH	700	turn off	[280]
Eu <sub>2</sub> IrLiO <sub>6</sub>	KOH-LiOH	700	turn off	[281]
Eu <sub>2</sub> IrMgO <sub>6</sub>	KOH	700–600	12	[282]
EuKNaNbO <sub>5</sub>	KOH-NaOH	450	turn off	[283]
Eu <sub>4</sub> K <sub>2</sub> Na <sub>2</sub> Nb <sub>2</sub> O <sub>13</sub>	KOH-NaOH	450–350	100	[284]
EuKNaTaO <sub>5</sub>	KOH-NaOH	600–500	2	[285]
Eu <sub>4</sub> K <sub>2</sub> Na <sub>2</sub> Ta <sub>2</sub> O <sub>13</sub>	KOH-NaOH	450–350	100	[284]
EuKPdO <sub>3</sub>	KOH	750–600	4.17	[113]
Gd <sub>2</sub> IrMgO <sub>6</sub>	KOH	700–600	12	[282]
Gd <sub>0.96</sub> IrNa <sub>1.04</sub> O <sub>4</sub>	CsOH-NaOH	700	turn off	[279]
GdKNaNbO <sub>5</sub>	KOH-NaOH	450	turn off	[283]
Gd <sub>4</sub> K <sub>2</sub> Na <sub>2</sub> Nb <sub>2</sub> O <sub>13</sub>	KOH-NaOH	450	70	[119]
GdKPdO <sub>3</sub>	KOH	750–600	4.17	[113]
Ge <sub>4</sub> K <sub>3.6</sub> Na <sub>8.4</sub> O <sub>14</sub>	KOH-NaOH	620	–	[286]
Ho <sub>0.90</sub> IrNa <sub>1.10</sub> O <sub>4</sub>	CsOH-NaOH	700	turn off	[279]
HoNaPd <sub>6</sub> O <sub>8</sub>	NaOH	700	turn off	[280]
IrK <sub>1.5</sub> La <sub>2.5</sub> O <sub>7</sub>	KOH	650	turn off	[287]
IrLa <sub>2</sub> LiO <sub>6</sub>	KOH-LiOH	700	turn off	[281]
IrLa <sub>2</sub> NaO <sub>6</sub>	NaOH	700	turn off	[288]
Ir <sub>4</sub> La <sub>9</sub> RbO <sub>24</sub>	RbOH	650	turn off	[116]
IrLiNd <sub>2</sub> O <sub>6</sub>	KOH-LiOH	700	turn off	[281]
IrLiPr <sub>2</sub> O <sub>6</sub>	KOH-LiOH	700	turn off	[281]
IrLiSm <sub>2</sub> O <sub>6</sub>	KOH-LiOH	700	turn off	[281]
IrMgNd <sub>2</sub> O <sub>6</sub>	KOH	700–600	12	[282]
IrMgPr <sub>2</sub> O <sub>6</sub>	KOH	700–600	12	[282]
IrMgSm <sub>2</sub> O <sub>6</sub>	KOH	700–600	12	[282]
IrNaNd <sub>2</sub> O <sub>6</sub>	NaOH	700	turn off	[288]
IrNaPr <sub>2</sub> O <sub>6</sub>	NaOH	700	turn off	[288]
IrNaSm <sub>2</sub> O <sub>6</sub>	CsOH-NaOH	650	turn off	[117]
IrNa <sub>1.07</sub> Tb <sub>0.93</sub> O <sub>4</sub>	CsOH-NaOH	700	turn off	[279]
IrNa <sub>1.08</sub> Y <sub>0.92</sub> O <sub>4</sub>	CsOH-NaOH	700	turn off	[279]
K <sub>2</sub> IrNd <sub>2</sub> O <sub>7</sub>	KOH	550	turn off	[289]
K <sub>2</sub> IrSm <sub>2</sub> O <sub>7</sub>	KOH	550	turn off	[289]
KLaNaNbO <sub>5</sub>	KOH-NaOH	400	60	[119]
KLa <sub>2</sub> NbO <sub>6</sub>	KOH	600	turn off	[290]
KLaPdO <sub>3</sub>	KOH	750–600	4.17	[113]
KNaNbNdO <sub>5</sub>	KOH-NaOH	600	turn off	[283]
K <sub>2</sub> Na <sub>2</sub> Nb <sub>2</sub> Nd <sub>4</sub> O <sub>13</sub>	KOH-NaOH	450–350	2.08	[284]
KNaNbPrO <sub>5</sub>	KOH-NaOH	400	turn off	[283]
KNaNbSmO <sub>5</sub>	KOH-NaOH	450	turn off	[283]
K <sub>2</sub> Na <sub>2</sub> Nb <sub>2</sub> Sm <sub>4</sub> O <sub>13</sub>	KOH-NaOH	450–350	100	[284]
K <sub>2</sub> Na <sub>2</sub> Sm <sub>4</sub> Ta <sub>2</sub> O <sub>13</sub>	KOH-NaOH	450–350	100	[284]
KNdPdO <sub>3</sub>	KOH	750–600	4.17	[113]
KPdPrO <sub>3</sub>	KOH	750–600	4.17	[113]
KPdSmO <sub>3</sub>	KOH	750–600	4.17	[113]
La <sub>2</sub> Li <sub>0.5</sub> Ni <sub>0.5</sub> O <sub>4</sub>	LiOH	800	–	[123]
La <sub>2</sub> LiOsO <sub>6</sub>	KOH-LiOH	625	turn off	[291]
La <sub>3</sub> Li <sub>5</sub> Ta <sub>2</sub> O <sub>12</sub>	LiOH	600	turn off	[292]
La <sub>2</sub> NaOsO <sub>6</sub>	NaOH	600	turn off	[293]
La <sub>2</sub> Na <sub>2</sub> PtO <sub>6</sub>	NaOH	700	turn off	[118]
La <sub>2.47</sub> Na <sub>1.53</sub> RhO <sub>6</sub>	NaOH	700	turn off	[79]
La <sub>2</sub> NaRuO <sub>6</sub>	NaOH	600–500	60	[294]
La <sub>2</sub> NaTaO <sub>6</sub>	NaOH	600	turn off	[295]
Li <sub>6</sub> Nb <sub>2</sub> Sr <sub>3</sub> O <sub>11</sub>	KOH-LiOH-Sr(OH) <sub>2</sub>	600–500	100	[296]
LiNd <sub>2</sub> OsO <sub>6</sub>	KOH-LiOH	600	turn off	[291]
Li <sub>5</sub> Nd <sub>3</sub> Ta <sub>2</sub> O <sub>12</sub>	LiOH	600	turn off	[292]
LiOsPr <sub>2</sub> O <sub>6</sub>	KOH-LiOH	600–400	60	[291]
LiOsSm <sub>2</sub> O <sub>6</sub>	KOH-LiOH	600	turn off	[291]
Li <sub>5</sub> Pr <sub>3</sub> Ta <sub>2</sub> O <sub>12</sub>	LiOH	600	turn off	[292]
LiReS <sub>2</sub> O <sub>6</sub>	LiOH-Sr(OH) <sub>2</sub>	750–600	5	[114]

Table 1: (Continued)

Composition	Flux	Temperature range [°C]	Cooling rate [°C/h]	Reference
LiRhSr <sub>3</sub> O <sub>6</sub>	KOH-LiOH-Sr(OH) <sub>2</sub>	600	remove	[297]
LiRuSr <sub>3</sub> O <sub>6</sub>	KOH-LiOH-Sr(OH) <sub>2</sub>	700–600	15	[83]
Li <sub>6</sub> Ta <sub>2</sub> Sr <sub>3</sub> O <sub>11</sub>	KOH-LiOH-Sr(OH) <sub>2</sub>	700–600	100	[296]
LuNaPd <sub>6</sub> O <sub>8</sub>	NaOH	700	turn off	[112]
MgPtSr <sub>3</sub> O <sub>6</sub>	KOH	1000–750	1	[298]
NaNbSr <sub>3</sub> O <sub>6</sub>	NaOH-Sr(OH) <sub>2</sub>	700–600	10	[110]
NaNd <sub>2</sub> O <sub>5</sub> O <sub>6</sub>	NaOH	650	turn off	[293]
Na <sub>2</sub> Nd <sub>2</sub> PtO <sub>6</sub>	NaOH	700	turn off	[79]
NaNd <sub>2</sub> RuO <sub>6</sub>	NaOH	600–500	60	[294]
Na <sub>3</sub> Nd <sub>14</sub> Ru <sub>6</sub> O <sub>36</sub>	NaOH	600	turn off	[111]
NaOsPr <sub>2</sub> O <sub>6</sub>	NaOH	600	turn off	[293]
NaPd <sub>6</sub> TbO <sub>8</sub>	NaOH	700	turn off	[280]
NaPd <sub>6</sub> TmO <sub>8</sub>	NaOH	700	turn off	[280]
NaPd <sub>6</sub> YO <sub>8</sub>	NaOH	700	turn off	[280]
NaPd <sub>6</sub> YbO <sub>8</sub>	NaOH	700	turn off	[280]
NaPr <sub>7</sub> RuO <sub>6</sub>	NaOH	600–500	60	[294]
Na <sub>3</sub> Pr <sub>14</sub> Ru <sub>6</sub> O <sub>36</sub>	NaOH	600–500	60	[111]
NaReSr <sub>2</sub> O <sub>6</sub>	NaOH-Sr(OH) <sub>2</sub>	750–600	5	[114]
NaRhSr <sub>3</sub> O <sub>6</sub>	NaOH-Sr(OH) <sub>2</sub>	600	remove	[297]
NaSr <sub>3</sub> TaO <sub>6</sub>	NaOH-Sr(OH) <sub>2</sub>	700–600	10	[110]
PtSr <sub>3</sub> ZnO <sub>6</sub>	KOH	1000–750	1	[277]
<b>Complex Melts (3.9)</b>				
Al <sub>6</sub> Ba <sub>46</sub> Cu <sub>24</sub> O <sub>84</sub>	BaCl <sub>2</sub> -Ba(OH) <sub>2</sub>	750–600	4.16	[126]
Ba <sub>3</sub> CaIr <sub>1.5</sub> Ru <sub>0.5</sub> O <sub>9</sub>	BaCl <sub>2</sub> -Ba(OH) <sub>2</sub>	1050	–	[125]
Ba <sub>3</sub> CaRu <sub>1.5</sub> Ta <sub>0.5</sub> O <sub>9</sub>	BaCl <sub>2</sub> -Ba(OH) <sub>2</sub>	1050	–	[125]
Ba <sub>46</sub> Cu <sub>24</sub> Fe <sub>6</sub> O <sub>84</sub>	BaCl <sub>2</sub> -Ba(OH) <sub>2</sub>	750–600	4.16	[126]
Ba <sub>46</sub> Cu <sub>24</sub> Ga <sub>6</sub> O <sub>84</sub>	BaCl <sub>2</sub> -Ba(OH) <sub>2</sub>	750–600	4.16	[126]
Ba <sub>46</sub> Cu <sub>24</sub> Ge <sub>6</sub> O <sub>84</sub>	BaCl <sub>2</sub> -Ba(OH) <sub>2</sub>	750–600	4.16	[126]
Ba <sub>46</sub> Cu <sub>24</sub> Ti <sub>6</sub> O <sub>84</sub>	BaCl <sub>2</sub> -Ba(OH) <sub>2</sub>	750–600	4.16	[126]
Ba <sub>46</sub> Cu <sub>24</sub> Zr <sub>6</sub> O <sub>84</sub>	BaCl <sub>2</sub> -Ba(OH) <sub>2</sub>	750–600	4.16	[126]
BaFe <sub>4</sub> Sn <sub>2</sub> O <sub>11</sub>	B <sub>2</sub> O <sub>3</sub> -BaCl <sub>2</sub>	1350	15	[134]
Ba <sub>3.44</sub> Ir <sub>2</sub> K <sub>1.56</sub> O <sub>10</sub>	Ba(OH) <sub>2</sub> -KOH-KO <sub>2</sub>	700–400	10	[271]
Ba <sub>3</sub> PbV <sub>4</sub> O <sub>14</sub>	PbO-V <sub>2</sub> O <sub>5</sub>	900–450	6	[299]
Be <sub>2</sub> Bi <sub>0.68</sub> Rh <sub>6</sub> O <sub>12</sub>	Bi <sub>2</sub> O <sub>3</sub> -V <sub>2</sub> O <sub>5</sub>	1100–700	5	[128]
Bi <sub>1.68</sub> Ca <sub>2</sub> Co <sub>1.69</sub> O <sub>7.38</sub>	Bi <sub>2</sub> O <sub>3</sub> -K <sub>2</sub> CO <sub>3</sub> -KCl	900–700	2	[137]
Bi <sub>0.67</sub> Ce <sub>0.33</sub> Rh <sub>2</sub> O <sub>5</sub>	Bi <sub>2</sub> O <sub>3</sub> -V <sub>2</sub> O <sub>5</sub>	1100–700	3	[300]
Bi <sub>0.75</sub> Fe <sub>0.75</sub> Pb <sub>0.25</sub> Ti <sub>0.25</sub> O <sub>3</sub>	Bi <sub>2</sub> O <sub>3</sub> -PbO	1200–800	2	[133]
Bi <sub>0.78</sub> Li <sub>2</sub> Rh <sub>6</sub> O <sub>12</sub>	Bi <sub>2</sub> O <sub>3</sub> -V <sub>2</sub> O <sub>5</sub>	1100–700	5	[128]
Bi <sub>2</sub> Mn <sub>1.33</sub> Ni <sub>0.67</sub> O <sub>6</sub>	Bi <sub>2</sub> O <sub>3</sub> -NaCl	875–820	0.5	[129]
Bi <sub>0.75</sub> Rh <sub>4.92</sub> Sc <sub>2.18</sub> O <sub>12</sub>	Bi <sub>2</sub> O <sub>3</sub> -V <sub>2</sub> O <sub>5</sub>	1100–700	5	[128]
Ca <sub>3.15</sub> IrLi <sub>0.85</sub> O <sub>6</sub>	K <sub>2</sub> CO <sub>3</sub> -KCl	1050	turn off	[83]
CrGe <sub>2</sub> LiO <sub>6</sub>	LiF-PbO-V <sub>2</sub> O <sub>5</sub>	1100–700	2	[301]
CrGe <sub>2</sub> NaO <sub>6</sub>	NaF-PbO-V <sub>2</sub> O <sub>5</sub>	1100–700	2	[301]
CuLiVO <sub>4</sub>	LiCl-LiVO <sub>3</sub>	560–520	1	[130]
EuGe <sub>2</sub> KO <sub>6</sub>	KF-MoO <sub>3</sub>	900–750	2	[302]
Fe <sub>1.78</sub> Ge <sub>2.11</sub> Mg <sub>0.11</sub> Pb <sub>2</sub> O <sub>9</sub>	B <sub>2</sub> O <sub>3</sub> -PbO	1050–800	1.8	[303]
Fe <sub>1.45</sub> K <sub>1.45</sub> Ti <sub>6.55</sub> O <sub>16</sub>	K <sub>2</sub> O-SiO <sub>2</sub> -V <sub>2</sub> O <sub>5</sub>	1450–900	6	[138]
Fe <sub>0.65</sub> Na <sub>2.65</sub> Ti <sub>3.35</sub> O <sub>9</sub>	Na <sub>2</sub> CO <sub>3</sub> -NaCl	1050–700	5	[304]
Gd <sub>1.88</sub> K <sub>1.88</sub> Sn <sub>8.12</sub> O <sub>16</sub>	B <sub>2</sub> O <sub>3</sub> -K <sub>2</sub> CO <sub>3</sub> -MoO <sub>3</sub>	1350–1000	2	[305]
Ge <sub>6</sub> La <sub>9</sub> NaO <sub>26</sub>	B <sub>2</sub> O <sub>3</sub> -Na <sub>2</sub> O-PbO	950–600	5	[306]
In <sub>0.5</sub> Nb <sub>0.5</sub> PbO <sub>3</sub>	B <sub>2</sub> O <sub>3</sub> -PbO	1040–990	–	[136]
In <sub>0.5</sub> PbTa <sub>0.5</sub> O <sub>3</sub>	B <sub>2</sub> O <sub>3</sub> -PbO	1060–1000	–	[136]
IrLiSr <sub>3</sub> O <sub>6</sub>	K <sub>2</sub> CO <sub>3</sub> -KCl	1050	turn off	[83]
K <sub>4</sub> La <sub>6</sub> Pt <sub>2</sub> O <sub>15</sub>	KF-KOH	650–300	4.86	[127]
K <sub>2</sub> Li <sub>6</sub> Pb <sub>2</sub> O <sub>8</sub>	Li <sub>2</sub> O-PbO <sub>2</sub>	660	–	[307]
K <sub>2</sub> Li <sub>14</sub> Pb <sub>3</sub> O <sub>14</sub>	Li <sub>2</sub> O-PbO <sub>2</sub>	595	–	[308]
K <sub>1.54</sub> Mg <sub>0.77</sub> Ti <sub>7.23</sub> O <sub>16</sub>	B <sub>2</sub> O <sub>3</sub> -KF-K <sub>2</sub> O	1310–1100	3	[309]
K <sub>2</sub> NbNdO <sub>6</sub>	KF-KOH	500–200	10	[290]
K <sub>4</sub> Nd <sub>6</sub> Pt <sub>2</sub> O <sub>15</sub>	KF-KOH	650–300	4.86	[127]
K <sub>2</sub> Nd <sub>2</sub> Ti <sub>3</sub> O <sub>10</sub>	KF-Na <sub>2</sub> B <sub>4</sub> O <sub>7</sub>	1100–1000	1	[131]
K <sub>4</sub> Pr <sub>6</sub> Pt <sub>2</sub> O <sub>15</sub>	KF-KOH	650–300	4.86	[127]
K <sub>4</sub> Pt <sub>2</sub> Sm <sub>6</sub> O <sub>15</sub>	KF-KOH	650–300	4.86	[127]

**Table 1:** (Continued)

Composition	Flux	Temperature range [°C]	Cooling rate [°C/h]	Reference
$\text{Li}_2\text{Pb}_{0.78}\text{Rh}_6\text{O}_{12}$	$\text{PbO-V}_2\text{O}_5$	1100–700	5	[128]
$\text{Mg}_{0.33}\text{PbTa}_{0.67}\text{O}_3$	$\text{B}_2\text{O}_3\text{-PbO-Pb}_3\text{O}_4$	1155–1130	–	[310]
$\text{Mg}_{0.5}\text{PbW}_{0.5}\text{O}_3$	$\text{B}_2\text{O}_3\text{-PbO-Pb}_3\text{O}_4$	1090–1055	–	[136]
$\text{Mn}_5\text{Pb}_3\text{V}_2\text{O}_{16}$	$\text{PbO-V}_2\text{O}_5$	950	–	[311]
$\text{MnSbVO}_6$	$\text{B}_2\text{O}_3\text{-V}_2\text{O}_5$	900–700	1.5	[135]
$\text{Nb}_{0.335}\text{PbSc}_{0.335}\text{Ti}_{0.33}\text{O}_3$	$\text{B}_2\text{O}_3\text{-PbO}$	1200–800	3	[312]
$\text{Nb}_{0.5}\text{PbYb}_{0.5}\text{O}_3$	$\text{B}_2\text{O}_3\text{-PbF}_2\text{-PbO}$	1200–1160	–	[136]
$\text{Pb}_{1.944}\text{Sc}_{0.506}\text{Ta}_{1.494}\text{O}_{6.438}$	$\text{B}_2\text{O}_3\text{-PbF}_2\text{-PbO}$	1200–950	0.5	[313]
$\text{PbTa}_{0.5}\text{Yb}_{0.5}\text{O}_3$	$\text{B}_2\text{O}_3\text{-PbF}_2\text{-PbO}$	1200–1160	–	[136]
$\text{Pb}_{0.5}\text{Th}_{0.5}\text{VO}_4$	$\text{PbO-V}_2\text{O}_5$	1000–750	5	[132]

[a] The actual compositions of  $\text{Na}_2\text{O}$ ,  $\text{K}_2\text{O}$ ,  $\text{Rb}_2\text{O}$ , and  $\text{Cs}_2\text{O}$  vary as  $\text{NaO}_x$  ( $x = 0.45, 0.46, 0.48, 0.5, 0.52$ ),  $\text{KO}_x$  ( $x = 0.45, 0.48, 0.5, 0.51, 0.52, 0.55$ ),  $\text{RbO}_x$  ( $x = 0.45, 0.49, 0.5, 0.58, 0.59, 0.7, 0.84$ ), and  $\text{CsO}_x$  ( $x = 0.5, 0.52, 0.55, 0.56$ ). The actual compositions of  $\text{Na}_2\text{O}_2$ ,  $\text{K}_2\text{O}_2$ , and  $\text{Cs}_2\text{O}_2$  vary as  $\text{NaO}_x$  ( $x = 1.0, 1.03$ ),  $\text{KO}_x$  ( $x = 1.0, 1.1$ ), and  $\text{CsO}_x$  ( $x = 1.0, 1.2$ ).

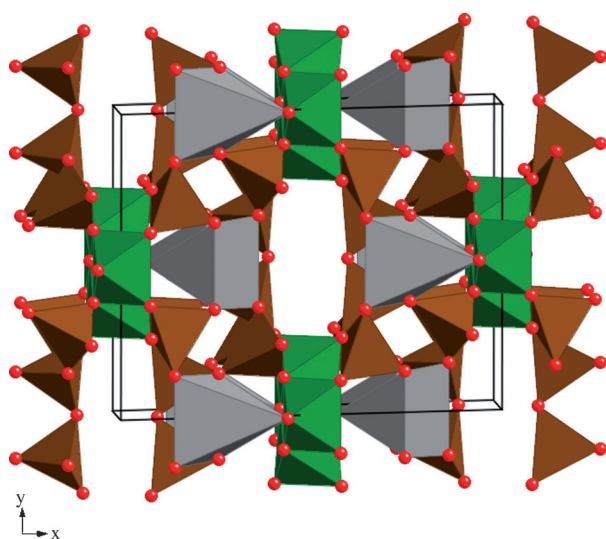


**Figure 5.** Crystal structure of  $\text{Pb}_3\text{MnAl}_{10}\text{O}_{20}$  viewed along [001].  $\text{PbO}_6$  and  $\text{PbO}_6$  polyhedra gray,  $\text{MnO}_6$  octahedra green,  $\text{AlO}_4$  tetrahedra brown, and  $\text{O}^{2-}$  ions red spheres.

but in neither case was lead fully incorporated into the product, although less lead contamination through substitution for Ca was reported when pre-reacted materials rather than the constituent oxides were used. Crystals of  $\text{Pb}_2\text{CoWO}_6$ <sup>[47]</sup> were successfully grown out of a  $\text{PbO}$  melt using a sealed platinum crucible. Polycrystalline  $\text{Pb}_2\text{CoWO}_6$  dissolved in  $\text{PbO}$  was slow cooled from 1130 °C to 830 °C at which time the flux was decanted by puncturing the crucible. This resulted in an easy isolation of  $3 \times 3 \times 3 \text{ mm}^3$  quasi-cubic crystals. Platinum containing crystals,  $\text{Sr}_4\text{PbPt}_4\text{O}_{11}$ ,<sup>[48]</sup> were grown out of  $\text{PbO}$  starting with Pt powder, suggesting that even platinum vessels may not be truly “inert” toward a  $\text{PbO}$  flux (a gold crucible was used for this synthesis). In this case, however, the presence of the basic strontium most likely facilitated the reaction with platinum to yield the first  $\text{Pt}_2^{6+}$  cation. The crystals were isolated as thin black needles upon cooling from 930 °C to 850 °C at a leisurely rate of 1 °C per hour, with the excess  $\text{PbO}$  flux removed by dissolution in hot acetic acid. Mixed transition-metal rare-earth-metal plumbate crystals,  $\text{Nd}_{0.75}\text{Pb}_{0.25}\text{MnO}_{2.72}$ ,<sup>[49]</sup> were grown out of a 1  $\text{PbO}$ :1.15  $\text{PbF}_2$  flux using a sixfold excess of flux. The binary reagents were dissolved in the flux at 1050 °C, slow cooled at 1.2 °C per hour to 885 °C, at which point excess flux was allowed to evaporate for 24 h prior to cooling to room temperature. Black cuboid crystals of  $2 \times 2 \times 3 \text{ mm}^3$  were isolated (Figure 6).

bate crystals,  $\text{Nd}_{0.75}\text{Pb}_{0.25}\text{MnO}_{2.72}$ ,<sup>[49]</sup> were grown out of a 1  $\text{PbO}$ :1.15  $\text{PbF}_2$  flux using a sixfold excess of flux. The binary reagents were dissolved in the flux at 1050 °C, slow cooled at 1.2 °C per hour to 885 °C, at which point excess flux was allowed to evaporate for 24 h prior to cooling to room temperature. Black cuboid crystals of  $2 \times 2 \times 3 \text{ mm}^3$  were isolated (Figure 6).

### 3.2. Bismuth Oxide

Bismuth oxide can be used as a safer alternative to  $\text{PbO}$  or  $\text{PbF}_2$ . As a melt (m.p. 817 °C), its physiochemical properties are similar to  $\text{PbO}$ , although it is somewhat less effective for dissolving oxides. It does have a significantly reduced volatility, however, owing to its high boiling point (1890 °C), which allows for longer soaking times during crystal growth. Owing to its large size and +3 charge, it can be used to grow crystals of complex oxides containing the large divalent cations with little likelihood of chemical substitution of  $\text{Bi}^{3+}$  for  $\text{M}^{2+}$ , however, it will readily substitute for some of the larger +3 cations, such as antimony or some of the larger rare-earth elements.

Typically, when  $\text{Bi}_2\text{O}_3$  fluxes are used for the growth of complex oxide single crystals, the bismuth cation is nearly always incorporated into the final product, an important consideration for using  $\text{Bi}_2\text{O}_3$  as a flux. An advantage, however, is that  $\text{Bi}_2\text{O}_3$  shows nearly the same versatility in the dissolution of all types of cations as  $\text{PbO}$  and/or  $\text{PbF}_2$ , once again the only exception being the alkali metals, which are a challenge to dissolve in  $\text{Bi}_2\text{O}_3$  and, hence, are rarely found in crystals grown out of  $\text{Bi}_2\text{O}_3$ . Reactions with  $\text{Bi}_2\text{O}_3$  are most often performed in open platinum crucibles, although alumina can also be used. Not only are longer soak times possible because of the lower volatility of  $\text{Bi}_2\text{O}_3$  compared with  $\text{PbO}$ , but also, for the same reason, higher temperatures, which can easily reach the range of 1000–1200 °C. Because the excess  $\text{Bi}_2\text{O}_3$  flux will not evaporate, following cooling, the solidified flux must be washed away with a dilute acid ( $\text{HCl}$  or  $\text{HNO}_3$ ) to isolate crystals of the final product. However, since the flux is quite dense ( $9.8 \text{ g cm}^{-3}$ ), the product often ends up



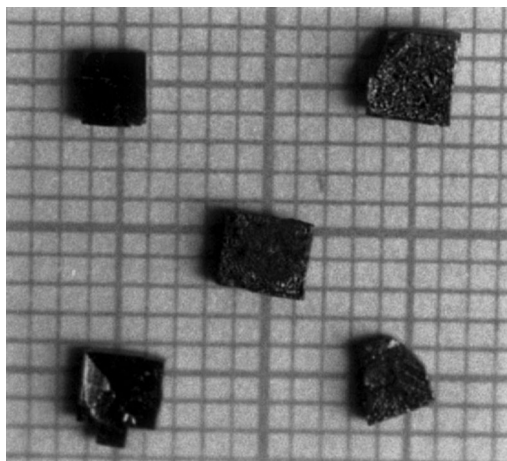


**Figure 6.** Photograph of cubic block crystals of  $\text{Nd}_{0.75}\text{Pb}_{0.25}\text{MnO}_{2.72}$  grown out of a  $\text{PbO-PbF}_2$  flux. Reprinted with permission from Ref. [139] Copyright 2003, Elsevier.

in the upper region of the solidified melt in the crucible, simplifying the isolation of the crystals.

$\text{Bi}_3\text{ScMo}_2\text{O}_{12}$ <sup>[50]</sup> was obtained as large yellow transparent anhedral crystals by the dissolution of the binary oxides in a  $\text{Bi}_2\text{O}_3$  flux. In addition to the target composition, side products include  $\text{Al}_2\text{O}_3$ , as well as  $\text{Sc}_2(\text{MoO}_4)$  and  $\text{Bi}_2\text{MoO}_6$  crystals. The melt was cooled from  $1150^\circ\text{C}$  to  $900^\circ\text{C}$  at a relatively quick rate of  $90^\circ\text{C}$  per hour, whereupon the furnace was turned off and allowed to cool to ambient temperature. Crystals of  $\text{Bi}_x\text{Ca}_y\text{MnO}_3$  ( $x=0.55$ ,  $y=0.45$ ;  $x=0.60$ ,  $y=0.40$ )<sup>[51]</sup> were successfully grown out of a  $\text{Bi}_2\text{O}_3$  flux at  $1094^\circ\text{C}$ , which was slow cooled at  $4^\circ\text{C}$  per hour to room temperature. Large cubic crystals with edges of up to 5 mm were isolated following removal of the flux using hot  $\text{HNO}_3$ . The zur Loye group prepared  $\text{Bi}_2\text{Fe}_2\text{Mn}_2\text{O}_{10}$ <sup>[52]</sup> and  $\text{Bi}_2\text{Fe}_2\text{Ga}_2\text{O}_9$ <sup>[53]</sup> from a fivefold excess of flux at  $1000^\circ\text{C}$  and  $950^\circ\text{C}$ , respectively. In each case the flux was cooled at  $5^\circ\text{C}$  per hour below the melting point of  $\text{Bi}_2\text{O}_3$  followed by rapid cooling to room temperature. The Mn compound formed as shiny black prisms with edges up to 1 mm, whereas the Ga compound formed significantly smaller brown prisms. Vanadates can be grown in  $\text{Bi}_2\text{O}_3$  fluxes, for example,  $\text{BiMg}_2\text{VO}_6$  (Figure 7)<sup>[54]</sup> was obtained as clear yellow needles from the dissolution of  $\text{MgO}$  and  $\text{NH}_4\text{VO}_3$  in  $\text{Bi}_2\text{O}_3$ . The mixture was cooled at  $15^\circ\text{C}$  per hour from  $1000^\circ\text{C}$  to  $500^\circ\text{C}$ , followed by furnace cooling.

Crystals of  $\text{BaBi}_{0.5}\text{Sb}_{0.5}\text{O}_3$ <sup>[55]</sup> were grown at  $1200^\circ\text{C}$  followed by slow cooling at  $5^\circ\text{C}$  per hour to  $800^\circ\text{C}$  in an alumina crucible covered with platinum foil. Dark brown crystals were separated mechanically from the flux.  $\text{Bi}_7\text{Ti}_4\text{NbO}_{21}$ <sup>[56]</sup> was prepared from the polycrystalline material dissolved in a fourfold excess of  $\text{Bi}_2\text{O}_3$  at  $1200^\circ\text{C}$  followed by cooling at  $5^\circ\text{C}$  per hour to  $700^\circ\text{C}$ . After washing with  $\text{HCl}$ , transparent mica-like crystals with a maximum dimension of 2.5 mm could be isolated.

Some non-Bi containing compositions have also been obtained from  $\text{Bi}_2\text{O}_3$  fluxes. For example,  $\text{BaFe}_{10.25}\text{Ir}_{0.85}\text{Co}_{0.85}\text{O}_{19}$  and  $\text{BaFe}_{10.90}\text{Ir}_{0.50}\text{Zn}_{0.50}\text{O}_{19}$ <sup>[57]</sup> were successfully grown from a  $\text{Bi}_2\text{O}_3$  flux at  $1250^\circ\text{C}$  followed by slow

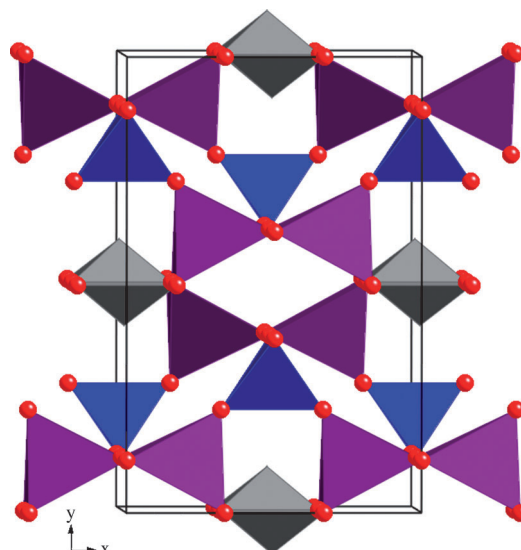


**Figure 7.** Crystal structure of  $\text{BiMg}_2\text{VO}_6$  viewed along  $[001]$ .  $\text{BiO}_5$  square pyramids gray,  $\text{MgO}_4$  tetrahedra purple,  $\text{VO}_4$  tetrahedra blue, and  $\text{O}^{2-}$  ions red spheres.

cooling at  $2^\circ\text{C}$  per hour to  $1000^\circ\text{C}$ . The hexagonal platelet crystals up to 3 mm across were extracted by dissolving the flux in hot dilute  $\text{HNO}_3$ , and according to microprobe analysis, contained less than 0.2% Bi impurity. Green-blue elongated prisms of  $\text{CuYb}_2\text{Ge}_4\text{O}_{12}$  (Figure 8)<sup>[58]</sup> were prepared from the dissolution of the binary oxides in a  $\text{Bi}_2\text{O}_3$  flux. Side products of this reaction also included crystals of  $\text{GeO}_2$  and  $\text{CuGeO}_3$ .  $\text{LaSr}_3(\text{Fe}_{0.8}\text{Al}_{0.2})_3\text{O}_{8.95}$ <sup>[59]</sup> was obtained by the step-wise heating of the binary oxides and  $\text{SrCO}_3$  in an alumina boat. Following heat treatments at  $1130^\circ\text{C}$ ,  $1125^\circ\text{C}$ , and  $1110^\circ\text{C}$ , the furnace was allowed to cool to  $600^\circ\text{C}$ , whereupon the sample was removed.

### 3.3. Boron Oxide or Alkali/Alkaline-Earth-Metal Borates

Boron oxide has a conveniently low melting point of  $450^\circ\text{C}$  and a high boiling point of  $1860^\circ\text{C}$ . This extended liquid range allows its use for many crystal growth applications. Its lack of toxicity compared with the lead-based systems also is an advantage. However, the viscosity of  $\text{B}_2\text{O}_3$  by itself is extremely high and not very attractive for crystal growth. As a result,  $\text{B}_2\text{O}_3$  is rarely used by itself. As mentioned above, the addition of monovalent cations can interfere with network formation and reduce the viscosity. Hence combinations of  $\text{A}_2\text{O}$  ( $\text{A} = \text{Li}, \text{Na}, \text{or K}$ ) and  $\text{B}_2\text{O}_3$  are preferred because of their more practical viscosity. Generally, for “complex” mixed-metal melts it is advantageous if a low-melting line phase exists that can generate the flux with the desired metal ratios upon melting. Hence, compounds such as  $\text{Na}_2\text{B}_4\text{O}_7$  ( $=\text{Na}_2\text{O} + 2\text{B}_2\text{O}_3$ ; m.p.  $743^\circ\text{C}$ ), or  $\text{K}_2\text{B}_4\text{O}_7$  ( $=\text{K}_2\text{O} + 2\text{B}_2\text{O}_3$ ; m.p.  $799^\circ\text{C}$ ), are convenient starting materials. Because  $\text{B}_2\text{O}_3$  is stable under extremely reducing conditions, boron oxide based fluxes can be used to grow oxide crystals containing metals in highly reduced oxidation states.

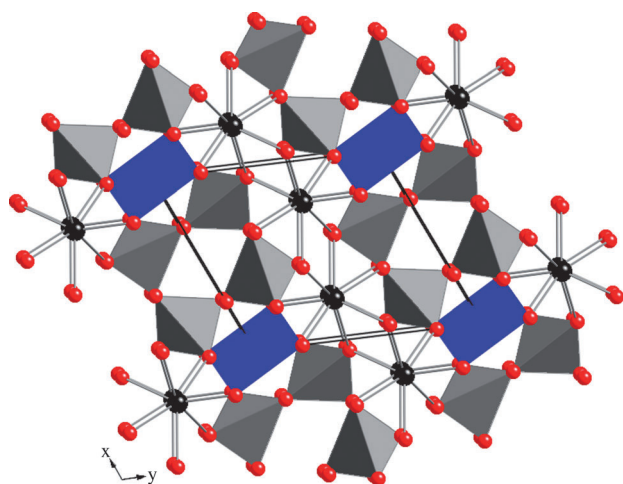


**Figure 8.** Crystal structure of  $\text{CuYb}_2\text{Ge}_4\text{O}_{12}$  viewed along  $c^*$ .  $\text{CuO}_4$  square planes blue,  $\text{Yb}^{3+}$  ions black spheres,  $\text{GeO}_4$  tetrahedra gray, and  $\text{O}^{2-}$  ions red spheres.

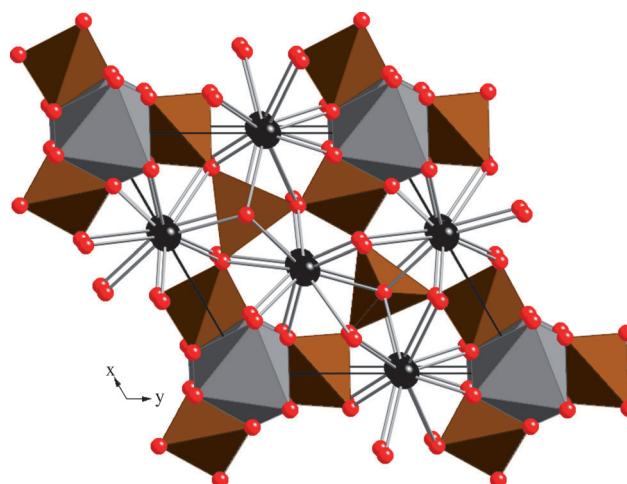


**Figure 9.** Crystal structure of  $\text{La}_3\text{SnGa}_5\text{O}_{14}$  viewed along  $c^*$ .  $\text{La}^{3+}$  ions black spheres,  $\text{SnO}_6$  octahedra gray,  $\text{GaO}_4$  tetrahedra brown, and  $\text{O}^{2-}$  ions red spheres.

Clearly, there is a very large variety of borate fluxes that can be used and while their properties are all similar, some are better for certain types of crystals than others. Furthermore, the choice between sodium and potassium, for example, as the additional monovalent cation, can influence whether or not chemical substitution of the monovalent cation will be a consideration during crystal growth. Of course, the small size of boron makes it unlikely for it to become substitutionally incorporated into complex oxides (as mentioned earlier, we have chosen to omit borates from the discussion of complex oxides). Borates show the same versatility for the dissolution of cations as the lead and bismuth fluxes, but can furthermore dissolve the alkali-metal cations. Because of the extremely high boiling point of boron oxide, the borates are typically used at temperatures in excess of  $1000^\circ\text{C}$ . Finally it is interesting to note that borate fluxes can have fairly high volatility and often evaporate during the crystal growth. If evaporation is not desired, the borates must be used in closed vessels, though they are even known to escape through grain boundaries from within sealed platinum capsules. Excess borate fluxes can be removed from the final product by washing in either hot water or hot acid ( $\text{HCl}$  or  $\text{HNO}_3$ ).

Both  $\text{SrLiCrTi}_4\text{O}_{11}$  and  $\text{SrLiFeTi}_4\text{O}_{11}$ <sup>[60]</sup> were grown out of  $\text{LiBO}_2$  fluxes, where the flux itself was prepared from  $\text{Li}_2\text{CO}_3$  and  $\text{H}_3\text{BO}_3$ . Crystals of  $\text{La}_3\text{SnGa}_5\text{O}_{14}$  (Figure 9)<sup>[61]</sup> were grown out of  $\text{LiBO}_2$ , although only 5 wt % of the flux was used. A pre-reacted powder of the product phase was used and crystals were obtained during slow cooling from  $1427^\circ\text{C}$  to  $1200^\circ\text{C}$  at  $20^\circ\text{C}$  per hour.  $\text{Sr}_6\text{TiNb}_4\text{O}_{18}$ <sup>[62]</sup> crystals were grown out of a  $\text{SrB}_4\text{O}_7$  flux prepared by heating  $\text{SrCO}_3$  and  $4\text{H}_3\text{BO}_3$ .  $\text{Sr}_6\text{TiNb}_4\text{O}_{18}$  was pre-synthesized and sealed together with the flux in a platinum capsule, heated to  $1400^\circ\text{C}$  and cooled at  $3^\circ\text{C}$  per hour to  $1130^\circ\text{C}$ . The flux was dissolved in warm  $\text{HCl}$ /ethanol to obtain block crystals. Crystals of  $\text{Ba}_4\text{CeNb}_{10}\text{O}_{30}$ <sup>[63]</sup> were obtained from a 1.0  $\text{BaO}$ :1.79  $\text{B}_2\text{O}_3$  flux contained in an alumina crucible. Again, pre-reacted powder of the product phase was mixed with the flux and the crucible, in this case,

was sealed inside a silica ampoule. Crystals were obtained during slow cooling from  $1050^\circ\text{C}$  to  $850^\circ\text{C}$  at  $6^\circ\text{C}$  per hour. Similarly, a  $\text{BaB}_2\text{O}_4$  flux was used in the growth of  $\text{BaMn}_{4.3}\text{Ti}_{1.4}\text{Fe}_{6.3}\text{O}_{19}$ <sup>[64]</sup> crystals (Figure 10) at  $1300^\circ\text{C}$ .

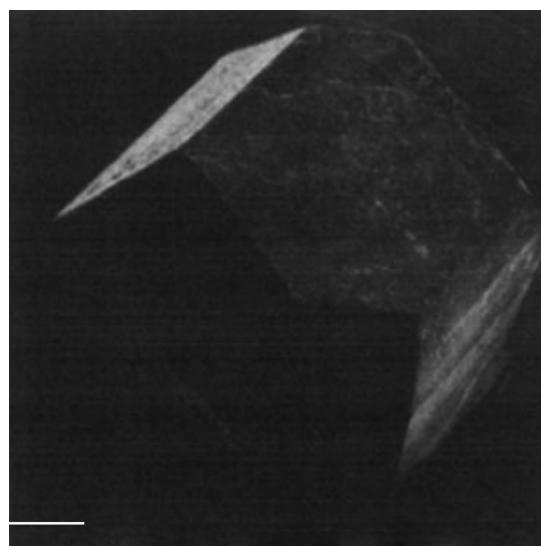


**Figure 10.** Scanning electron micrograph of a large prismatic crystal of  $\text{BaMn}_{4.3}\text{Ti}_{1.4}\text{Fe}_{6.3}\text{O}_{19}$  grown out of a  $\text{BaB}_2\text{O}_4$  flux. Scale bar 1 mm. Reprinted with permission from Ref. [64] Copyright 1987, Elsevier.

A potassium borate flux, 9  $\text{K}_2\text{O}$ :100  $\text{B}_2\text{O}_3$ , was used to crystallize  $\text{K}_9\text{BiU}_6\text{O}_{24}$ <sup>[65]</sup> by heating the binary oxides in the flux at  $1200^\circ\text{C}$  for 15 h and small transparent red crystals were isolated by dissolving the flux in boiling water. Another example of a potassium borate flux is  $\text{KBO}_2$ , which was used to obtain crystals of  $\text{Ba}_{12}\text{Fe}_{28}\text{Ti}_{15}\text{O}_{84}$ <sup>[66]</sup>. The binary oxides and carbonates were dissolved in the flux at  $1300^\circ\text{C}$ , held at that temperature for 36 h before slow cooling at  $3^\circ\text{C}$  per hour to  $1050^\circ\text{C}$ . The flux was dissolved in hot water to isolate shiny black plate crystals. Single crystals of

$\text{Ba}_{0.16}\text{Na}_{0.84}\text{Nb}_{0.84}\text{Ti}_{0.16}\text{O}_3$ <sup>[67]</sup> were successfully grown from a  $\text{Na}_2\text{B}_4\text{O}_7$  flux in a platinum crucible. The appropriate metal carbonates and oxides were dissolved in the flux at 1100 °C, before slow cooling to 850 °C; crystals up to  $1 \times 0.5 \times 0.5 \text{ mm}^3$  (Figure 11) could be isolated by washing in hot dilute nitric acid.

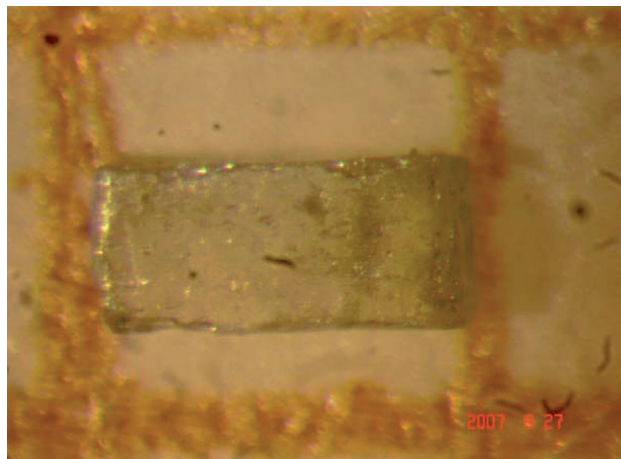


**Figure 11.** Photograph of a block-like single crystal of  $\text{Ba}_{0.16}\text{Na}_{0.84}\text{Nb}_{0.84}\text{Ti}_{0.16}\text{O}_3$  grown out of a  $\text{Na}_2\text{B}_4\text{O}_7$  flux. Reprinted with permission from Ref. [67] Copyright 2009, Elsevier.

### 3.4. Alkali- and/or Alkaline-Earth-Metal Halides

The alkali- and alkaline-earth-metal halides are very successful fluxes for oxide crystal growth. Their melting points—LiCl (m.p. 605 °C), NaCl (m.p. 801 °C), KCl (m.p. 770 °C), NaF (m.p. 993 °C), KF (m.p. 858 °C),  $\text{SrCl}_2$  (m.p. 874 °C), and  $\text{BaCl}_2$  (m.p. 962 °C)—fall into the useful range and they have a reasonable ability to dissolve oxides. Some of the fluorides such as  $\text{SrF}_2$  (m.p. 1477 °C) or  $\text{BaF}_2$  (m.p. 1368 °C), have somewhat inconveniently high melting points that typically preclude their use as neat melts, but they can be used as one component of a eutectic halide melt. In particular the fluorides have enhanced ability to dissolve oxides, where the fluoride anion can function as a mineralizer. Some of the more complex halides, such as a  $\text{Na}_3\text{AlF}_6$  (m.p. 1012 °C) are quite formidable solvents and, just like NaF and KF, cannot be contained in oxide crucibles, necessitating the use of platinum crucibles. The chlorides, on the other hand, can easily be contained in the less expensive alumina crucibles and the majority of crystal growth experiments have in fact been performed using alkali- and alkaline-earth-metal chlorides. Furthermore, a significant advantage of halide melts is the ease with which the flux can be removed upon completion of the crystal growth experiment by simply dissolving the flux with water. Of course, this may not even be necessary since using halide melts at temperatures in excess of roughly 1000 °C can lead to significant flux evaporation that can positively affect the crystal growth by creating supersaturation in the melt, as well as help with crystal isolation if all the flux has evaporated.

Halide melts can be used to dissolve a wide range of elements, including transition metals, main-group metals, rare-earths, and actinides. The alkali- and alkaline-earth metals are typically introduced as the carbonates if they themselves are not part of the halide flux. Owing to their high stability, halide melts can be used to grow crystals of oxides containing metals in reduced oxidation states. The specific reaction conditions vary with the melting point of the specific flux and the need for various amounts of flux excess for the specific oxide. The temperatures are typically at least 900 °C and rarely in excess of 1400 °C. The most common temperatures fall into the 1000–1100 °C range.

A large variety of oxide structure types and compositions have been crystallized from halide melts. Single crystals of various members of the extended perovskite families have been obtained, such as  $\text{Ba}_6\text{Al}_2\text{Rh}_2\text{Ho}_2\text{O}_{15}$ ,<sup>[68]</sup> which was grown out of a  $\text{BaCl}_2 \cdot 2\text{H}_2\text{O}$  melt contained in an alumina boat by slow cooling from 1040 °C to room temperature at 10 °C per hour. To obtain the black hexagonal plates, the rhodium was introduced as the metal and oxidized during the crystal growth process. Similarly,  $\text{Ba}_3\text{CaRu}_2\text{O}_9$ <sup>[69]</sup> was obtained in the form of light brown platelets by starting with Ru powder,  $\text{CaCO}_3$ , and  $\text{BaCl}_2 \cdot 2\text{H}_2\text{O}$  as the flux upon soaking at 1025 °C for three weeks. Since most of the flux had evaporated by this time, the isolation of the large black hexagonal plates was trivial. The preparation of  $\text{Ca}_3\text{IrCuO}_6$ ,<sup>[70]</sup> a 2H-perovskite related oxide, using a  $\text{CaF}_2/\text{KF}$  1:1 melt in tenfold excess over  $\text{Ca}(\text{OH})_2$ , CuO, and Ir powder (1:1:1) in a platinum boat succeeded after soaking at 1020 °C for 8 days followed by cooling to room temperature at 20 °C per hour. Crystals of another 2H-perovskite related oxide,  $\text{Sr}_3\text{NiPbO}_6$ ,<sup>[71]</sup> were obtained by starting with the pre-formed  $\text{Sr}_3\text{PbNiO}_6$  in a 10-fold excess of NaCl in an alumina crucible. Heating to 1000 °C for 24 h followed by rapid cooling at 50 °C per hour to 750 °C and then quenching to 25 °C resulted in black faceted block crystals (Figure 12) that were isolated by dissolving the flux in water.

A number of vanadates, molybdates, and tungstates have been grown out of halide melts, such as  $\text{K}_6(\text{UO}_2)_5(\text{VO}_4)_2\text{O}_5$  (Figure 13),<sup>[72]</sup> which was grown in a 30-fold excess of KCl. Orange crystals were produced by soaking the starting

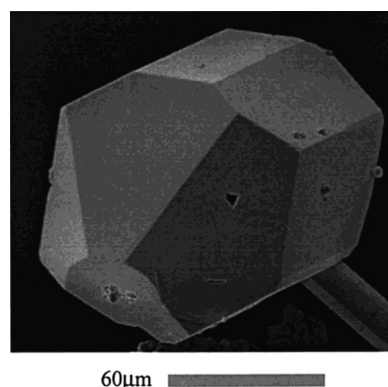


**Figure 12.** Scanning electron micrograph of a large prismatic crystal of  $\text{Sr}_3\text{PbNiO}_6$  grown out of a NaCl flux. Reprinted with permission from Ref. [71] Copyright 1999, American Chemical Society.



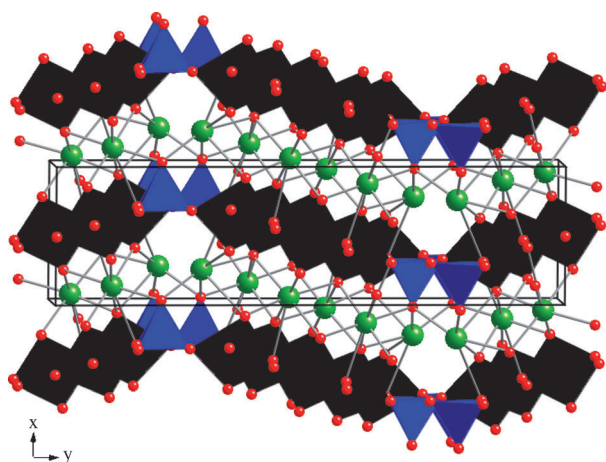


**Figure 13.** Crystal structure of  $K_6(UO_2)_5(VO_4)_2O_5$  viewed along  $[001]$ .  $K^+$  ions green spheres,  $UO_6$  octahedra black,  $VO_4$  tetrahedra blue, and  $O^{2-}$  ions red spheres.

material  $(UO_2)_3(VO_4)_2$  in the flux at  $775^\circ\text{C}$  for 3 days followed by slow cooling to  $25^\circ\text{C}$  and removing the KCl by washing with water. Crystals of  $Li_3Sc(MoO_4)_3$  [73] with sizes up to 0.5 mm in length were grown out of NaF contained in a covered platinum crucible by soaking  $MoO_3$ ,  $Sc_2O_3$ ,  $Al_2O_3$ , and  $TiO_2$  at  $1150^\circ\text{C}$  for 6 h followed by cooling at  $90^\circ\text{C}$  per hour to  $900^\circ\text{C}$  then quenching to room temperature. Neither the aluminum nor the titanium were incorporated into the major product, however, small colorless octahedra of  $LiAl_5O_8$  and  $(Al_xSc_{1-x})_2TiO_5$  were isolated in minor yield.  $Na_7Nb_{15}W_{13}O_{80}$  [74] crystallized in a melt of NaCl at  $897^\circ\text{C}$ , followed by slow cooling at  $1^\circ\text{C}$  per hour to generate small platelets. The spinel compound  $Li_{0.65}Co_{1.29}Mn_{1.06}O_4$  [75] was prepared from a 1:1 ratio of  $CoCl_2$  and  $MnCl_2$  with a sixty fold excess of LiCl serving as a flux. The mixture was heated at  $750^\circ\text{C}$  for 60 h, before cooling to room temperature and dissolving the flux in water to reveal black octahedral crystals (Figure 14).

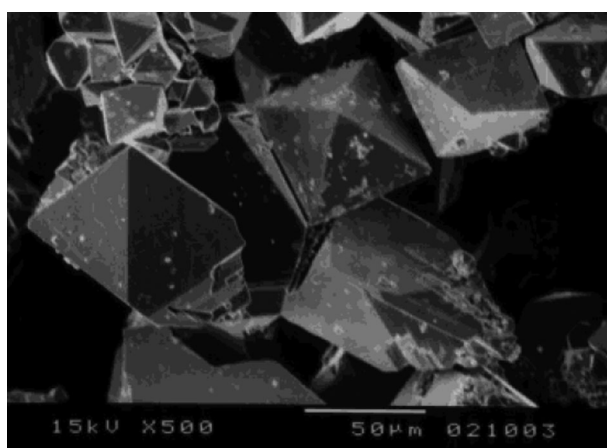


**Figure 14.** Scanning electron micrograph of octahedral crystals of  $Li_{0.65}Co_{1.29}Mn_{1.06}O_4$  grown out of a LiCl flux. Reprinted with permission from Ref. [75] Copyright 2003, American Chemical Society.

A complex reduced niobate,  $Rb_4Al_2Nb_{35}O_{70}$  [76] was crystallized in an alumina boat sealed inside an evacuated silica tube.  $Na_3NbO_4$  and NbO were dissolved in a tenfold excess of RbCl at  $1050^\circ\text{C}$  by soaking for 12 h followed by slow cooling at  $10^\circ\text{C}$  per hour to  $700^\circ\text{C}$ . Another reduced niobate grown out of a halide flux is  $Na_3Al_2Nb_{34}O_{64}$  [77] which was crystallized over the course of one week from NaF,  $Al_2O_3$ , NbO<sub>2</sub>, and NbO in a 3:1:8:2 ratio at  $850^\circ\text{C}$ , and dark gold metallic platelets were isolated by dissolving any residual materials in concentrated HCl.

### 3.5. Alkali-Metal Carbonates

The alkali-metal carbonates are very effective melts for oxides and can also be used successfully with platinum group elements to grow crystals of complex oxides containing platinum group metals. Unlike the alkaline-earth-metal carbonates, which decompose by  $CO_2$  loss on heating, the alkali-metal carbonates dissociate into the alkali-metal cation and the carbonate anion. The melting points of  $Na_2CO_3$  (m.p.  $851^\circ\text{C}$ ) and  $K_2CO_3$  (m.p.  $891^\circ\text{C}$ ) are convenient. The lighter lithium and sodium carbonates can exhibit some volatility, which is often beneficial in order to induce supersaturation of the reagents in solution.

Alkali-metal carbonate fluxes have been utilized for the growth of numerous oxide single crystals; however, it is difficult to predict a priori whether or not the alkali-metal cation will be incorporated into the final product. Alkaline-earth metals, main-group metals, and transition metals all appear to be highly soluble in carbonate melts. Unfortunately rare-earth and actinide elements are seemingly less soluble in an alkali-metal carbonate flux, although there are some examples of crystals grown from carbonate melts that contain these elements. The alkali-metal carbonates are most often used in alumina crucibles as there is no reaction with the alumina. Common soak temperatures for the alkali-metal carbonates range from  $1000$ – $1150^\circ\text{C}$ , with typical soak times of 24–48 h. Removal of the flux following crystal growth is easy due to the high solubility of carbonates in water.

A number of complex oxides containing platinum group elements have been grown as single crystals from carbonate melts by the zur Loye group. Both  $Sr_3NiPtO_6$  and  $Sr_3CuPtO_6$  [78] were prepared from the dissolution of  $SrCO_3$ , Pt metal, and the corresponding binary oxide in a  $K_2CO_3$  melt. Smaller, but higher quality crystals (suitable for single-crystal X-ray diffraction) were obtained with a reaction temperature of  $1050^\circ\text{C}$ , whereas larger crystals (suitable for physical property measurements) up to 5 mm in length were obtained with a higher reaction temperature of  $1150^\circ\text{C}$ . Crystals of  $Pr_{2.45}Na_{1.55}RhO_6$  and  $Nd_{2.45}Na_{1.55}RhO_6$  [79] were successfully grown from a  $Na_2CO_3$  flux at  $1050^\circ\text{C}$  and small black blocks were isolated by the dissolution of the flux in water aided by sonication.  $Ca_3CuRhO_6$  [80] was obtained from  $CaCO_3$ , Cu, and Rh in a  $K_2CO_3$  melt at  $1050^\circ\text{C}$ . Hexagonal crystals (Figure 15) could be isolated after washing the flux away with water. Two rhodates with the same elemental content but different composition,  $SrFe_{0.71}Rh_{0.29}O_3$  and  $Sr_4Fe_{0.73}Rh_{2.27}O_9$  [81] were prepared from  $K_2CO_3$  melts under the same heating and



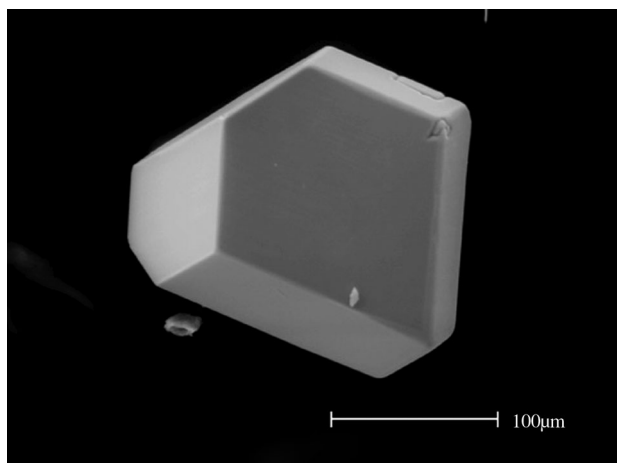


**Figure 15.** Scanning electron micrograph of a hexagonal crystal of  $\text{Ca}_3\text{CuRhO}_6$  grown out of a  $\text{K}_2\text{CO}_3$  flux. Reprinted with permission from Ref. [80] Copyright 2003, Elsevier.

cooling conditions. The only difference in the crystal growth process was the reagents that were used as the Sr sources:  $\text{SrCO}_3$  for the former, and  $\text{SrCl}_2 \cdot 6\text{H}_2\text{O}$  for the latter, and it was hypothesized that the  $\text{Cl}^-$  anion in the flux mixture may have favored the formation of the Rh-rich phase. Long hexagonal rods (Figure 16) of  $\text{Ba}_8\text{CoRh}_6\text{O}_{21}$  were prepared by the dissolution of  $\text{BaCO}_3$ ,  $\text{Co}_3\text{O}_4$ , and Rh in a  $\text{K}_2\text{CO}_3$  melt

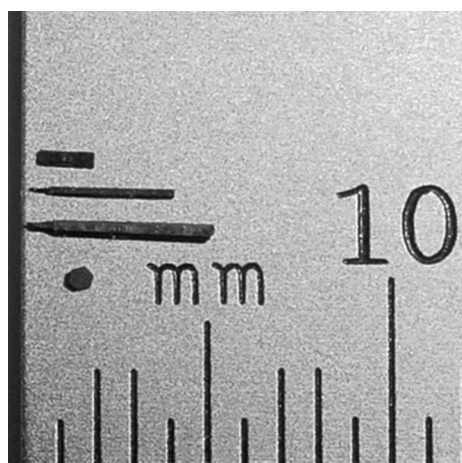


**Figure 16.** Photograph of long hexagonal rods of  $\text{Ba}_8\text{CoRh}_6\text{O}_{21}$  grown out of a  $\text{K}_2\text{CO}_3$  flux. Reprinted with permission from Ref. [82] Copyright 2001, American Chemical Society.

at  $1050^\circ\text{C}$ . Another platinum group based oxide,  $\text{Ca}_3\text{LiRuO}_6$ ,<sup>[83]</sup> was obtained as dark red hexagonal rods from the polycrystalline material dissolved in a tenfold mass excess of flux, which consisted of a 1:1 mixture of  $\text{Li}_2\text{CO}_3$  and  $\text{K}_2\text{CO}_3$ . The melt was cooled from  $1025^\circ\text{C}$  to  $750^\circ\text{C}$  at  $6^\circ\text{C}$  per hour, whereupon the furnace was turned off and allowed to cool to room temperature.

Crystals of oxides containing early transition elements, such as transparent crystals of  $\text{Li}_7\text{La}_3\text{Zr}_2\text{O}_{12}$ ,<sup>[84]</sup> were successfully grown from a  $\text{Li}_2\text{CO}_3$  flux. The polycrystalline materials

was mixed with the flux in a gold crucible and heated at  $1040^\circ\text{C}$  for 48 h.  $\text{Na}_3\text{Ca}_2\text{TaO}_6$ <sup>[85]</sup> and  $\text{Na}_2\text{Ca}_3\text{Ta}_2\text{O}_9$ <sup>[86]</sup> were obtained as colorless transparent crystals from the dissolution of  $\text{CaCO}_3$  and  $\text{Ta}_2\text{O}_5$  in a  $\text{Na}_2\text{CO}_3$  flux. The starting materials were pressed into a pellet, which was heated at  $1000^\circ\text{C}$  on a platinum plate, before being cooled at  $3^\circ\text{C}$  per hour to  $800^\circ\text{C}$ , at which point the furnace was turned off. A higher ratio of flux to  $\text{Ta}_2\text{O}_5$  in the starting materials was reflected in the ratio of Na to Ta in the final products. The Abraham group prepared a series of uranium containing oxides including  $\text{A}_2(\text{UO}_2)_2\text{MO}_6$  ( $\text{A} = \text{K}, \text{Rb}$ ;  $\text{M} = \text{Mo}, \text{W}$ ) and  $\text{K}_8(\text{UO}_2)_8(\text{MoO}_5)_3\text{O}_6$ <sup>[87,88]</sup> from a  $\text{A}_2\text{CO}_3$  melt heated to  $950^\circ\text{C}$  in a platinum crucible. The melt was cooled at  $5^\circ\text{C}$  per hour to  $25^\circ\text{C}$ , and the excess flux was washed away with ethanol to isolate the crystals.

$\text{K}_{1.76}\text{Mg}_{3.25}\text{Sb}_{4.75}\text{O}_{16}$ <sup>[89]</sup> was obtained as transparent needle crystals from the dissolution of the binary oxides in a  $\text{K}_2\text{CO}_3$  flux. The starting materials were sealed in a platinum tube, which was heated to  $1500^\circ\text{C}$  for 150 min, cooled at  $10^\circ\text{C}$  per hour to  $1300^\circ\text{C}$ , at which point the tube was removed from the furnace. Crystals of  $\text{BaZn}_2\text{Fe}_{16}\text{O}_{27}$ <sup>[90]</sup> were successfully grown out of a  $\text{Na}_2\text{CO}_3$  melt at  $1340^\circ\text{C}$ . The reaction was performed in a covered platinum crucible; after cooling the reaction to room temperature, the excess flux was removed with hot nitric acid. The Darriet group prepared both  $\text{Sr}_4\text{Mn}_2\text{NiO}_9$ <sup>[91]</sup> and  $\text{Sr}_4\text{Mn}_2\text{CuO}_9$ <sup>[92]</sup> from the dissolution of  $\text{SrCO}_3$ ,  $\text{Mn}_2\text{O}_3$ , and the corresponding metal oxide in a  $\text{K}_2\text{CO}_3$  flux. The reactions took place at  $1100^\circ\text{C}$  and  $927^\circ\text{C}$ , respectively; after cooling to room temperature, small block crystals were isolated by washing the flux away with water. Crystals of  $\text{Li}_{1.746}\text{Nd}_{4.494}\text{FeO}_{9.493}$  (Figure 17)<sup>[93]</sup> were obtained from polycrystalline  $\text{Li}_5\text{Nd}_4\text{FeO}_{10}$  heated in a 70 wt %  $\text{Li}_2\text{CO}_3$  melt for  $760^\circ\text{C}$  for 2 weeks. The flux was removed using a combination of water, alcohol, and dilute acetic acid, revealing black polyhedral crystals.

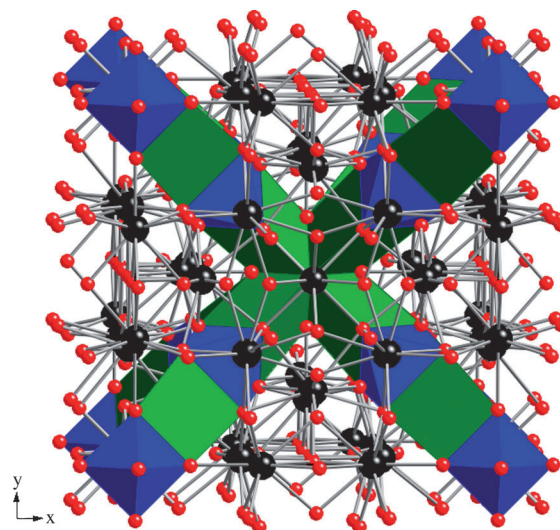


**Figure 17.** Crystal structure of  $\text{Li}_{1.746}\text{Nd}_{4.494}\text{FeO}_{9.493}$  viewed along [001].  $\text{LiO}_6$  trigonal prisms green,  $\text{Nd}^{3+}$  ions black spheres,  $\text{FeO}_6$  octahedra blue, and  $\text{O}^{2-}$  ions red spheres.

### 3.6. (Alkali-Metal) Vanadates, Molybdates, and/or Tungstates

The binary oxides,  $V_2O_5$  (m.p. 690°C),  $MoO_3$  (m.p. 795°C), and  $WO_3$  (m.p. 1473°C) have all been used as fluxes in spite of their significant volatility. In fact, crystals of the simple oxides can readily be grown from the vapor phase. The sodium salts,  $NaVO_3$  (m.p. 630°C),  $Na_3VO_4$  (m.p. 858°C),  $Na_2MoO_4$  (m.p. 687°C),  $Na_2Mo_2O_7$  (m.p. 876°C),  $Na_2WO_4$  (m.p. 698°C), and  $Na_2W_2O_7$  (m.p. 746°C) on the other hand are much more attractive for oxide crystal growth, both because of their ability to dissolve oxides, but mostly for their reduced volatility. In addition, the sodium salts are water-soluble and can, thus, be readily removed. The lithium salts, such as  $Li_2MoO_4$  (m.p. 705°C) and eutectics containing  $Li_2MoO_4$ , have been used to prepare beryllium-containing oxides and, thus, apparently create a more covalent melt. Typically there is little concern about substitutional processes due to the high oxidation states, as  $V^{5+}$ ,  $Mo^{6+}$ , and  $W^{6+}$  frequently occupy their own crystallographic site in the product phase.

These fluxes are very versatile as far as the dissolution of cations is concerned, with only alkaline-earth metals rarely being found in crystals grown from these fluxes. Nearly any type of reaction vessel can be used with this family of fluxes. The optimal temperature range is commonly below 800°C, where higher temperatures necessitate the use of closed vessels to prevent excessive evaporation. The alkali-metal vanadates, molybdates, and tungstates can easily be dissolved in water or hot alkali solutions to remove leftover flux from the crystalline product.

A uranium-containing oxide,  $Pb(UO_2)(V_2O_7)$ ,<sup>[94]</sup> was obtained from a vanadate flux by the dissolution of  $PbO$  and  $U_3O_8$  in  $V_2O_5$ . The reaction mixture was heated in a platinum crucible approximately at the melting point of  $V_2O_5$  for 2 h, before cooling to room temperature at 5°C per hour; the product was washed with ethanol to isolate the yellow crystals. Thorium containing oxides also are accessible using these fluxes, where  $K_2Th(MoO_4)_3$ <sup>[95]</sup> and  $K_8Th(MoO_4)_6$ <sup>[96]</sup> were prepared as triangular prism and plate crystals respectively from  $Th(MoO_4)_2$  and  $K_2MoO_4$ . The more potassium-rich phase could be obtained by adjusting the ratio of flux to reagent from 3:2 to 3:1 and using a quicker cooling rate.

The compounds  $NaCa_2MV_3O_{12}$  ( $M = Mg, Co, Ni$ )<sup>[97]</sup> were prepared by reacting the polycrystalline material with  $NaVO_3$  in ratios ranging from 2:3 to 4:1. The mixtures were soaked at temperatures of 756°C (Ni), 735°C (Mg), and 705°C (Co) for 20 h, cooled 65°C in 30 min, heated at that temperature for an additional 50 h, and then quenched to produce crystals (Figure 18).  $RbMnVO_4$ <sup>[98]</sup> crystals were grown from  $MnO$  dissolved in a  $RbVO_3$  melt contained within a gold tube sealed in a silica tube, and heated to 950°C. The yellow hexagonal block crystals of  $RbMnVO_4$  were accompanied by clear crystals of  $RbVO_3$ , dark green crystals of  $MnO$ , and yellow-green crystals of  $Rb_2MnV_2O_7$ . Red block crystals of  $Ln_2(Mo_4Sb_2O_{18})$  ( $Ln = Y, La, Nd, Sm, Dy$ ) (Figure 19)<sup>[99]</sup> were successfully grown in evacuated quartz tubes. The binary oxides  $Ln_2O_3$  and  $Sb_2O_3$  were reacted with molten  $MoO_3$  at 900°C for 4 days. Following the reaction, excess  $MoO_3$  flux was washed away with a 2%  $Na_2CO_3$  solution.

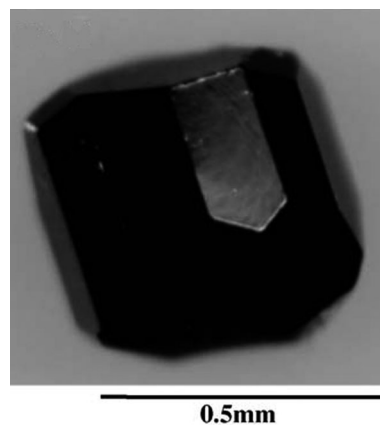


**Figure 18.** Scanning electron micrograph of a prismatic crystal of  $NaCa_2CoV_3O_{12}$  grown out of a  $NaVO_3$  flux. Reprinted with permission from Ref. [97] Copyright 2006, Elsevier.

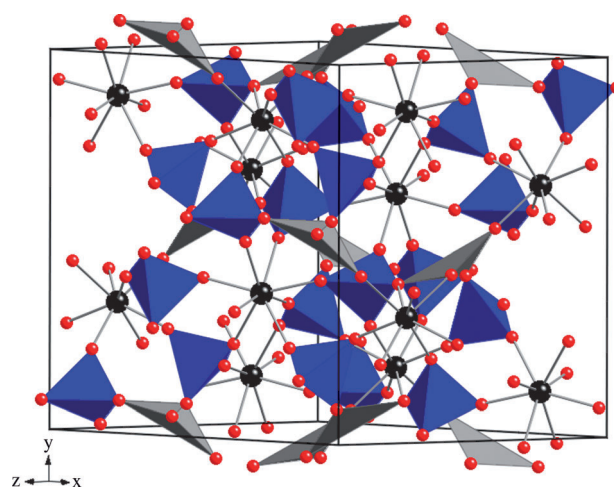


**Figure 19.** Crystal structure of  $Ln_2(Mo_4Sb_2O_{18})$  ( $Ln = Y, La, Nd, Sm, Dy$ ).  $Ln^{3+}$  ions black spheres,  $MoO_4$  tetrahedra blue,  $SbO_5$  square pyramids gray, and  $O^{2-}$  ions red spheres.

Deep blue needles of  $Na_{1.7}Cr_{1.7}Ti_{6.3}O_{16}$ <sup>[100]</sup> were obtained at 1300°C from  $Na_2CO_3$ ,  $Cr_2O_3$ , and  $TiO_2$  in a fourteen fold mass excess of  $Na_2MoO_4$  as flux.  $Na_2MoO_4$  was generated in situ from the reaction of  $Na_2CO_3$  and  $MoO_3$ , and could be washed away after the reaction with water.  $InGaO_3(ZnO)_2$ <sup>[101]</sup> hexagonal plates (Figure 20) were grown as single crystals in a sealed platinum tube at 1350°C. The binary oxides were dissolved in molten  $K_2MoO_4$  in a 1:20 ratio by mass. Crystals of  $Rb_3LiZn_2(MoO_4)_4$ <sup>[102]</sup> were successfully grown from the polycrystalline material dissolved in a melt of  $Rb_2Mo_2O_7$ . After cooling the mixture at 3°C per hour from 500°C to 400°C, colorless cubes with edges up to 2 mm were isolated. The compounds  $ANbW_2O_9$  ( $A = K, Rb$ )<sup>[103]</sup> were obtained as crystals from  $Nb_2O_5$  reacted in a flux consisting of  $K_2O-WO_3$  or  $Rb_2O-WO_3$ . Cooling of the mixture at 1°C per hour from 1050°C to 700°C produced large hexagonal plate-like or prismatic crystals between 5 and 10 mm. Light brown hexagonal prisms of  $KFeGeO_4$ <sup>[104]</sup> were grown with a 1:1 mixture of  $KVO_3$  to  $K_2MoO_4$  as flux. The polycrystalline

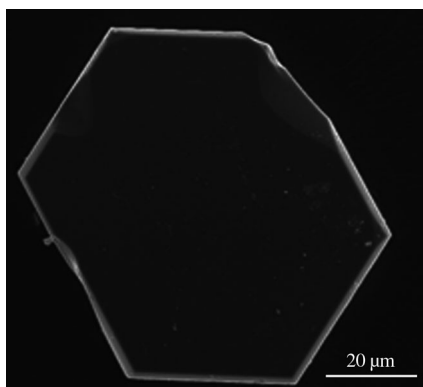


**Figure 20.** Scanning electron micrograph of a hexagonal plate of  $\text{InGaO}_3(\text{ZnO})_2$  grown out of a  $\text{K}_2\text{MoO}_4$  flux. Reprinted with permission from Ref. [101] Copyright 2009, Wiley.

material was heated in the melt at  $875^\circ\text{C}$  for 3 days, and then cooled at an extremely low rate of  $0.6^\circ\text{C}$  per hour to  $725^\circ\text{C}$ ; following cooling to room temperature, the excess flux was removed by soaking in hot water.

### 3.7. Alkali-Metal Oxides, Peroxides, and/or Superoxides

One extensive collection of oxides that have been used as fluxes for the preparation of many water sensitive compounds is the binary alkali-metal oxides, peroxides and superoxides. As a group they are extremely moisture sensitive and react violently with water to form the hydroxides. These simple oxides,  $\text{Na}_2\text{O}$  (m.p.  $1132^\circ\text{C}$ ),  $\text{K}_2\text{O}$  (m.p.  $707^\circ\text{C}$ ),  $\text{Rb}_2\text{O}$  (m.p.  $> 500^\circ\text{C}$ ),  $\text{Cs}_2\text{O}$  (m.p.  $490^\circ\text{C}$ ), the peroxides  $\text{Na}_2\text{O}_2$  (m.p.  $675^\circ\text{C}$ ) and  $\text{K}_2\text{O}_2$  (m.p.  $490^\circ\text{C}$ ), and the superoxides  $\text{KO}_2$  (m.p.  $\approx 490\text{--}530^\circ\text{C}$ ), and  $\text{CsO}_2$  (m.p.  $432^\circ\text{C}$ ) have been used as melts for the growth of many alkali-metal–transition-metal oxides, especially by the group of Hoppe.

The alkali-metal oxides, peroxides, and superoxides have been used with all families of elements throughout the periodic table. In a typical crystal growth reaction, the binary oxides are mixed with additional oxide reagents—carefully dried prior to use—and heated slightly above the melting point of the binary oxides and held at that temperature for weeks and even months. The reaction has to be contained inside a nickel, silver, gold or platinum ampoule that, in turn, is typically sealed under vacuum within a silica tube. This assures the absence of moisture during the reaction. This approach is well suited to prepare alkali-metal-rich oxide compositions that as a rule are extremely moisture sensitive. Due to this acute moisture sensitivity, no solvent can be used to wash away the excess flux, so crystals must be mechanically isolated. (As a note, we were unable to find photographs of any crystals grown from these fluxes due to their rapid decomposition in ambient conditions.)

The synthesis of  $\text{Cs}_2\text{Na}_2[\text{IrO}_4]$  (Figure 21),<sup>[5]</sup> for example, was achieved by mixing  $\text{CsO}_{0.52}$ ,  $\text{Na}_2\text{O}_2$ ,  $\text{IrO}_2$ , and iridium metal in a 3.52:1.3:1:1 ratio in a silver tube contained inside a sealed silica tube. The mixture was heated quickly to  $400^\circ\text{C}$ , then slowly to  $760^\circ\text{C}$  and held there for 46 days to yield very

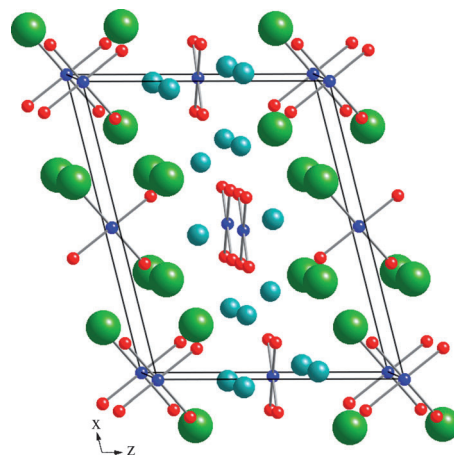


**Figure 21.** Crystal structure of  $\text{Cs}_2\text{Na}_2[\text{IrO}_4]$  viewed along  $b^*$ .  $\text{Cs}^+$  ions green spheres,  $\text{Na}^+$  ions turquoise spheres,  $\text{Ir}^{4+}$  ions blue spheres, and  $\text{O}^{2-}$  ions red spheres.

water sensitive black block crystals. Similarly,  $\text{CsK}_5[\text{RuO}_5]\text{--}[\text{RuO}_4]$ <sup>[105]</sup> was prepared by heating intimate mixtures of the binary oxides,  $\text{KO}_{1.1}$ ,  $\text{CsO}_{1.2}$ ,  $\text{RuO}_2$ , in a ratio of K:Cs:Ru 2.2:1:1, in a silver tube contained inside a sealed silica tube at  $750^\circ\text{C}$  for 34 days. Dark green water sensitive block shaped crystals could be isolated. The synthesis of  $\text{Cs}_2[\text{Li}_3\text{GaO}_4]$ <sup>[106]</sup> was carried out by heating a mixture of  $\text{Cs}_2\text{O}$  and  $\text{Li}_5\text{GaO}_4$  in a ratio of 2:1 in a sealed platinum tube which in turn was sealed inside a silica tube, at  $750^\circ\text{C}$  for 8 weeks. Colorless, irregularly shaped air sensitive crystals were formed. Similarly, crystals of  $\text{Rb}_3\text{NaPbO}_4$ <sup>[107]</sup> were obtained from the reaction of  $\text{Na}_2\text{PbO}_3$  and  $\text{RbO}_{0.84}$ , using a ratio of Rb:Na:Pb = 4:2:1 contained in a silver boat inside a silica tube. The mixture was heated at  $5^\circ\text{C}$  per hour to  $480^\circ\text{C}$  for 180 days and then cooled at a rate of  $3^\circ\text{C}$  per hour to room temperature to yield colorless water sensitive crystals.

Reactions that used a large excess of the alkali metal—implicitly as a flux—were used to prepare oxides like  $\text{Sr}_{12}\text{NaNi}_7\text{O}_{23}$ .<sup>[108]</sup> In this crystal growth experiment, an excess of  $\text{Na}_2\text{O}_2$  was added to a mixture of  $\text{SrCO}_3$  and  $\text{NiO}$  in a 2:1 ratio that had been pre-reacted at  $1000^\circ\text{C}$  for one day. With the  $\text{Na}_2\text{O}_2$  functioning as the flux, the reaction mixture was contained in a sealed silver tube and heated at  $750^\circ\text{C}$  for six days to yield black crystals of  $\text{Sr}_{12}\text{NaNi}_7\text{O}_{23}$ . The preparation of single crystals of  $\text{Ba}_3\text{In}_2\text{Zn}_5\text{O}_{11}$  (Figure 22)<sup>[109]</sup> using a  $\text{KO}_2$  flux illustrates the rare example where the alkali metal is not incorporated into the final product.  $\text{BaO}$ ,  $\text{ZnO}$  and  $\text{In}_2\text{O}_3$  as reactants together with  $\text{KO}_2$  as the flux in a ratio of 2:1:1:2 were sealed inside a silver tube and heated at  $750^\circ\text{C}$  for 12 days. The tube was cooled at  $2.5^\circ\text{C}$  per hour to room temperature to yield colorless octahedral crystals.

### 3.8. Alkali- and/or Alkaline-Earth-Metal Hydroxides

Hydroxides have been used extensively for oxide crystal growth and are in many ways a more complex flux than other simple inorganic salts, as their water content has a significant effect on the oxo-acidity ( $pH_2\text{O}$ ) of the melt. The hydroxides



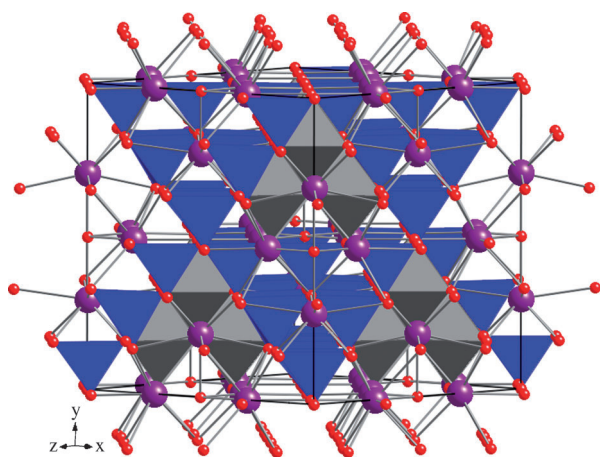


**Figure 22.** Crystal structure of  $\text{Ba}_3\text{In}_2\text{Zn}_5\text{O}_{11}$ .  $\text{Ba}^{2+}$  ions purple spheres,  $\text{InO}_6$  octahedra gray,  $\text{ZnO}_4$  tetrahedra blue, and  $\text{O}^{2-}$  ions red spheres.

have low melting points, such as 462 °C for LiOH, 318 °C for NaOH, 420 °C for KOH, 301 °C for RbOH, 342 °C for CsOH, 375 °C for  $\text{Sr}(\text{OH})_2$ , and 407 °C for  $\text{Ba}(\text{OH})_2$ . These can be further reduced to below 200 °C for eutectic combinations. In addition, the water content of the hydroxides (commercially available hydroxides have a water content of 15–20 wt %) will influence the melting point, which decreases with increasing water content up to the limit of forming an aqueous solution. Consequently, their melting points can change upon heating and water loss, unless they are kept in a closed system. In the extreme case they will transform into the simple oxide anhydrides. The water content is critical to determining the solution chemistry, which can range from highly acidic for hydrated hydroxides (high  $p\text{H}_2\text{O}$ ), to extremely basic for the oxide anhydrides (low  $p\text{H}_2\text{O}$ ), as described by the Lux-Flood concept of oxo-acidity.<sup>[32,33]</sup> Different metal cations will be soluble in specific ranges of acidity, and essentially every element in the periodic table can be dissolved in hydroxide melts, albeit not all at the same  $p\text{H}_2\text{O}$ . A detailed report on the use of hydroxide melts to grow platinum metal containing oxides was recently published, which focuses on the many peculiarities of crystal growth using hydroxide fluxes.<sup>[2]</sup>

As a class, hydroxides are capable of dissolving essentially every element of the periodic table and, when performed in air, have a tendency to stabilize the metals in high and sometimes unusually high oxidation states. Typically the hydroxide melts are contained in alumina or silver crucibles. The alumina crucibles can be attacked by the flux which may lead to aluminum contamination of the product phase, however, they can be used to very high temperatures. By contrast the useful temperature range of silver crucibles or silver tubes, which are inert toward the hydroxide flux, are limited by the melting point of silver (m.p. 961 °C). In sealed silver tubes, the water content and hence the acidity needed to dissolve certain metal oxides, such as the rare-earths, can be maintained for many days at high temperatures. Following the reactions, the solidified hydroxide melt can be dissolved in water, or for moisture sensitive compositions, methanol.

Single crystals of many complex transition-metal containing oxides have grown by the zur Loye group utilizing

hydroxide fluxes. Both  $\text{Sr}_3\text{NaNbO}_6$  and  $\text{Sr}_3\text{NaTaO}_6$ <sup>[110]</sup> were obtained from the dissolution of  $\text{Nb}_2\text{O}_5$  or  $\text{Ta}_2\text{O}_5$  in a  $\text{Sr}(\text{OH})_2$ -NaOH melt. Pale green hexagonal prisms were found in reactions performed in sealed silver tubes, whereas light brown rods were found in reactions contained in loosely covered silver crucibles. Although both crystals gave the same structure solution, the differences in color were attributed to slight oxygen deficiencies introduced by performing the reaction in an open versus a closed system. Black hexagonal block crystals of the ruthenates  $\text{Ln}_{14}\text{Na}_3\text{Ru}_6\text{O}_{36}$  ( $\text{Ln} = \text{Pr}, \text{Nd}$ )<sup>[111]</sup> were successfully grown with a NaOH flux at 600 °C. The Pr compound required the addition of Os metal to the reaction mixture to act as a sacrificial reductant to preserve the +3 oxidation state for Pr.  $\text{LuNaPd}_6\text{O}_8$  (Figure 23)<sup>[112]</sup> was

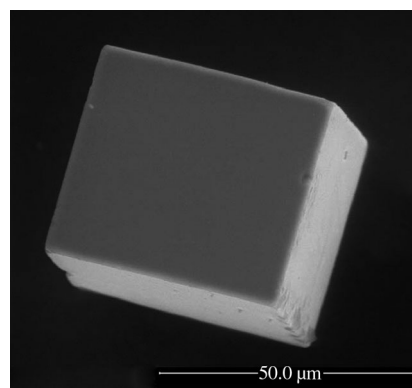


**Figure 23.** Scanning electron micrograph of a cubic block crystal of  $\text{LuNaPd}_6\text{O}_8$  grown out of a NaOH flux. Reprinted with permission from Ref. [112] Copyright 2006, Elsevier.

obtained from the dissolution of  $\text{Lu}_2\text{O}_3$  and  $\text{Pd}(\text{NH}_3)_2\text{Cl}_2$  or Pd metal in a NaOH melt at 700 °C; the black cubic crystals were isolated by dissolving the flux in water. Other palladates, such as  $\text{LnKPD}_3$  ( $\text{Ln} = \text{La}, \text{Pr}, \text{Nd}, \text{Sm}, \text{Eu}, \text{Gd}$ )<sup>[113]</sup> were grown as golden-brown needles from the early rare-earth oxides and Pd metal in a KOH melt at 750 °C.

The rhenates  $\text{Sr}_2\text{LiReO}_6$ ,  $\text{Sr}_2\text{NaReO}_6$ ,  $\text{Ba}_2\text{LiReO}_6$ , and  $\text{Ba}_2\text{NaReO}_6$ <sup>[114]</sup> were prepared from  $\text{NH}_4\text{ReO}_4$  or Re metal in the corresponding alkali- and alkaline-earth-metal hydroxides. The reaction mixtures were heated at either 700 °C or 750 °C for 12 h, with a higher yield obtained at 700 °C, but better crystal quality at 750 °C. Interestingly, for  $\text{Sr}_2\text{LiReO}_6$ , the single-crystal X-ray structure reveals cubic symmetry, whereas the powder obtained from a standard solid-state route shows tetragonal symmetry. Thus, the flux route to crystal growth may be isolating a kinetic product not possible at higher temperatures where thermodynamic stability becomes the overriding factor. Shiny black prismatic crystals (Figure 24) of  $\text{Ba}_2\text{LiOsO}_6$  and  $\text{Ba}_2\text{NaOsO}_6$ <sup>[115]</sup> were successfully grown in alumina crucibles at 600 °C. Os metal was dissolved in a melt of  $\text{Ba}(\text{OH})_2 \cdot 8\text{H}_2\text{O}$  and either a  $\text{LiOH} \cdot \text{H}_2\text{O}$ -KOH eutectic or NaOH. The iridates  $\text{La}_9\text{RbIr}_4\text{O}_{24}$ <sup>[116]</sup> and  $\text{Sm}_2\text{NaIrO}_6$ <sup>[117]</sup> were obtained as black crystals from the dissolution of Ir metal and the appropriate rare-earth oxide in a hydroxide flux at 650 °C. For  $\text{La}_9\text{RbIr}_4\text{O}_{24}$ , the flux was RbOH, whereas for  $\text{Sm}_2\text{NaIrO}_6$  it



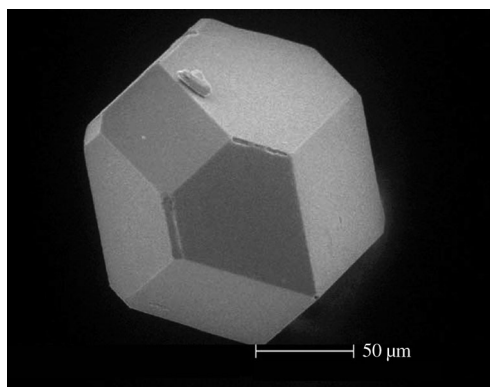


**Figure 24.** Scanning electron micrograph of a prismatic crystal of  $\text{Ba}_2\text{NaOsO}_6$  grown out of a  $\text{Ba}(\text{OH})_2$ -NaOH flux. Reprinted with permission from Ref. [115] Copyright 2002, Elsevier.

was a NaOH-CsOH eutectic mixture. Yellow prismatic crystals of  $(\text{NaLa}_2)\text{NaPtO}_6$ <sup>[118]</sup> were obtained from a NaOH melt.  $\text{La}_2\text{O}_3$  and  $(\text{NH}_4)_2\text{PtCl}_6$ , as well as 2 g of water, were added to 10 g of NaOH flux in a silver crucible, and heated at 700 °C for 12 h, before turning off the furnace and allowing it to cool to ambient temperature.

Many other groups have also prepared oxide single crystals from hydroxide melts.  $\text{NaKLaNbO}_5$  and  $\text{Na}_2\text{K}_2\text{Gd}_4\text{Nb}_2\text{O}_{13}$ <sup>[119]</sup> were grown as thin rectangular plates from the dissolution of  $\text{Nb}_2\text{O}_5$  and the corresponding rare-earth oxide with a NaOH-KOH eutectic mixture. The reagents were placed in a platinum crucible and heated to either 400 °C (La) or 450 °C (Gd); after cooling to room temperature, excess flux was removed by washing with water. The Stacy group obtained  $\text{Sr}_{18}\text{Ru}_{1.9}\text{Bi}_{4.1}\text{O}_{33}$ <sup>[120]</sup> from  $\text{RuO}_2$  and  $\text{Bi}_2\text{O}_3$  in a melt consisting of  $\text{Sr}(\text{OH})_2$  and KOH. After heating at 750 °C for 6 h, the mixture was slowly cooled to 600 °C over 48 h, and then quenched to room temperature, which revealed ruby red crystals that could be isolated mechanically. Amber prisms of  $\text{BaKFeO}_3$  (Figure 25)<sup>[121]</sup> were successfully grown from the dissolution at 750 °C of  $\text{Fe}_2\text{O}_3$  in a flux of  $\text{Ba}(\text{OH})_2$

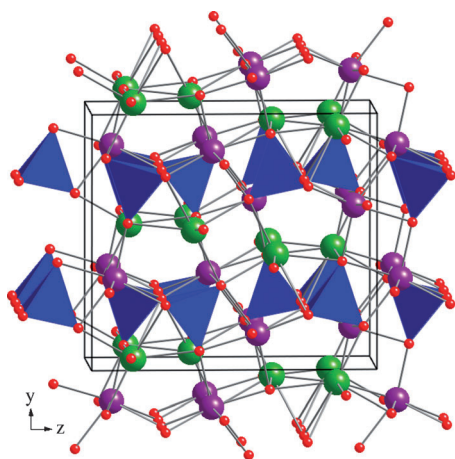


**Figure 25.** Crystal structure of  $\text{BaKFeO}_3$  viewed along [100].  $\text{Ba}^{2+}$  ions purple spheres,  $\text{K}^+$  ions green spheres,  $\text{FeO}_4$  tetrahedra blue, and  $\text{O}^{2-}$  ions red spheres.

and KOH. Clear tablet shaped crystals of  $\text{Ba}_4\text{Ti}_{10}\text{Al}_2\text{O}_{27}$ <sup>[122]</sup> were prepared by the Müller-Buschbaum group.  $\text{BaCO}_3$  and  $\text{TiO}_2$  were reacted with a twofold excess of NaOH at 1300 °C, followed by cooling to room temperature. The compounds  $\text{La}_2\text{Li}_{0.5}\text{M}_{0.5}\text{O}_4$  ( $\text{M} = \text{Co}, \text{Ni}, \text{Cu}, \text{Au}$ )<sup>[123,124]</sup> were grown as single crystals from a LiOH flux. In the case of the Au compound, Au powder and  $\text{La}(\text{OH})_3$  were used, whereas the remaining examples started with  $\text{La}_2\text{O}_3$  and the respective binary metal oxide. The reaction mixture was heated in a corundum boat at 750 °C (Au) or 800 °C (Co, Ni, Cu) until most of the excess LiOH flux had evaporated. After cooling, any remaining solidified flux was removed by washing in boiling water.

### 3.9. Complex Melts

In addition to fluxes consisting of a single component, there are an even greater number of fluxes that consist of combinations of inorganic materials, for example the  $\text{PbO-PbF}_2$  or the  $\text{B}_2\text{O}_3\text{-Na}_2\text{O}$  combinations mentioned earlier. Often a line phase exists, such as  $\text{Na}_2\text{B}_4\text{O}_7$ , but even when one does not, the combination of several fluxes to enhance each other is a common technique to improve the crystal growth process. Thus combinations of the type  $\text{Ba}(\text{OH})_2\text{-BaCl}_2$ ,  $\text{Bi}_2\text{O}_3\text{-V}_2\text{O}_5$ ,  $\text{PbO-PbF}_2\text{-B}_2\text{O}_3$ , etc., have been used with great success, where different components contribute to different aspects of the fluxes overall utility. As mentioned,  $\text{B}_2\text{O}_3$  widens the temperature range in which the metastable region for crystal growth exists, as well as reduces the overall vapor pressure. Mineralizers like KF can facilitate the stabilization of metal cations in melts. Finding the single “best” flux is difficult, but finding a “very good” flux is certainly feasible, as there is generally more than one flux that will yield high-quality crystals. Clearly when contemplating using such complex melts it would be advantageous to have access to the relevant phase diagrams which, for the simple fluxes, can be found in the literature providing us with melting points for various compositions. Once we include the reagents, however, it becomes increasingly unlikely that such a complex phase diagram (often consisting of 4 or more components) has been worked out. That, however, should not prevent the inclusion of additional components for optimizing the crystal growth process, since the addition of a few percent of an additional component, while impacting for example the solubility of the reagents in the flux, will typically not significantly change the melting point. In all cases, of course, some degree of exploratory work to identify practical crystal growth conditions (temperature, time, flux, concentration) is required.

The Müller-Buschbaum group obtained  $\text{Ba}_3\text{CaRu}_{1.5}\text{Ta}_{0.5}\text{O}_9$  and  $\text{Ba}_3\text{CaRu}_{0.5}\text{Ir}_{1.5}\text{O}_9$ <sup>[125]</sup> from a flux consisting of a 5:1 ratio of  $\text{BaCl}_2\cdot 2\text{H}_2\text{O}$  to  $\text{Ba}(\text{OH})_2\cdot 8\text{H}_2\text{O}$ .  $\text{BaCO}_3$ ,  $\text{CaCO}_3$ , Ru, and  $\text{Ta}_2\text{O}_5$  or  $\text{IrO}_2$  were reacted in the melt at 1050 °C for 9 days, with the  $\text{BaCl}_2\cdot 2\text{H}_2\text{O}$  continually replenished to compensate for evaporative losses. After cooling, the excess flux was dissolved with dilute HCl to reveal black hexagonal platelets. Using the same flux, the Stacy group grew black hexagonal crystals of the compound

$M_6Ba_{46}Cu_{24}O_{84}$  ( $M = Al, Ti, Fe, Ga, Ge, Zr$ ) (Figure 26).<sup>[126]</sup> The appropriate binary metal oxide (or  $Fe(NO_3)_3$  in the case of iron) and  $CuO$  were dissolved in the flux at  $750^\circ C$ , before

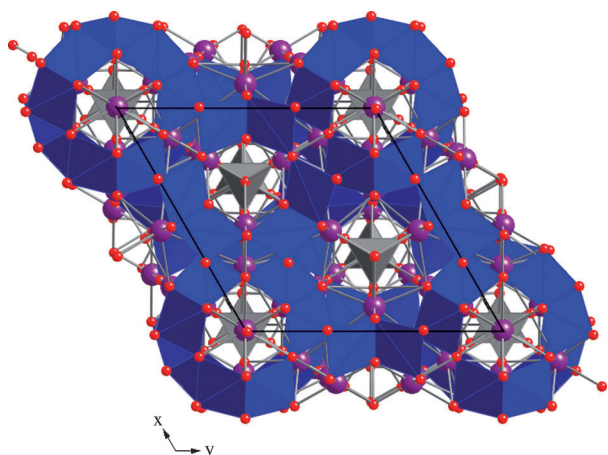


**Figure 26.** Crystal structure of  $M_6Ba_{46}Cu_{24}O_{84}$  ( $M = Al, Ti, Fe, Ga, Ge, Zr$ ) viewed along  $[001]$ .  $MO_4$  tetrahedra gray,  $Ba^{2+}$  ions purple spheres,  $CuO_4$  tetrahedra blue, and  $O^{2-}$  ions red spheres.

cooling to  $600^\circ C$  over 36 h, and then the furnace was shut off. Cubic crystals (Figure 27) of  $K_4[Ln_6Pt_2O_{15}]$  ( $Ln = La, Pr, Nd, Sm$ )<sup>[127]</sup> were successfully grown by the zur Loye group with a melt consisting of  $KOH$  and  $KF$ . The rare-earth oxide and  $(NH_4)_2PtCl_6$  were reacted in the flux at  $650^\circ C$  for between 12 and 24 h, before slow cooling; sonication in water was used to isolate the crystals from the excess flux.

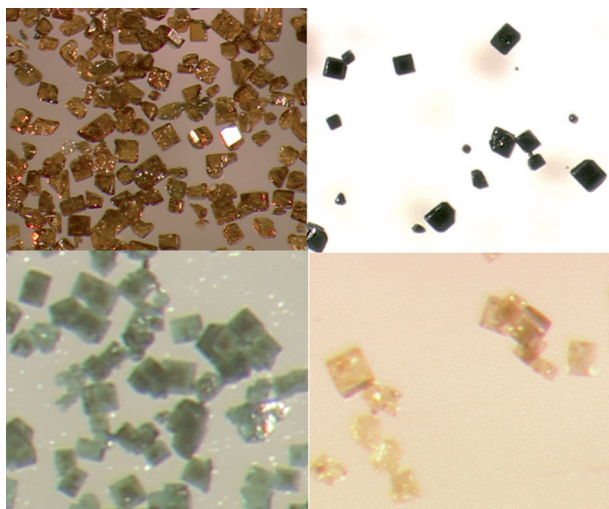


**Figure 27.** Photograph of cubic block crystals of  $K_4[Ln_6Pt_2O_{15}]$  ( $Ln = La$  (top left),  $Pr$  (top right),  $Nd$  (bottom left),  $Sm$  (bottom right)), grown out of a  $KOH$ - $KF$  flux. Reprinted with permission from Ref. [127] Copyright 2009, American Chemical Society.

The complex oxides  $Bi_{0.78}Li_2Rh_6O_{12}$ ,  $Bi_{0.75}Sc_{1.10}(Rh_{4.92}Sc_{1.08})O_{12}$ , and  $Bi_{0.68}Be_2Rh_6O_{12}$ <sup>[128]</sup> were prepared at  $1100^\circ C$  from  $Rh_2O_3$  and  $Li_2CO_3$ ,  $Sc_2O_3$ , or  $BeO$ , in a melt composed of 75 %  $Bi_2O_3$  and 25 %  $V_2O_5$ . After cooling,

the flux was dissolved in  $HNO_3$  at  $87^\circ C$  to reveal black shiny needles (Figure 28) up to 4 mm in length. The Rosseinsky group was able to grow cubic crystals with edges up to 1 mm

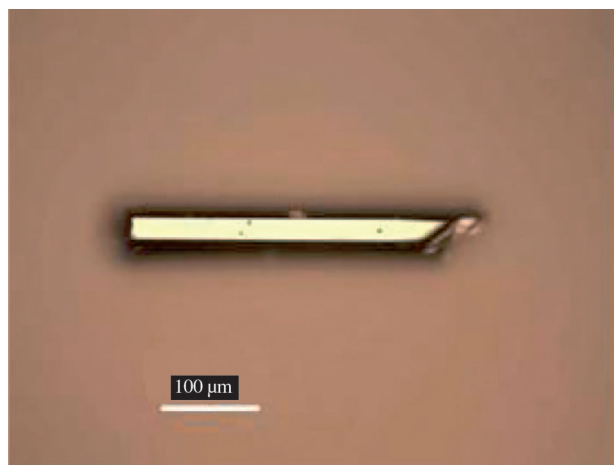


**Figure 28.** Photograph of a metallic columnar crystal of  $Bi_{0.78}Li_2Rh_6O_{12}$  grown out of a  $Bi_2O_3$ - $V_2O_5$  flux. Reprinted with permission from Ref. [128] Copyright 2009, American Chemical Society.

of  $Bi_2Mn_{1.33}Ni_{0.67}O_6$ <sup>[129]</sup> from a flux of  $Bi_2O_3$  and  $NaCl$ . The oxides  $MnO_2$  and  $NiO$  were step-wise heated in the melt at temperatures of  $800^\circ C$ ,  $850^\circ C$ , and  $875^\circ C$ , before cooling at  $0.5^\circ C$  per hour to  $820^\circ C$  and then quickly to room temperature.  $LiCuVO_4$ <sup>[130]</sup> was obtained as large black crystals up to  $4 \times 2 \times 1 \text{ mm}^3$  with a flux containing 47 mol %  $LiCl$  and 53 mol %  $LiVO_3$ . The polycrystalline material was dissolved in the melt at  $560^\circ C$  before slow cooling to  $520^\circ C$  and then turning off the furnace.

The Greedan group grew thin colorless plates of  $K_2Nd_2Ti_3O_{10}$ <sup>[131]</sup> in a melt containing  $KF$  and  $Na_2B_4O_7$ . The binary oxides  $Nd_2O_3$  and  $TiO_2$  were heated in the flux at  $1100^\circ C$  for 2 h, and then cooled at  $1^\circ C$  per hour to  $1000^\circ C$ , at which point the reaction was removed from the furnace and the excess flux was poured out of the platinum crucible.  $Th_{0.5}Pb_{0.5}VO_4$ <sup>[132]</sup> was prepared with a flux of  $2PbO:1V_2O_5$ , which forms  $Pb_2V_2O_7$  in situ.  $ThO_2$  was dissolved in the melt at  $1000^\circ C$ , and then cooled to  $750^\circ C$ , when the crucible was inverted so that the molten flux could flow into the lid of the crucible. After fully cooling the reaction, the solidified flux on the lid was removed by immersing in hot, dilute  $HNO_3$ , and plates with edges up to 10 mm could be isolated. Metallic crystals of  $(Bi_{0.75}Pb_{0.25})(Fe_{0.75}Ti_{0.25})O_3$ <sup>[133]</sup> were grown at  $1200^\circ C$  from a melt composition of 70 %  $PbO$  and 30 %  $Bi_2O_3$ ; the excess flux could be dissolved in glacial acetic acid.

A number of other compounds were grown as crystals with the addition of  $B_2O_3$  to other fluxes. In the case of  $BaSn_2Fe_4O_{11}$ ,<sup>[134]</sup> the oxides  $BaO$ ,  $Fe_2O_3$ , and  $SnO_2$  were dissolved in a melt of  $BaCl_2$  and  $B_2O_3$ . Because the reaction was heated at  $1350^\circ C$ , some of the flux evaporated, while the remainder was washed away with dilute  $HNO_3$  to reveal large red-brown hexagonal platelets. Black shiny parallelepiped crystals of  $MnVSbO_6$ <sup>[135]</sup> were obtained from a flux of 90.4 wt %  $V_2O_5$  and 9.6 wt %  $B_2O_3$ .  $Sb_2O_5$  and manganese

carbonate or manganese acetate tetrahydrate were heated in the melt at 900 °C for 3 h, before cooling at 1.5 °C per hour to 700 °C, at which point the molten flux was poured out on a steel plate and washed away with dilute HCl. Crystals of  $\text{PbYb}_{0.5}\text{M}_{0.5}\text{O}_3$  ( $\text{M}=\text{Nb}, \text{Ta}$ ) and  $\text{PbMg}_{0.5}\text{W}_{0.5}\text{O}_3$ <sup>[136]</sup> were successfully grown with a flux of  $\text{PbO-PbF}_2\text{-B}_2\text{O}_3$  with a maximum soak temperature of 1200 °C. During the cooling of the reactions, molten flux was decanted at 880 °C, and following cooling to room temperature, any remaining solidified flux was washed away in hot acetic acid and dilute nitric acid, which yielded octahedral crystals (Figure 29) up to 6 mm in size. A melt consisting of  $\text{Bi}_2\text{O}_3$ ,  $\text{K}_2\text{CO}_3$ , and KCl was



**Figure 29.** Photograph of prismatic crystals of  $\text{PbYb}_{0.5}\text{Nb}_{0.5}\text{O}_3$  (top) and  $\text{PbMg}_{0.5}\text{W}_{0.5}\text{O}_3$  (bottom) grown out of a  $\text{PbO-PbF}_2\text{-B}_2\text{O}_3$  flux. Reprinted with permission from Ref. [136] Copyright 2008, Elsevier.

employed to grow hexagonal plates with an area of 5–10 mm<sup>2</sup> of  $[\text{Bi}_{0.84}\text{CaO}_2]_2[\text{CoO}_2]_{1.69}$ .<sup>[137]</sup> A pre-reacted powder of  $\text{Bi}_2\text{O}_3$ ,  $\text{CaCO}_3$ , and  $\text{Co}_3\text{O}_4$  was dissolved in the melt at 900 °C for 20 h, before cooling at 2 °C per hour to 700 °C, and then turning off the furnace. Dark red prismatic crystals of  $\text{K}_{1.45}\text{Fe}_{1.45}\text{Ti}_{6.55}\text{O}_{16}$ <sup>[138]</sup> were prepared at 1450 °C from a flux composition  $\text{K}_2\text{O-SiO}_2\text{-V}_2\text{O}_5$ . Once the reaction had cooled, the flux could be removed in dilute  $\text{HNO}_3$ .

#### 4. Summary and Outlook

The utility of fluxes for materials discovery by exploratory crystal growth has been and continues to be a rewarding undertaking, as illustrated in this Review. Numerous researchers have used fluxes for many years to grow crystals of all types of materials, not just oxides, and in the process have established flux growth as an important tool for materials chemistry. The field of flux growth is, of course,

much too large to be covered in a single Review, which is why we decided to focus on only a small subset, the flux growth of crystals of quaternary or higher order oxides, and the goal was to be illustrative rather than inclusive. In addition, by demonstrating the efficacy of the most commonly used fluxes we intended to provide the reader with a “how-to” manual for the flux crystal growth of oxides.

The fluxes discussed in this Review, lead oxide and/or lead fluoride, bismuth oxide, boron oxide or alkali/alkaline-earth-metal borates, alkali and/or alkaline-earth-metal halides, alkali-metal carbonates, vanadates, molybdates and/or tungstates, alkali-metal oxides, peroxides and/or superoxides, alkali- and/or alkaline-earth-metal hydroxides, and various complex melts, were chosen because they are some of the best fluxes for oxide crystal growth and hence the most commonly used. They are certainly not the only fluxes in the literature and for some systems, not even the best. However, for the vast majority of oxides that might be targeted, these fluxes will work.

To grow crystals of future materials, in particular structures containing a larger number of elements, the flux, by necessity, must be able to solubilize simultaneously a more diverse mix of oxide reagents. Since simple fluxes may not be up to this task, it is probable that the crystal growth of complex oxides will require more complex fluxes, and it will be up to the researchers to adapt and modify existing fluxes for this purpose. The crystal growth from high-temperature solutions is an adaptive field and we expect that new flux combinations will come into use and lead to the growth of new complex oxides.

Finally, as new opportunities arise for millimeter-sized crystals, for example, for single-crystal neutron diffraction on high-intensity neutron sources, it will become desirable to utilize fluxes to target the growth of larger crystals. There is, of course, always the tension between crystal size and crystal growth throughput, and while growing large crystals can be very rewarding for measuring properties, it is also typically more time consuming. The crystal growth from high-temperature solutions remains an excellent approach for exploratory, discovery-oriented work that can rapidly generate a multitude of new materials in the form of sub-millimeter-sized crystals. Fortunately, adapting the approach from targeting sub-millimeter-sized crystals for X-ray structural characterization to millimeter-sized crystals for property measurements and neutron diffraction work is mostly a matter of scale—and time—and we expect to see more reports detailing the flux growth of larger crystals for physical property measurements in the coming years.

*We gratefully acknowledge financial support from the National Science Foundation through grant DMR:0804209 and from the Department of Energy, BES, through the Center for Heterogeneous Functional Materials for Energy Systems, Award Number DE-SC0001061.*

Received: April 18, 2011

Published online: January 27, 2012



- [1] D. Elwell, H. J. Scheel, *Crystal Growth from High-Temperature Solutions*, Academic Press, New York, **1975**.
- [2] S. J. Mugavero III, W. R. Gemmill, I. P. Roof, H.-C. zur Loye, *J. Solid State Chem.* **2009**, *182*, 1950–1963.
- [3] M. G. Kanatzidis, R. Pöttgen, W. Jeitschko, *Angew. Chem.* **2005**, *117*, 7156–7184; *Angew. Chem. Int. Ed.* **2005**, *44*, 6996–7023.
- [4] D. Fischer, R. Hoppe, K. M. Mogare, M. Jansen, *Z. Naturforsch. B* **2005**, *60*, 1113–1117.
- [5] K. Mader, R. Hoppe, *J. Alloys Compd.* **1992**, *183*, 198–209.
- [6] S. Voigt, R. Hoppe, *J. Less-Common Met.* **1989**, *156*, 97–104.
- [7] S. T. Schiffler, H. K. Müller-Buschbaum, *J. Less-Common Met.* **1987**, *128*, 117–123.
- [8] D. E. Bugaris, J. A. Ibers, *Dalton Trans.* **2010**, *39*, 5949–5964.
- [9] M. Sofin, E.-M. Peters, M. Jansen, *Solid State Sci.* **2004**, *6*, 339–344.
- [10] J. A. Campá, M. P. Gutierrez, M. A. Monge, I. Rasines, C. Ruiz-Valero, *J. Solid State Chem.* **1994**, *108*, 230–235.
- [11] D. Arney, B. Porter, B. Greve, P. A. Maggard, *J. Photochem. Photobiol. A* **2005**, *199*, 1113–1117.
- [12] F. R. Cruickshank, D. M. Taylor, F. P. Glasser, *J. Inorg. Nucl. Chem.* **1964**, *26*, 937–941.
- [13] F. Galasso, L. Katz, *Acta Crystallogr.* **1961**, *14*, 647–650.
- [14] G. Liu, J. E. Greedan, *J. Solid State Chem.* **1995**, *115*, 174.
- [15] J. L. Luce, A. M. Stacy, *Chem. Mater.* **1997**, *9*, 1508–1515.
- [16] J. B. Parise, C. C. Torardi, M.-H. Whangbo, C. J. Rawn, R. S. Roth, B. P. Burton, *Chem. Mater.* **1990**, *2*, 454–458.
- [17] J. Shannon, L. Katz, *Acta Crystallogr. Sect. B* **1970**, *26*, 102–105.
- [18] R. W. Smith, J. L. Luce, D. A. Keszler, *Inorg. Chem.* **1992**, *31*, 4679–4682.
- [19] G. Svensson, J. Köhler, A. Simon, *Acta Chem. Scand.* **1992**, *46*, 244–248.
- [20] G. Svensson, J. Köhler, A. Simon, *J. Alloys Compd.* **1991**, *176*, 123–132.
- [21] J. T. Vaughey, J. B. Wiley, K. R. Poeppelmeier, *Z. Anorg. Allg. Chem.* **1991**, *598–599*, 327–338.
- [22] S. Wang, S.-J. Hwu, *Inorg. Chem.* **1995**, *34*, 166–171.
- [23] A. Wold, K. Dwight, *J. Solid State Chem.* **1990**, *88*, 229–238.
- [24] S. Wang, S.-J. Hwu, *J. Am. Chem. Soc.* **1992**, *114*, 6920–6922.
- [25] M. Jansen, *Angew. Chem.* **2002**, *114*, 3896–3917; *Angew. Chem. Int. Ed.* **2002**, *41*, 3746–3766.
- [26] F. J. DiSalvo, *Science* **1990**, *247*, 649–655.
- [27] K. R. Poeppelmeier, *Chem. Mater.* **1998**, *10*, 2577–2578.
- [28] M. Jansen, J. C. Schön, *Angew. Chem.* **2006**, *118*, 3484–3490; *Angew. Chem. Int. Ed.* **2006**, *45*, 3406–3412.
- [29] J. Hulliger, M. Aslam Awan, *Chem. Eur. J.* **2004**, *10*, 4694–4702.
- [30] V. M. Goldschmidt, *Mater.-Nat. Kl.* **1926**, *2*, 117.
- [31] D. M. Giaquinta, H.-C. zur Loye, *Chem. Mater.* **1994**, *6*, 365–372.
- [32] H. Lux, *Z. Elektrochem.* **1939**, *45*, 303–309.
- [33] H. Flood, T. Florand, *Acta Chem. Scand. B* **1947**, *1*, 592–604.
- [34] N. Pienack, W. Bensch, *Angew. Chem.* **2011**, *123*, 2062–2083; *Angew. Chem. Int. Ed.* **2011**, *50*, 2014–2034.
- [35] D. Kashchiev, *Nucleation*, Butterworth-Heinemann, Oxford, **2000**.
- [36] I. V. Markov, *Crystal Growth for Beginners*, World Scientific, Singapore, **2003**.
- [37] P. Cubillas, M. W. Anderson in *Zeolites and Catalysis: Synthesis Reactions and Applications* (Eds.: J. Čejka, A. Corma, S. Zones), Wiley-VCH, Weinheim, **2010**, Chap. 1.
- [38] W. K. Burton, N. Cabrera, F. C. Frank, *Philos. Trans. R. Soc. London Ser. A* **1951**, *243*, 299–358.
- [39] K. Wichmann, I. P. Roof, H.-C. zur Loye, **2011**, unpublished results.
- [40] K.-B. Plötz, H. K. Müller-Buschbaum, *Z. Anorg. Allg. Chem.* **1982**, *491*, 253–258.
- [41] A. Teichert, H. K. Müller-Buschbaum, *J. Alloys Compd.* **1993**, *202*, 37–40.
- [42] A. Teichert, H. K. Müller-Buschbaum, *J. Less-Common Met.* **1991**, *170*, 315–320.
- [43] M. Scheikowski, H. K. Müller-Buschbaum, *Z. Anorg. Allg. Chem.* **1993**, *619*, 1755–1758.
- [44] A. Roesler, D. Reinen, *Z. Anorg. Allg. Chem.* **1981**, *479*, 119–124.
- [45] J. Bredthauer, N. Wagner, M. Jansen, *Z. Anorg. Allg. Chem.* **1991**, *593*, 193–199.
- [46] J. Ostorero, M. Nanot, F. Queyroux, J. C. Gilles, H. Makram, *J. Cryst. Growth* **1983**, *65*, 576–579.
- [47] B. N. Sun, R. Boutellier, P. Sciau, E. Burkhardt, V. Rodriguez, H. Schmid, *J. Cryst. Growth* **1991**, *112*, 71–83.
- [48] C. Renard, P. Roussel, A. Rubbens, S. Daviero-Minaud, F. Abraham, *J. Solid State Chem.* **2006**, *179*, 2101–2110.
- [49] N. Ghosh, S. Elizabeth, H. L. Bhat, G. Nalini, B. Muktha, T. N. Guru Row, *J. Solid State Chem.* **2005**, *178*, 120–127.
- [50] U. Kolitsch, E. Tillmanns, *Acta Crystallogr. Sect. E* **2003**, *59*, i43–i46.
- [51] M. Giot, P. Beran, O. Pérez, S. Malo, M. Hervieu, B. Raveau, M. Nevriya, K. Knizek, P. Roussel, *Chem. Mater.* **2006**, *18*, 3225–3236.
- [52] D. M. Giaquinta, H.-C. zur Loye, *J. Alloys Compd.* **1992**, *184*, 151–160.
- [53] D. M. Giaquinta, G. C. Papaefthymiou, W. M. Davis, H.-C. zur Loye, *J. Solid State Chem.* **1992**, *99*, 120–133.
- [54] J. Huang, A. W. Sleight, *J. Solid State Chem.* **1992**, *100*, 170–178.
- [55] W. T. Fu, R. de Gelder, R. A. G. de Graaff, *Mater. Res. Bull.* **1997**, *32*, 657–662.
- [56] D. Mercurio, G. Trolliard, T. Hansen, J. P. Mercurio, *Int. J. Inorg. Mater.* **2000**, *2*, 397–406.
- [57] H. Vincent, E. Brando, B. Sugg, *J. Solid State Chem.* **1995**, *120*, 17–22.
- [58] J. A. Campá, C. Cascales, E. Gutiérrez-Puebla, M. A. Monge, I. Rasines, C. Ruiz Valero, *J. Solid State Chem.* **1996**, *124*, 17–23.
- [59] J. Y. Lee, J. S. Swinnea, H. Steinfink, W. M. Reiff, S. Pei, J. D. Jorgensen, *J. Solid State Chem.* **1993**, *103*, 1–15.
- [60] I. Imaz, S. Péchev, I. Koseva, F. Bourée, P. Gravereau, P. Peshev, J.-P. Chaminade, *Acta Crystallogr. Sect. B* **2007**, *63*, 26–36.
- [61] S. Park, D. A. Keszler, *Solid State Sci.* **2002**, *4*, 799–802.
- [62] A. R. Drews, W. Wong-Ng, T. A. Vanderah, R. S. Roth, *J. Alloys Compd.* **1997**, *255*, 243–247.
- [63] A. V. Mironov, S. Y. Istomin, O. G. D'yachenko, E. V. Antipov, *J. Solid State Chem.* **2001**, *157*, 1–7.
- [64] F. Licci, T. Besagni, J. Lábár, *Mater. Res. Bull.* **1987**, *22*, 467–476.
- [65] M. Gasperin, J. Rebizant, J. P. Dancausse, D. Meyer, A. Cousson, *Acta Crystallogr. Sect. C* **1991**, *47*, 2278–2279.
- [66] I. E. Grey, A. Collomb, X. Obradors, *J. Solid State Chem.* **1991**, *91*, 131–139.
- [67] L. Gacem, D. Ouadjaout, J.-P. Chaminade, M. Maglione, R. Von der Mühl, S. Pechev, *Mater. Res. Bull.* **2009**, *44*, 2240–2245.
- [68] D. Schlüter, H. K. Müller-Buschbaum, *J. Alloys Compd.* **1993**, *191*, 305–308.
- [69] J. Wilkens, H. K. Müller-Buschbaum, *J. Alloys Compd.* **1991**, *177*, L31L33.
- [70] A. Tomaszewska, H. K. Müller-Buschbaum, *Z. Anorg. Allg. Chem.* **1993**, *619*, 534–536.
- [71] M. D. Smith, J. K. Stalick, H.-C. zur Loye, *Chem. Mater.* **1999**, *11*, 2984–2988.
- [72] C. Dion, S. Obbade, E. Raekelboom, F. Abraham, M. Saadi, *J. Solid State Chem.* **2000**, *155*, 342–353.
- [73] U. Kolitsch, E. Tillmanns, *Acta Crystallogr. Sect. E* **2003**, *59*, i55–i58.

- [74] B.-O. Marinder, M. Sundber, *Acta Crystallogr. Sect. C* **1984**, *40*, 1303–1306.
- [75] J. Akimoto, Y. Gotoh, Y. Takahashi, *Cryst. Growth Des.* **2003**, *3*, 627–629.
- [76] M. J. Geselbracht, A. M. Stacy, *J. Solid State Chem.* **1994**, *110*, 1–5.
- [77] J. Köhler, A. Simon, *Z. Anorg. Allg. Chem.* **1987**, *553*, 106–122.
- [78] J. B. Claridge, R. C. Layland, W. H. Henley, H.-C. zur Loye, *Chem. Mater.* **1999**, *11*, 1376–1380.
- [79] R. B. Macquart, W. R. Gemmill, M. J. Davis, M. D. Smith, H.-C. zur Loye, *Inorg. Chem.* **2006**, *45*, 4391–4395.
- [80] M. J. Davis, M. D. Smith, H.-C. zur Loye, *J. Solid State Chem.* **2003**, *173*, 122–129.
- [81] J. N. Mwamuka, W. R. Gemmill, K. E. Stitzer, M. D. Smith, H.-C. zur Loye, *J. Alloys Compd.* **2004**, *377*, 91–97.
- [82] H.-C. zur Loye, K. E. Stitzer, M. D. Smith, A. El Abed, J. Darriet, *Inorg. Chem.* **2001**, *40*, 5152–5156.
- [83] M. J. Davis, M. D. Smith, K. E. Stitzer, H.-C. zur Loye, *J. Alloys Compd.* **2003**, *351*, 95–100.
- [84] J. Awaka, N. Kijima, H. Hayakawa, J. Akimoto, *J. Solid State Chem.* **2009**, *182*, 2046–2052.
- [85] H. Yamane, H. Takahashi, T. Kajiwarra, M. Shimada, *Acta Crystallogr. Sect. C* **2000**, *56*, 1177–1178.
- [86] H. Yamane, H. Takahashi, T. Kajiwarra, M. Shimada, *Acta Crystallogr. Sect. C* **1999**, *55*, 1978–1980.
- [87] S. Obbade, S. Yagoubi, C. Dion, M. Saadi, F. Abraham, *J. Solid State Chem.* **2003**, *174*, 19–31.
- [88] S. Obbade, C. Dion, E. Bekaert, S. Yagoubi, M. Saadi, F. Abraham, *J. Solid State Chem.* **2003**, *172*, 305–318.
- [89] Y. Michiue, *J. Solid State Chem.* **2007**, *180*, 1840–1845.
- [90] M. N. Deschizeaux-Cheruy, M. Vallet-Regi, J. C. Joubert, *J. Solid State Chem.* **1985**, *57*, 234–239.
- [91] A. El Abed, E. Gaudin, S. Lemaux, J. Darriet, *Solid State Sci.* **2001**, *3*, 887–897.
- [92] A. El Abed, E. Gaudin, J. Darriet, *Acta Crystallogr. Sect. C* **2002**, *58*, i138–i140.
- [93] M. Drofenik, I. Ban, D. Makovec, D. Hanžel, A. Golobič, L. Golič, *J. Solid State Chem.* **2007**, *180*, 2–7.
- [94] S. Obbade, C. Dion, M. Saadi, S. Yagoubi, F. Abraham, *J. Solid State Chem.* **2004**, *177*, 3909–3917.
- [95] M. Huyghe, M.-R. Lee, M. Quarton, F. Robert, *Acta Crystallogr. Sect. C* **1991**, *47*, 244–246.
- [96] M. Huyghe, M.-R. Lee, S. Jaulmes, M. Quarton, *Acta Crystallogr. Sect. C* **1993**, *49*, 950–954.
- [97] K. Iishi, J. Utsumi, *J. Cryst. Growth* **2006**, *291*, 436–441.
- [98] H. Ben Yahia, E. Gaudin, J. Darriet, *J. Solid State Chem.* **2008**, *181*, 3103–3109.
- [99] G. Kalpana, K. Vidyasagar, *J. Solid State Chem.* **2007**, *180*, 1708–1712.
- [100] Y. Michiue, M. Watanabe, *J. Solid State Chem.* **1995**, *116*, 296–299.
- [101] I. Keller, W. Assenmacher, G. Schnakenburg, W. Mader, *Z. Anorg. Allg. Chem.* **2009**, *635*, 2065–2071.
- [102] Z. A. Solodovnikova, S. F. Solodovnikov, E. S. Zolotova, *Acta Crystallogr. Sect. C* **2006**, *62*, i6–i8.
- [103] V. K. Yanovsky, V. I. Voronkova, *J. Cryst. Growth* **1981**, *52*, 654–659.
- [104] R. Hammond, J. Barbier, *Acta Crystallogr. Sect. C* **1999**, *55*, IUC9900074.
- [105] D. Fischer, R. Hoppe, *Z. Anorg. Allg. Chem.* **1992**, *617*, 37–44.
- [106] H.-P. Müller, R. Hoppe, *Z. Anorg. Allg. Chem.* **1990**, *581*, 159–172.
- [107] B. Brazel, R. Hoppe, *Z. Anorg. Allg. Chem.* **1983**, *499*, 161–168.
- [108] M. Strunk, H. K. Müller-Buschbaum, *Z. Anorg. Allg. Chem.* **1994**, *620*, 1565–1568.
- [109] M. Scheikowski, H. K. Müller-Buschbaum, *Z. Anorg. Allg. Chem.* **1993**, *619*, 559–562.
- [110] M. Bharathy, V. A. Rassolov, H.-C. zur Loye, *Chem. Mater.* **2008**, *20*, 2268–2273.
- [111] W. R. Gemmill, M. D. Smith, H.-C. zur Loye, *Inorg. Chem.* **2007**, *46*, 2132–2138.
- [112] S. J. Mugavero III, M. D. Smith, H.-C. zur Loye, *J. Solid State Chem.* **2006**, *179*, 3586–3589.
- [113] S. J. Mugavero III, M. D. Smith, H.-C. zur Loye, *Inorg. Chem.* **2007**, *46*, 3116–3122.
- [114] M. Bharathy, H.-C. zur Loye, *J. Solid State Chem.* **2008**, *181*, 2789–2795.
- [115] K. E. Stitzer, M. D. Smith, H.-C. zur Loye, *Solid State Sci.* **2002**, *4*, 311–316.
- [116] S. J. Mugavero III, M. D. Smith, H.-C. zur Loye, *Inorg. Chem.* **2006**, *45*, 946–948.
- [117] S. J. Mugavero III, I. V. Puzdrjakova, M. D. Smith, H.-C. zur Loye, *Acta Crystallogr. Sect. E* **2005**, *61*, i3–i5.
- [118] M. J. Davis, M. D. Smith, H.-C. zur Loye, *Inorg. Chem.* **2003**, *42*, 6980–6982.
- [119] J.-H. Liao, M.-C. Tsai, *Cryst. Growth Des.* **2002**, *2*, 83–85.
- [120] M. S. Martín-González, J. L. Delattre, A. M. Stacy, *J. Solid State Chem.* **2003**, *173*, 203–208.
- [121] J. L. Delattre, A. M. Stacy, *J. Solid State Chem.* **2003**, *172*, 261–264.
- [122] J. Schmachtel, H. K. Müller-Buschbaum, *Z. Anorg. Allg. Chem.* **1981**, *472*, 89–94.
- [123] S. Abou-Warda, W. Pietzuch, G. Berghöfer, U. Kesper, W. Massa, D. Reinen, *J. Solid State Chem.* **1998**, *138*, 18–31.
- [124] W. Pietzuch, S. A. Warda, W. Massa, D. Reinen, *Z. Anorg. Allg. Chem.* **2000**, *626*, 113–117.
- [125] S. T. Scheske, H. K. Müller-Buschbaum, *J. Alloys Compd.* **1993**, *198*, 173–176.
- [126] P. D. VerNooy, M. A. Dixon, F. J. Hollander, A. M. Stacy, *Inorg. Chem.* **1990**, *29*, 2837–2841.
- [127] H.-C. zur Loye, T. J. Hansen, Q. Zhao, S. J. Mugavero III, R. L. Withers, M. D. Smith, *Inorg. Chem.* **2009**, *48*, 414–416.
- [128] H. Mizoguchi, L. N. Zakharov, W. J. Marshall, A. W. Sleight, M. A. Subramanian, *Chem. Mater.* **2009**, *21*, 994–999.
- [129] H. Hughes, M. M. B. Allix, C. A. Bridges, J. B. Claridge, X. Kuang, H. Niu, S. Taylor, W. Song, M. J. Rosseinsky, *J. Am. Chem. Soc.* **2005**, *127*, 13790–13791.
- [130] A. V. Prokofiev, D. Wichert, W. Assmus, *J. Cryst. Growth* **2000**, *220*, 345–350.
- [131] G. Amow, J. E. Greedan, *Acta Crystallogr. Sect. C* **1998**, *54*, 1053–1055.
- [132] G. D. Andreotti, G. Calestani, A. Montenero, M. Bettinelli, *J. Cryst. Growth* **1985**, *71*, 289–294.
- [133] T. L. Burnett, T. P. Comyn, A. J. Bell, *J. Cryst. Growth* **2005**, *285*, 156–161.
- [134] M. Drofenik, D. Hanžel, D. Hanžel, M. N. Deschizeaux-Chérui, J. C. Joubert, *J. Solid State Chem.* **1989**, *79*, 119–125.
- [135] L. Rambert, P. Bordet, A. Sulpice, P. Strobel, *J. Solid State Chem.* **2004**, *177*, 268–273.
- [136] A. Kania, *J. Cryst. Growth* **2008**, *310*, 2767–2773.
- [137] H. Muguerra, D. Grebille, E. Guilmeau, R. Cloots, *Inorg. Chem.* **2008**, *47*, 2464–2471.
- [138] M. Drofenik, D. Hanžel, *Mater. Res. Bull.* **1982**, *17*, 1457–1460.
- [139] N. Ghosh, S. Elizabeth, H. L. Bhat, G. N. Subanna, M. Sahana, *J. Magn. Magn. Mater.* **2003**, *256*, 286–292.
- [140] W. Depmeier, H. Schmid, N. Setter, M. L. Werk, *Acta Crystallogr. Sect. C* **1987**, *43*, 2251–2255.
- [141] T. R. Wagner, T. J. Styranec, *J. Solid State Chem.* **1998**, *138*, 313–320.
- [142] J. Tellier, P. Boullay, M. Manier, D. Mercurio, *J. Solid State Chem.* **2004**, *177*, 1829–1837.
- [143] E. Guilmeau, M. Pollet, D. Grebille, M. Hervieu, H. Muguerra, R. Cloots, M. Mikami, R. Funahashi, *Inorg. Chem.* **2007**, *46*, 2124–2131.



- [144] J. S. Kim, J. Y. Lee, J. S. Swinnea, H. Steinfink, W. M. Reiff, P. Lightfoot, S. Pei, J. D. Jorgensen, *J. Solid State Chem.* **1991**, *90*, 331–343.
- [145] F. Sandiumenge, S. Galí, R. Rodríguez-Clemente, *Mater. Res. Bull.* **1992**, *27*, 417–424.
- [146] F. Sandiumenge, S. Galí, R. Rodríguez-Clemente, *J. Cryst. Growth* **1991**, *110*, 617–622.
- [147] M. Gasperin, *Acta Crystallogr. Sect. C* **1984**, *40*, 9–11.
- [148] D.-G. Chen, W.-D. Cheng, D.-S. Wu, H. Zhang, Y.-C. Zhang, Y.-J. Gong, Z.-G. Kan, *J. Solid State Chem.* **2004**, *177*, 3927–3933.
- [149] H. A. Graetsch, *Acta Crystallogr. Sect. C* **2002**, *58*, i152–i153.
- [150] E. Cavalli, G. Calestani, A. Belletti, E. Bovero, *J. Alloys Compd.* **2008**, *451*, 143–145.
- [151] M. M. Ftini, M. Krifa, H. Amor, *Acta Crystallogr. Sect. C* **2002**, *58*, i106–i108.
- [152] A. R. Drews, W. Wong-Ng, R. S. Roth, T. A. Vanderah, *Mater. Res. Bull.* **1996**, *31*, 153–162.
- [153] D. Schüter, H. K. Müller-Buschbaum, *J. Alloys Compd.* **1993**, *197*, 51–55.
- [154] M. Abed, H. K. Müller-Buschbaum, *J. Alloys Compd.* **1993**, *198*, L9–L10.
- [155] I. Rüter, H. K. Müller-Buschbaum, *Z. Anorg. Allg. Chem.* **1989**, *573*, 89–94.
- [156] M. Neubacher, H. K. Müller-Buschbaum, *Z. Anorg. Allg. Chem.* **1991**, *594*, 133–138.
- [157] H. K. Müller-Buschbaum, M. Abed, *Z. Anorg. Allg. Chem.* **1990**, *591*, 174–180.
- [158] C. H. Lang, H. K. Müller-Buschbaum, *Z. Anorg. Allg. Chem.* **1989**, *568*, 29–34.
- [159] P. Sonne, H. Müller-Buschbaum, *Z. Anorg. Allg. Chem.* **1993**, *619*, 1004–1006.
- [160] D. Schülter, H. K. Müller-Buschbaum, *J. Alloys Compd.* **1993**, *190*, L43–L44.
- [161] B. Schüpp-Niewa, L. Shlyk, S. Kryukov, L. E. De Long, R. Niewa, *Z. Naturforsch. B* **2007**, *62*, 753–758.
- [162] C. H. Lang, H. K. Müller-Buschbaum, *J. Less-Common Met.* **1990**, *161*, 1–6.
- [163] C. H. Lang, H. K. Müller-Buschbaum, *J. Less-Common Met.* **1990**, *157*, 301–306.
- [164] J. Wilkens, H. K. Müller-Buschbaum, *J. Alloys Compd.* **1991**, *176*, 141–146.
- [165] N. Harre, D. Mercurio, G. Trolliard, B. Frit, *Eur. J. Solid State Inorg. Chem.* **1998**, *35*, 77–90.
- [166] S. Alablanche, J. Thery, D. Vivien, *Mater. Res. Bull.* **1989**, *24*, 475–482.
- [167] J. Wilkens, H. K. Müller-Buschbaum, *Z. Anorg. Allg. Chem.* **1993**, *619*, 517–520.
- [168] A. Lenz, H. K. Müller-Buschbaum, *J. Less-Common Met.* **1990**, *161*, 141–146.
- [169] M. J. Davis, M. D. Smith, H.-C. zur Loye, *Acta Crystallogr. Sect. C* **2001**, *57*, 1234–1236.
- [170] J. B. Claridge, R. C. Layland, W. H. Henley, H.-C. zur Loye, *Z. Anorg. Allg. Chem.* **1998**, *624*, 1951–1955.
- [171] R. Niewa, L. Shlyk, B. Schüpp-Niewa, L. E. De Long, *Z. Anorg. Allg. Chem.* **2010**, *636*, 331–336.
- [172] C. C. Torardi, C. Page, L. H. Brixner, G. Blasse, G. J. Dirksen, *J. Solid State Chem.* **1987**, *69*, 171–178.
- [173] M. A. Monge, E. Gutiérrez-Puebla, C. Cascales, J. A. Campa, *Chem. Mater.* **2000**, *12*, 1926–1930.
- [174] M. Labeau, B. Bochu, J. C. Joubert, J. Chenavas, *J. Solid State Chem.* **1980**, *33*, 257–261.
- [175] H. Watelet, J.-P. Picard, G. Baud, J.-P. Besse, R. Chevalier, *Mater. Res. Bull.* **1981**, *16*, 877–882.
- [176] S. G. Ebbinghaus, *J. Solid State Chem.* **2004**, *177*, 817–823.
- [177] J. Köhler, G. Miller, A. Simon, *Z. Anorg. Allg. Chem.* **1989**, *568*, 8–21.
- [178] S. Grupe, M. S. Wickleder, *Z. Anorg. Allg. Chem.* **2003**, *629*, 955–958.
- [179] S. Obbade, C. Dion, L. Duvieubourg, M. Saadi, F. Abraham, *J. Solid State Chem.* **2003**, *173*, 1–12.
- [180] M. Zakhour-Nakhl, J. Darriet, J. B. Claridge, H.-C. zur Loye, J. M. Perez-Mato, *Int. J. Inorg. Mater.* **2000**, *2*, 503–512.
- [181] W. H. Henley, J. B. Claridge, P. L. Smallwood, H.-C. zur Loye, *J. Cryst. Growth* **1999**, *204*, 122–127.
- [182] K. E. Stitzer, A. El Abed, J. Darriet, H.-C. zur Loye, *J. Solid State Chem.* **2004**, *177*, 1405–1411.
- [183] C. Dussarrat, R. A. Howie, G. C. Mather, L. M. Torres-Martinez, A. R. West, *J. Mater. Chem.* **1997**, *7*, 2103–2106.
- [184] I. V. Puzdrjakova, R. B. Macquart, M. D. Smith, H.-C. zur Loye, *Acta Crystallogr. Sect. E* **2007**, *63*, i95–i96.
- [185] J. B. Claridge, R. C. Layland, R. D. Adams, H.-C. zur Loye, *Z. Anorg. Allg. Chem.* **1997**, *623*, 1131–1134.
- [186] M. Gasperin, *Acta Crystallogr. Sect. C* **1987**, *43*, 404–406.
- [187] M. Gasperin, *J. Solid State Chem.* **1987**, *67*, 219–224.
- [188] T. J. Hansen, R. B. Macquart, M. D. Smith, H.-C. zur Loye, *Solid State Sci.* **2007**, *9*, 785–791.
- [189] O. Sedello, H. K. Müller-Buschbaum, *J. Alloys Compd.* **1994**, *210*, 331–334.
- [190] P. E. Tomaszewski, A. Pietraszko, M. Mączka, J. Hanuza, *Acta Crystallogr. Sect. E* **2002**, *58*, i119–i120.
- [191] S. Yoshikado, I. Taniguchi, M. Watanabe, Y. Onoda, Y. Fujiki, *Solid State Ionics* **1995**, *79*, 34–39.
- [192] U. Kolitsch, M. Mackza, J. Hanuza, *Acta Crystallogr. Sect. E* **2003**, *59*, i10–i13.
- [193] D. Lévy, J. Barbier, *Acta Crystallogr. Sect. C* **1999**, *55*, 1611–1614.
- [194] A. Sarapulova, D. Mikhailova, A. Senyshyn, H. Ehrenberg, *J. Solid State Chem.* **2009**, *182*, 3262–3268.
- [195] Y. Fujiki, M. Watanabe, T. Sasaki, T. Mitsushashi, Y. Onoda, S. Yoshikado, T. Ohachi, I. Taniguchi, *Solid State Ionics* **1990**, *40/41*, 136–138.
- [196] D. Zhao, F. Li, W. Cheng, H. Zhang, *Acta Crystallogr. Sect. E* **2010**, *66*, i2.
- [197] D. Lévy, J. Barbier, *Acta Crystallogr. Sect. C* **1998**, *54*, IUC9800043.
- [198] A. van der Lee, M. Beaurain, P. Armand, *Acta Crystallogr. Sect. C* **2008**, *64*, i1–i4.
- [199] J. Barbier, M. E. Fleet, *J. Solid State Chem.* **1987**, *71*, 361–370.
- [200] M. Watanabe, Y. Fujiki, S. Yoshikado, T. Ohachi, *Solid State Ionics* **1989**, *35*, 369–375.
- [201] Y. Michiue, M. Watanabe, Y. Fujiki, *Mater. Res. Bull.* **1991**, *26*, 597–603.
- [202] Y. Michiue, M. Watanabe, Y. Kitami, Y. Fujiki, *Acta Crystallogr. Sect. C* **1992**, *48*, 607–610.
- [203] Y. Michiue, M. Watanabe, *Solid State Ionics* **1994**, *70/71*, 186–190.
- [204] K. Wang, J. Zhang, J. Wang, W. Yu, H. Zhang, X. Wang, Z. Wang, M. Ba, *J. Cryst. Growth* **2005**, *281*, 407–410.
- [205] G. J. Redhammer, G. Roth, D. Topa, G. Amthauer, *Acta Crystallogr. Sect. C* **2008**, *64*, i21–i26.
- [206] M. Touboul, P. Toledano, *J. Solid State Chem.* **1981**, *38*, 386–393.
- [207] M. Huyghe, M. R. Lee, M. Quarton, F. Robert, *Acta Crystallogr. Sect. C* **1991**, *47*, 1797–1799.
- [208] B. M. Gatehouse, M. C. Nesbit, *J. Solid State Chem.* **1981**, *39*, 1–6.
- [209] B. M. Gatehouse, M. C. Nesbit, *J. Solid State Chem.* **1980**, *33*, 153–158.
- [210] M. Sugahara, A. Yoshiasa, T. Yamanaka, H. Takei, *Acta Crystallogr. Sect. E* **2003**, *59*, i61–i63.
- [211] V. Volkov, C. Cascales, A. Kling, C. Zaldo, *Chem. Mater.* **2005**, *17*, 291–300.

- [212] J.-J. Grebe, H. Stoll, R. Hoppe, *Z. Anorg. Allg. Chem.* **1988**, 559, 17–26.
- [213] G. Tams, H. K. Müller-Buschbaum, *Z. Anorg. Allg. Chem.* **1992**, 617, 19–22.
- [214] M. Scheikowski, H. K. Müller-Buschbaum, *Z. Anorg. Allg. Chem.* **1994**, 620, 313–318.
- [215] M. Scheikowski, H. K. Müller-Buschbaum, *Z. Anorg. Allg. Chem.* **1994**, 620, 155–159.
- [216] D. Fischer, R. Hoppe, *J. Solid State Chem.* **1992**, 96, 7–12.
- [217] G. Wehrum, R. Hoppe, *Z. Anorg. Allg. Chem.* **1992**, 617, 45–52.
- [218] D. Schultdt, R. Hoppe, *Z. Anorg. Allg. Chem.* **1991**, 594, 87–94.
- [219] D. Schultdt, R. Hoppe, *Z. Anorg. Allg. Chem.* **1989**, 575, 77–89.
- [220] O. Kerp, A. Möller, *Acta Crystallogr. Sect. E* **2006**, 62, i204–i206.
- [221] R. Hoppe, J. Birx, *Z. Anorg. Allg. Chem.* **1988**, 557, 171–181.
- [222] J. Birx, R. Hoppe, *Z. Anorg. Allg. Chem.* **1990**, 591, 67–76.
- [223] J. Birx, R. Hoppe, *Z. Anorg. Allg. Chem.* **1991**, 597, 19–26.
- [224] J. Birx, R. Hoppe, *Z. Anorg. Allg. Chem.* **1990**, 588, 7–18.
- [225] H.-P. Müller, R. Hoppe, *Z. Anorg. Allg. Chem.* **1989**, 569, 16–30.
- [226] J. Köhler, R. Hoppe, *Z. Anorg. Allg. Chem.* **1984**, 511, 201–211.
- [227] J. Hofmann, R. Hoppe, *Z. Anorg. Allg. Chem.* **1991**, 605, 43–50.
- [228] R. Brandes, R. Hoppe, *Z. Anorg. Allg. Chem.* **1995**, 621, 713–718.
- [229] H. Glaum, R. Hoppe, *Z. Anorg. Allg. Chem.* **1991**, 595, 95–114.
- [230] N. Kumada, N. Kinomura, A. W. Sleight, *Acta Crystallogr. Sect. C* **1996**, 52, 1063–1065.
- [231] D. Fischer, R. Hoppe, *Z. Anorg. Allg. Chem.* **1992**, 618, 59–62.
- [232] K. Bernet, J. Kissel, R. Hoppe, *Z. Anorg. Allg. Chem.* **1991**, 593, 17–34.
- [233] J. Kissel, R. Hoppe, *Z. Anorg. Allg. Chem.* **1989**, 571, 113–126.
- [234] C. Weiß, R. Hoppe, *Z. Anorg. Allg. Chem.* **1995**, 621, 1447–1453.
- [235] C. Weiß, R. Hoppe, *Z. Anorg. Allg. Chem.* **1996**, 622, 1715–1720.
- [236] J. Kissel, R. Hoppe, *Z. Anorg. Allg. Chem.* **1990**, 587, 29–38.
- [237] W. Losert, R. Hoppe, *Z. Anorg. Allg. Chem.* **1984**, 515, 87–94.
- [238] K. Mader, R. Hoppe, *Z. Anorg. Allg. Chem.* **1991**, 602, 155–167.
- [239] R. Luge, R. Hoppe, *Z. Anorg. Allg. Chem.* **1985**, 520, 39–50.
- [240] J. Köhler, R. Hoppe, *Z. Anorg. Allg. Chem.* **1982**, 495, 7–15.
- [241] R. Werthmann, R. Hoppe, *Z. Anorg. Allg. Chem.* **1984**, 509, 7–22.
- [242] J. Hofmann, R. Hoppe, *Z. Anorg. Allg. Chem.* **1993**, 619, 811–818.
- [243] P. Kroeschell, R. Hoppe, *Z. Anorg. Allg. Chem.* **1986**, 537, 106–114.
- [244] K. Mader, R. Hoppe, *J. Alloys Compd.* **1994**, 206, 271–276.
- [245] K. Mader, R. Hoppe, *Z. Anorg. Allg. Chem.* **1994**, 620, 225–233.
- [246] R. Hoppe, E. Seipp, *Z. Anorg. Allg. Chem.* **1985**, 522, 33–38.
- [247] D. Fischer, R. Hoppe, *Z. Anorg. Allg. Chem.* **1990**, 586, 106–114.
- [248] G. Wehrum, R. Hoppe, *Z. Anorg. Allg. Chem.* **1993**, 619, 149–157.
- [249] W. Scheld, G. Wehrum, R. Hoppe, *Z. Anorg. Allg. Chem.* **1993**, 619, 337–342.
- [250] R. Wolf, R. Hoppe, *Z. Anorg. Allg. Chem.* **1987**, 554, 34–42.
- [251] J. Kissel, R. Hoppe, *Z. Anorg. Allg. Chem.* **1989**, 570, 109–118.
- [252] R. Baier, R. Hoppe, *Z. Anorg. Allg. Chem.* **1985**, 522, 23–32.
- [253] E. Seipp, R. Hoppe, *J. Less-Common Met.* **1985**, 108, 279–288.
- [254] D. Fischer, R. Hoppe, *J. Alloys Compd.* **1992**, 183, 187–197.
- [255] P. Kroeschell, R. Hoppe, *Z. Anorg. Allg. Chem.* **1984**, 509, 127–137.
- [256] R. Werthmann, R. Hoppe, *Z. Anorg. Allg. Chem.* **1985**, 523, 54–62.
- [257] J. Köhler, R. Hoppe, *J. Less-Common Met.* **1985**, 108, 269–278.
- [258] R. Hoffmann, R. Hoppe, *Z. Anorg. Allg. Chem.* **1989**, 573, 143–156.
- [259] R. Hoppe, R. Baier, *Z. Anorg. Allg. Chem.* **1984**, 511, 161–175.
- [260] D. Fischer, R. Hoppe, *Angew. Chem.* **1990**, 102, 835–836; *Angew. Chem. Int. Ed.* **1990**, 29, 800–801.
- [261] E. Seipp, R. Hoppe, *Z. Anorg. Allg. Chem.* **1986**, 538, 123–130.
- [262] C. Weiß, R. Hoppe, *Z. Anorg. Allg. Chem.* **1994**, 620, 2064–2069.
- [263] T. Betz, R. Hoppe, *Z. Anorg. Allg. Chem.* **1985**, 522, 11–22.
- [264] R. Wolf, R. Hoppe, *Z. Anorg. Allg. Chem.* **1986**, 539, 127–140.
- [265] R. Baier, R. Hoppe, *Z. Anorg. Allg. Chem.* **1989**, 568, 136–146.
- [266] C. Weiß, R. Hoppe, *Z. Anorg. Allg. Chem.* **1996**, 622, 603–610.
- [267] R. Baier, R. Hoppe, *Z. Anorg. Allg. Chem.* **1987**, 546, 122–136.
- [268] V. A. Carlson, A. M. Stacy, *J. Solid State Chem.* **1992**, 96, 332–343.
- [269] M. Bharathy, H. S. Khalsa, M. D. Smith, H.-C. zur Loye, *Solid State Sci.* **2009**, 11, 294–298.
- [270] W. R. Gemmill, M. D. Smith, H.-C. zur Loye, *Solid State Sci.* **2007**, 9, 380–384.
- [271] S.-J. Kim, M. D. Smith, J. Darriet, H.-C. zur Loye, *J. Solid State Chem.* **2004**, 177, 1493–1500.
- [272] S. J. Mugavero III, M. Bharathy, J. McAlu, H.-C. zur Loye, *Solid State Sci.* **2008**, 10, 370–376.
- [273] K. E. Stitzer, A. El Abed, M. D. Smith, M. J. Davis, S.-J. Kim, J. Darriet, H.-C. zur Loye, *Inorg. Chem.* **2003**, 42, 947–949.
- [274] K. E. Stitzer, M. D. Smith, W. R. Gemmill, H.-C. zur Loye, *J. Am. Chem. Soc.* **2002**, 124, 13877–13885.
- [275] K. E. Stitzer, W. R. Gemmill, M. D. Smith, H.-C. zur Loye, *J. Solid State Chem.* **2003**, 175, 39–45.
- [276] E. Quarez, M. Huve, P. Roussel, O. Mentré, *J. Solid State Chem.* **2002**, 165, 214–227.
- [277] M. D. Smith, H.-C. zur Loye, *Acta Crystallogr. Sect. C* **2001**, 57, 337–338.
- [278] S. L. Stoll, A. M. Stacy, C. C. Torardi, *Inorg. Chem.* **1994**, 33, 2761–2765.
- [279] S. J. Mugavero III, M. D. Smith, H.-C. zur Loye, *Solid State Sci.* **2007**, 9, 555–563.
- [280] S. J. Mugavero III, M. D. Smith, H.-C. zur Loye, *Cryst. Growth Des.* **2008**, 8, 494–500.
- [281] S. J. Mugavero III, M. D. Smith, H.-C. zur Loye, *J. Solid State Chem.* **2005**, 178, 200–206.
- [282] S. J. Mugavero III, A. H. Fox, M. D. Smith, H.-C. zur Loye, *J. Solid State Chem.* **2010**, 183, 465–470.
- [283] I. P. Roof, T.-C. Jagau, W. G. Zeier, M. D. Smith, H.-C. zur Loye, *Chem. Mater.* **2009**, 21, 1955–1961.
- [284] T.-C. Jagau, I. P. Roof, M. D. Smith, H.-C. zur Loye, *Inorg. Chem.* **2009**, 48, 8220–8226.
- [285] I. P. Roof, M. D. Smith, S. Park, H.-C. zur Loye, *J. Am. Chem. Soc.* **2009**, 131, 4202–4203.
- [286] E. Halwax, H. Völlenkle, *Acta Crystallogr. Sect. C* **1991**, 47, 1353–1356.
- [287] S. J. Mugavero III, M. D. Smith, H.-C. zur Loye, *J. Solid State Chem.* **2005**, 178, 3176–3182.
- [288] M. J. Davis, S. J. Mugavero III, K. I. Glab, M. D. Smith, H.-C. zur Loye, *Solid State Sci.* **2004**, 6, 413–417.
- [289] S. J. Mugavero III, M. D. Smith, W.-S. Yoon, H.-C. zur Loye, *Angew. Chem.* **2009**, 121, 221–224; *Angew. Chem. Int. Ed.* **2009**, 48, 215–218.
- [290] I. P. Roof, S. Park, T. Vogt, V. Rassolov, M. D. Smith, S. Omar, J. Nino, H.-C. zur Loye, *Chem. Mater.* **2008**, 20, 3327–3335.
- [291] W. R. Gemmill, M. D. Smith, H.-C. zur Loye, *J. Solid State Chem.* **2006**, 179, 1750–1756.
- [292] I. P. Roof, M. D. Smith, E. J. Cussen, H.-C. zur Loye, *J. Solid State Chem.* **2009**, 182, 295–300.

- [293] W. R. Gemmill, M. D. Smith, R. Prozorov, H.-C. zur Loye, *Inorg. Chem.* **2005**, *44*, 2639–2646.
- [294] W. R. Gemmill, M. D. Smith, H.-C. zur Loye, *J. Solid State Chem.* **2004**, *177*, 3560–3567.
- [295] I. P. Roof, M. D. Smith, H.-C. zur Loye, *J. Cryst. Growth* **2008**, *310*, 240–244.
- [296] M. Bharathy, V. A. Rassolov, S. Park, H.-C. zur Loye, *Inorg. Chem.* **2008**, *47*, 9941–9945.
- [297] B. A. Reisner, A. M. Stacy, *J. Am. Chem. Soc.* **1998**, *120*, 9682–9683.
- [298] M. D. Smith, H.-C. zur Loye, *Acta Crystallogr. Sect. E* **2003**, *59*, i75–i76.
- [299] T. Sivakumar, H. Y. Chang, P. S. Halasyamani, *Solid State Sci.* **2007**, *9*, 370–375.
- [300] H. Mizoguchi, A. P. Ramirez, L. N. Zakharov, A. W. Sleight, M. A. Subramanian, *J. Solid State Chem.* **2008**, *181*, 56–60.
- [301] G. J. Redhammer, G. Roth, G. Amthauer, *Acta Crystallogr. Sect. C* **2008**, *64*, i97–i102.
- [302] P.-L. Chen, P.-Y. Chiang, H.-C. Yeh, B.-C. Chang, K.-H. Lii, *Dalton Trans.* **2008**, 1721–1726.
- [303] J. Barbier, D. Lévy, *Acta Crystallogr. Sect. C* **1998**, *54*, 2–5.
- [304] J. Akimoto, Y. Takahashi, N. Kijima, Y. Gotoh, *Solid State Ionics* **2004**, *172*, 495–497.
- [305] K. Fujimoto, S. Ito, M. Watanabe, *Solid State Ionics* **2006**, *177*, 1901–1904.
- [306] M. Takahashi, K. Uematsu, Z.-G. Ye, M. Sato, *J. Solid State Chem.* **1998**, *139*, 304–309.
- [307] B. Brazel, R. Hoppe, *Z. Anorg. Allg. Chem.* **1983**, *497*, 176–184.
- [308] B. Brazel, R. Hoppe, *Z. Anorg. Allg. Chem.* **1982**, *493*, 93–103.
- [309] H. U. Beyeler, C. Schüler, *Solid State Ionics* **1980**, *1*, 77–86.
- [310] A. Kania, *J. Cryst. Growth* **2007**, *300*, 343–346.
- [311] N. Henry, L. Burylo-Dhuime, F. Abraham, O. Mentré, *Solid State Sci.* **2002**, *4*, 1023–1029.
- [312] Y. Yamashita, S. Shimanuki, *Mater. Res. Bull.* **1996**, *31*, 887–895.
- [313] D. Petrova, S. Dobрева, M. Veleva, J. Macicek, M. Gospodinov, *Mater. Res. Bull.* **1997**, *32*, 1543–1549.